COOMET Key comparison COOMET.PR-K1.a.2018 for Spectral Irradiance 250 nm to 2500 nm.

Final Report

Boris Khlevnoy[1], Maksim Solodilov[1], Svetlana Kolesnikova[1], Denis Otryaskin[1], Ivan Korseko[2], Siarhey Nikanenka[2,3], Mykola Huriev[4], Ferhat Sametoğlu[5]

1 All-Russian Research Institute for Optical and Physical Measurements (VNIIOFI), Russia
2 Belarusian State Institute of Metrology (BelGIM), Belarus
3 B.I. Stepanov Institute of Physics of the National Academy of Sciences of Belarus
4 National Scientific Centre «Institute of Metrology» (NSC IM), Ukraine
5 National Metrology Institute of Türkiye (TÜBİTAK UME), Türkiye

Pilot: All-Russian Research Institute for Optical and Physical Measurement (VNIIOFI). Russia

Moscow, 2024

ABSTRACT

This report describes the Key Comparison COOMET.R-K1.a.2018 for Spectral Irradiance in the wavelength range of 250 nm to 2500 nm, conducted by the Regional Metrology Organization "Euro-Asian Cooperation of National Metrological Institutions" (COOMET). The comparison was, in fact, a combination of three bilateral comparisons with the same link/pilot laboratory – The All-Russian Research Institute for Optical and Physical Measurements (VNIIOFI), the Russian Federation. The non-link laboratories were the Belarusian State Institute of Metrology (BelGIM), Belarus, the National Scientific Centre «Institute of Metrology» (NSC IM), Ukraine, and the National Metrology Institute of Türkiye (TÜBİTAK UME), Türkiye.

The aim of the comparison was to link the BelGIM, NSC IM and TÜBİTAK UME measurement results to the CIPM key comparison CCPR-K1.a.2017, conducted by the Consultative Committee for Photometry and Radiometry (CCPR).

Tungsten quartz halogen lamps of the FEL type (1000 W) were used as artefacts. Each participant used its own set of lamps. The sequence of measurements was *participant – pilot – participant*. The pilot measurements of the described here COOMET comparison were performed in a short time (within three months) after completing the measurements of CCPR-K1.a.2017, where VNIIOFI also was a pilot, which provided a high quality link.

NSC IM performed measurements in the full spectral range, from 250 nm to 2500 nm, while BelGIM and TÜBİTAK UME managed to cover the range from 250 nm to 1100 nm only.

The analysis of the comparison was performed following the approach described in the Appendix A of the Guidelines for CCPR and RMO Bilateral Key Comparisons (CCPR-G5). Differences from KCRV of BelGIM and TÜBİTAK UME, for the most of the measured wavelengths, do not exceed 2% and are within the expanded uncertainties. For NSC IM the differences from KCRV are within or comparable with the uncertainties in the IR range, from 900 nm to 2500 nm, but become larger with decreasing wavelength in the visible and UV reaching 9% at 250 nm.

Content

1. Introduction

This report describes the Key Comparison COOMET.R-K1.a.2018 for Spectral Irradiance in the wavelength range of 250 nm to 2500 nm, organised and conducted by the Regional Metrology Organization (RMO) Euro-Asian Cooperation of National Metrological Institutions (COOMET).

The CIPM Mutual Recognition Arrangement (CIPM MRA) of the International Committee for Weights and Measures (CIPM) was signed in 1999 with the objectives of establishing the degree of equivalence of national measurement standards and providing for the mutual recognition of calibration and measurement certificates issued by National Metrology Institutes (NMIs) [1]. Under the CIPM MRA the equivalence of national measurement standards maintained by the NMIs is determined by a set of Key Comparisons which are chosen and organised by the Consultative Committees of the CIPM.

The Consultative Committee for Photometry and Radiometry (CCPR) identified several key comparisons in the field of optical radiation metrology. In particular, CCPR decided that a key comparison of spectral irradiance is to be carried out in two spectral ranges: from 250 nm to 2500 nm (identification code is CCPR-K1.a) and from 200 nm to 350 nm (CCPR-K1.b). The first CCPR-K1.a comparison was piloted by The National Physical Laboratory (NPL), the NMI of the United Kingdom, and was completed in 2006 [2]. The second round of the CCPR-K1.a. key comparison was started in 2017 with the code is CCPR-K1.a.2017 and piloted by the All-Russian Research Institute for Optical and Physical Measurements (VNIIOFI), the NMI of the Russian Federation. The final report of CCPR-K1.a.2017 was published in August 2023 [3].

The COOMET Technical Committee on Photometry and Radiometry (COOMET TC-PR) decided to carry out the RMO K1.a key comparison and appointed VNIIOFI as a pilot and a link laboratory. The comparison was started in 2018 with the code of COOMET.R-K1.a.2018. Originally PTB, the NMI of Germany, was appointed as the second link laboratory. However, later, on the stage of Pre-Draft A, PTB was forced to refuse further participation in the comparisons for reasons beyond its control. After that, in agreement with the COOMET TC-PR and the CCPR working group for key comparisons (CCPR-WGRC), the COOMET.R-K1.a.2018 comparison was considered as three combined bilateral comparisons with the same pilot/link laboratory, VNIIOFI, and the same technical protocol.

The Technical Protocol of COOMET.R-K1.a.2018 followed the guidelines established by the CIPM [4] and the CCPR [5, 6] and was written as closed as possible to the Technical Protocol of CCPR-K1a.2017 and takes into account of the experience gained from the previous K1a comparisons carried out by CCPR [2] and RMOs [7-10]. The same type of artefacts, FEL 1000 W tungsten quartz halogen lamps, were used for both, COOMET and CCPR, comparisons.

Measurements within COOMET.R-K1.a.2018 were performed in the period from 2018 to 2022. The pilot measurements of the COOMET.R-K1.a.2018 participants lamps were carried out in short time, within three months, after completing the pilot measurements of the CCPR-K1.a.2017 participants lamps with the same measurement procedure, which provided the best link.

Data analysis and the report preparation were done in accordance with [5] and the CCPR-G2 Guidelines for CCPR Key Comparison Report Preparation [11].

2. Organization of comparison

2.1. Participants

The list of the COOMET.PR-K1.a.2018 is presented in Table 2.1.

Table 2.1. List of participants and contact information

NMI			NMI Contact	
Short name	**Full name and Address**	**RMO**	**Name**	**Telephone, email address**
VNIIOFI (pilot, link)	All-Russian Research Institute for Optical and Physical Measurements (VNIIOFI) 46 Ozernaya Str. 119361 Moscow, RUSSIA	COOMET	Boris Khlevnoy	TEL: +7 (495) 437-29-88 khlevnoy-m4@vniiofi.ru
BelGIM (non-link)	Belarusian State Institute of Metrology 93 Starovilensky trakt, 220053 Minsk, REPUBLIC OF BELARUS (with assistance of B.I.Stepanov Institute of Physics of the National Academy of Sciences of Belarus)	COOMET	Siarhey Nikanenka	TEL: +375-17-2840794 s.nikonenko@ifanbel.bas-net.by
NSC IM (non-link)	National Scientific Centre «Institute of Metrology» 42 Mironositskaya st, 61002 Kharkov, UKRAINE	COOMET	Mykola Huriev	TEL: +38 057 704 97 72 ngurev@yandex.ru
TÜBİTAK UME (non-link)	National Metrology Institute of Türkiye TÜBİTAK Gebze Yerleşkesi, 41470, TÜRKIYE	EURAMET, COOMET, GULFMET	Ferhat Sametoğlu	TEL: +90 262 679 5000 ext.3301 ferhat.sametoglu@tubitak.gov.tr

VNIIOFI acted as the pilot laboratory and was responsible for developing the comparison protocol, registering the comparison, writing the Pre-Draft A and subsequent work.
NOTE: VNIIOFI was a pilot of the CCPR-K1a.2017 comparison.

VNIIOFI was a link laboratory.

Other three participants were non-linked laboratories and needed to be linked to CCPR-K1a.2017. They had to be able to demonstrate independent realization of spectral irradiance, or make clear the route of traceability to the quantity via another named laboratory.

2.2. Form of comparison

COOMET.PR-K1.a.2018 was a set of three bilateral key comparisons with the same pilot and link laboratory and the same technical protocol.

The measurements of all three bilateral comparisons were carried out in parallel in approximately the same period in the **Star form** with the following measurement sequence:

Participant – Pilot – Participant.

The artifacts were initially calibrated by a participant. Then they were transported to the pilot for pilot calibration. They were finally returned to the participant and calibrations were repeated to monitor possible drift. The pilot measurements of all three bilateral comparisons were done simultaneously in March-April 2019, soon after the CCPR-K1a.2017 pilot measurements, which were completed in January 2019.

2.3. Comparison artifacts

The comparison was carried out through calibration of groups of traveling standard lamps (traveling standards). Each participant provided its own set of three traveling standard lamps.

Traveling standard lamps were FEL type tungsten halogen lamps with nominal voltage and electrical power of 120 V and 1000 W, respectively. The same artifacts were used for CCPR-K1.a.2017 [3]. The lamps were operated at constant DC current. Each lamp set was equipped with an alignment jig that allowed for precise lamp alignment. A full description of the traveling standard lamps is given in section 4.

All traveling standards were transported from participants to the pilot and back by hand.

2.4. Timetable

The Technical Protocol of COOMET.PR-K1.a.2018 was approved by CCPR-WGKC and registered in the KCDB in December 2018.

The original timetable published in the Technical Protocol assumed that all the measurements to be finished by March 2019 and the Draft A report to be distributed by August 2019. The actual dates were significantly different from that originally planed. The main reason of the delay was late completing of the CIPM key comparison CCPR-K1.a.2017. COOMET.PR-K1.a.2018 was to be linked CCPR-K1.a.2017. Therefore, COOMET.PR-K1.a.2018 report could not be completed before publishing of the CCPR-K1.a.2017 final report, which was published in August 2023. The actual measurement timetable is presented in Table 2.3.

Table 2.2. Measurement timetable of COOMET.PR-K1.a.2018

NMI	1st round measurement	Lamps delivered to pilot	Pilot measurements	2st round measurement	Measurement data submitted to Pilot
BelGIM	February 2019	March 2019	March-April 2019	by April 2023	April 2023
NSC IM	February 2019	March 2019	April 2019	November 2020	December 2020
TÜBİTAK UME	November 2018	November 2018	March 2019	August 2019	November 2019

3. Measurand

The measurand of the comparison is the **spectral irradiance** (unit $W \cdot m^{-2} \cdot nm^{-1}$) of a lamp, which is properly aligned (see alignment procedures in section 4.4) at the distance of 500 mm from the lamp reference plane (see the definition of the reference plane in the section 4.4.9) at the following wavelengths (in nm):

250, 260, 270, 280, 290, 300, 320, 340, 360, 380, 400, 450, 500, 555, 600, 700, 800, 900, 1000, 1100, 1300, 1500, 1700, 2000, 2200, 2300, 2400 and 2500.

NOTE: Only NSC IM was able to measure spectral irradiance at all wavelengths. BelGIM and TÜBİTAK UME perform their measurements in the range of 250 nm to 1100 nm.

The spectral irradiance of each lamp had to be measured for the defined operating current. The measurements should be performed in suitable laboratory conditions maintained at a temperature of 20 °C to 25 °C.

The spectral irradiances of each lamp should be measured independently at least three times. Each independent measurement should consist of the lamp being realigned in the measurement facility. But only the mean or final spectral irradiance values for each lamp should be reported by the participants as a combination of the results of these independent measurements.

4. Description of the traveling standards and measurement instructions

4.1. Type of the Traveling Standards

The traveling standards (artifacts) were tungsten halogen lamps of the FEL type with nominal power of 1000 W and nominal voltage of 120 V produced by OSRAM-Sylvania. The same artifacts were used for CCPR-K1.a.2017 [3]. This lamp consists of a double-coiled tungsten filament, supported at the top and bottom of the filament and operated in a bromine-filled quartz envelope. Each lamp had to be equipped with an alignment jig.

Each participant used three aged and calibrated traveling lamps.

The technical protocol recommended the participants to use commercially available lamps of the type described above, which had been mounted and pre-aged by the company Gigahertz-Optik GmbH (Germany), the product number is BN-9101-02. The same type of lamps was used as the traveling standards for CCPR-K1.a.2017 [3]. The lamp BN-9101-02 and the alignment jig are shown in Figure 4.1. All participants except NSC IM used the lamps BN-9101-02. NSC IM used lamps, pre-aged and mounted by the company Newport (USA). The lamp itself was the same FEL lamp produced by OSRAM-Sylvania. NSC IM equipped the lamps with the holder and alignment jig similar to that of the BN-9101-02 lamp. The NSC IM lamp is shown in Figure 4.2.

Figure 4.1. Measurement artifact used by all participants except NSC IM – tungsten halogen lamp of FEL 120V-1000W type mounted by Gigahertz-Optik with alignment jig (right).

Figure 4.2. Measurement artifact used by NSC IM – tungsten halogen lamp of FEL 120V-1000W type mounted by Newport: in a traveling box (left), with holder and alignment jig (right).

4.2. Electrical Parameters

The traveling standards were operated with DC electrical power, with the positive (+) and negative (-) polarity terminals clearly marked for each lamp.

BN-9101-02 lamps were operated at the fixed electrical current of 8.100 A. The NSC IM lamps were operated at the current of 8.200 A.

4.3. Aligning the lamps

Before measuring spectral irradiance, each lamp had to be aligned using an alignment laser defining the optical axis of the spectral irradiance facility. It is assumed that the laser points towards the facility entrance optics, and the lamp is placed between the laser and the facility.

Alignment had to be performed by moving/rotating the lamp such that the laser hits the centre of the alignment jig target and the laser beam is back-reflected back to the laser (Figure.4.3).
Then the lamp had to be placed at the defined distance. For that the lamp moved towards to the facility until the front plate of the lamp was 500 mm from the entrance reference plane of the spectral irradiance measurement facility. The area of the front plate to measure the distance from was above the upper central screw, as shown in Figure 4.4.

Then the procedures of alignment and setting distance had to be repeated.

Finally, the alignment jig had to be removed.

More details of the alignment procedure are described in the comparison technical protocol.

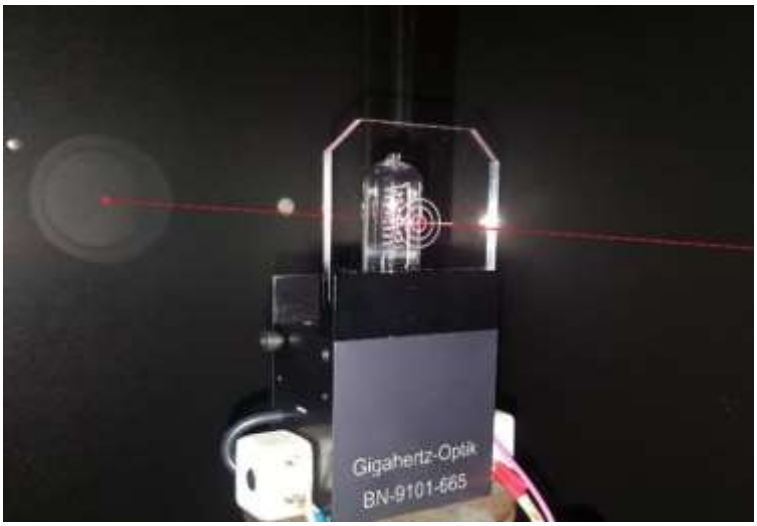

Figure 4.3. Aligning the lamp.

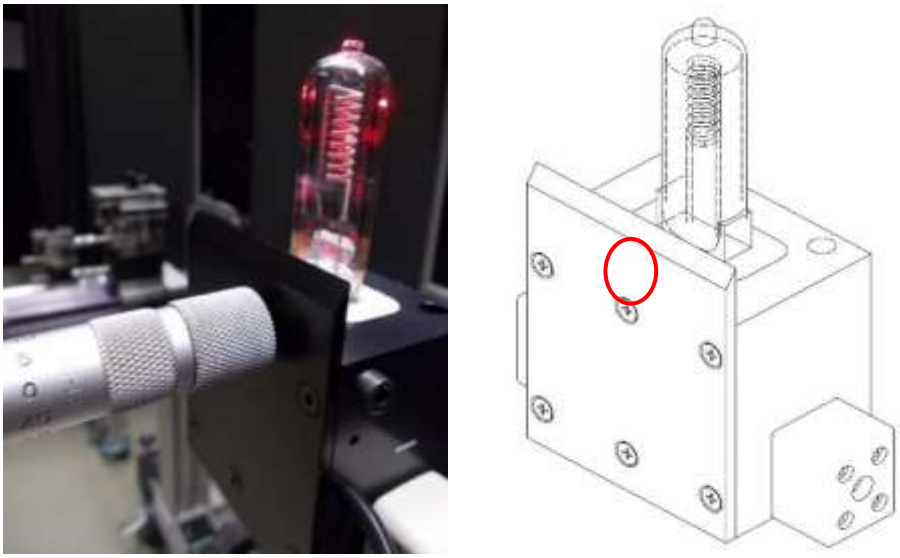

Figure 4.4. Measuring distance: The area of the front plate of the lamp to measure the distance from is marked by a red a circle.

4.4. Instruction of lamp warming-up and cooling-down

All participants had to use the following instructions for warming-up and cooling-down the lamps:

- The lamps should be turned on slowly by increasing the electrical current over a 2 minute period to prevent sudden thermal shock;

- Each lamp must be warmed up at the operational current for at least 20 minutes prior to the measurements being taken.

- After operation the lamp should be cooled down slowly by decreasing the electrical current over a 2 minutes period to prevent sudden thermal shock;

- The lamp should not be moved after switching off until the lamp base is cool enough to be touched (for approximately 20 to 30 minutes).

4.5. Measurement instruction

Before use, the lamps had to be inspected for any damage or contamination to the lamp envelope, lamp filament or lamp mount. Any damage had to be documented with photos or a drawing.

Spectral irradiance of each lamp had to be measured at the distance of 500 mm from the lamp reference plane for the defined operating current in suitable ambient temperature of 20 to 25 °C. The ambient temperature of the laboratory should be reported.

The bandwidth used to measure the spectral irradiance had to be less than 10 nm and ideally less than 5 nm in the visible and UV spectral regions.

The spectral irradiance of each lamp had to be measured independently at least 3 times, each time after realignment of the lamp in the measurement facility. But only the mean or final spectral irradiance value for each lamp should be reported.

The operating time for each lamp should be recorded and reported to the pilot.

More details of the measurement instruction can be found in the comparison technical protocol.

5. Measurement facilities and uncertainty budgets

Measurement facilities and procedures as well as uncertainty budgets of all participants are described below as submitted by the participants.

5.1. VNIIOFI (Pilot), Russia

5.1.1. VNIIOFI Measurement facility

During the COOMET.PR-K1.a.2018 comparison VNIIOFI used exactly the same facility and measurement procedure that were used for CCPR-K1.a.2017 [3] where VNIIOFI acted as a pilot. Therefore, the participant lamps in both comparisons were measured exactly in the same way.

VNIIOFI used a group of standard lamps for monitoring stability/reproducibility of its facility between two comparisons. VNIIOFI calibrated its lamps during the CCPR-K1.a.2017 campaign and then after completing the COOMET.PR-K1.a.2018 campaign to estimate stability or probable difference (and associated uncertainty) in measurements between the comparisons.

The VNIIOFI spectral irradiance facility is shown schematically in Figure 5.1.1. The facility consists of the following elements:

1. High-temperature blackbody of BB3500M type
2. Precision aperture
3. Lamps to be measured
4. Alignment lasers
5. Radiation thermometer
6. Integrating sphere
7. Monochromator
8. Detectors
9. Focusing mirror
10. Flat mirrors
11. Alignment laser
12. Set of light shields
13. Shutters

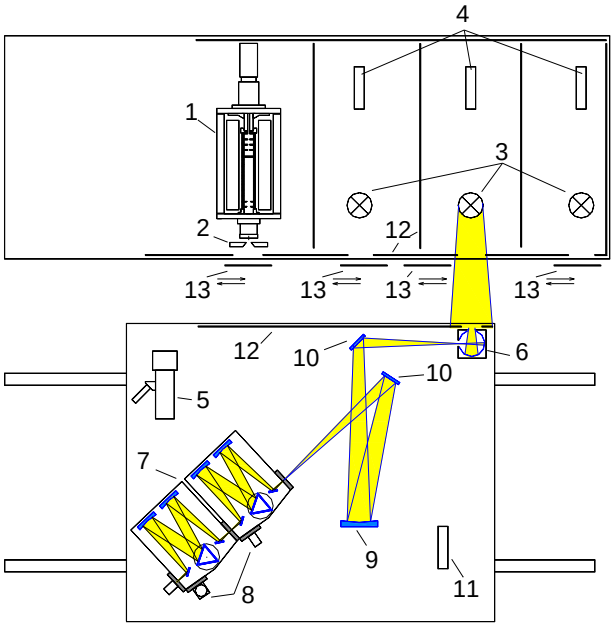

Figure 5.1.1. Spectral Irradiance facility of VNIIOFI

The blackbody and lamps were installed on an optical table and covered with a light tight box with holes in front of the sources equipped with shutters (13).

In front of the sources there was a spectral comparator that consisted of the integrating sphere (6), monochromator (7), focusing optics (9, 10) and detectors (8). The comparator was assembled on a translation stage, moving along the sources. The radiation thermometer (5) and the alignment laser (11) were installed on the same translation stage. The optical table top of the translation stage was covered with a light tight box with holes in front of the sphere and thermometer.

Spectral irradiance of the sources was measured in the plane of the entrance aperture of the integrating sphere. The distance from the lamps to the sphere was 500 mm, and the distance from the blackbody aperture to the sphere was approximately 470 mm. The exit aperture of the sphere was imaged to the monochromator entrance slit by the focusing mirror through the flat mirrors.

Each lamp measured at VNIIOFI was measured by comparing with the blackbody.

There were two lamp posts in the facility. Two lamps simultaneously were aligned and prepared for measurement. However, the lamps were measured one by one. Only one lamp was ON and measured each time.

5.1.1.1. Blackbody

Blackbody used was the high-temperature blackbody of the BB3500M type developed at VNIIOFI with a pyrolytic graphite radiator and the temperature range from 1200 K to 3500 K [12]. During the present comparison the blackbody was used at the temperature of 2750 K.

The emissivity was estimated to be 0.9995 using the STEEP321 modeling software [13, 14] based on the Monte Carlo ray tracing method for axially symmetric non-isothermal cavities.

An optical feedback system was used for stabilizing the blackbody radiation. The typical noise and drift of the blackbody temperature was ± 0.02 K and 0.1K/h, respectively, at the level of 2750 K.

The temperature of the blackbody was measured with a radiation thermometer of the TSP type [15] with central wavelength of 650 nm, bandwidth of 20 nm and target size of approximately 1.0 x 1.5 mm. The thermometer was originally calibrated against three high-temperature fixed

points (HTFP): Co-C (1567.39 K), Re-C (2747.84 K) and WC-C (3020.6 K) [16-19]. Then TSP calibration was periodically checked and, if necessary, corrected against the Re-C point.

In front of the blackbody there was an aperture with diameter of 12 mm in a water-cooled jacket. The precise average diameter of the aperture was measured at the facility traceable to the national standard of metre. The temperature of the aperture holder was stabilised at the level of 20 ºC using a water circulating thermostat.

5.1.1.2. Integrating sphere

The integrating sphere had an internal diameter of 40 mm and was covered inside with PTFE. The sphere had two apertures located on orthogonal sides: a circular entrance aperture with diameter of 11 mm and an exit slit with the dimensions of 4×15 mm.

5.1.1.3. Monochromator

The monochromator used was an additive-mode double grating monochromator of the DTMc300 type (producer is Bentham Instruments Limited) with focal length of 300 mm. Three pairs of gratings were used: presented in Table 1.1. In the range from 1700 nm to 2500 nm the monochromator was used as a single one, i.e. a detector was attached to the exit slit of the first monochromator.

Wavelength accuracy and wavelength repeatability of the monochromator were 0.15 nm and 0.05 nm, respectively.

Table 5.1.1. Monochromator gratings used at the VNIIOFI facility.

Spectral range, nm	Line density, g/mm	Blaze wavelength, nm	Linear dispersion, nm/mm
250-400	1200	250	1.35 (additive)
400-1000	1200	500	1.35 (additive)
1000-2500	600	1600	2.7 (additive) 5.4 (single)

The slit width used was 2.2 mm for both entrance and exit slits in whole spectral range. Therefore, the bandwidth was:

3 nm for the range from 250 nm to 1100 nm
6 nm for the range from 1100 nm to 1700 nm
12 nm for the range from 1700 nm to 2500 nm

5.1.1.4. Bandwidth correction

Bandwidth correction was applied following analysis presented in the section 5.4.2.1 of the CCPR-K1b final report [20]. The correction factor was calculated as

$$k_{BW}(\lambda_i) = \frac{\left(S_{Lamp}(\lambda_i) + \Delta S_{Lamp}(\lambda_i)\right)/\left(S_{BB}(\lambda_i) + \Delta S_{BB}(\lambda_i)\right)}{R(\lambda_i)} \qquad (5.1.1)$$

where $S_{Lamp}(\lambda_i)$ and $S_{BB}(\lambda_i)$ are signals of the lamp and blackbody, respectively, at the wavelength λ_i. $R(\lambda_i)$ is the measured ratio of lamp-to-blackbody signals. $\Delta S_{Lamp}(\lambda_i)$ and $\Delta S_{BB}(\lambda_i)$ are corrections to the signals of the lamp and blackbody, respectively, calculated as

$$\Delta S(\lambda_i) = -\frac{b^2}{12}\left[\frac{S(\lambda_{i-1}) - 2S(\lambda_i) + S(\lambda_{i+1})}{(\Delta\lambda)^2}\right] \quad (5.1.2)$$

where b is the bandwidth (4.05 nm, 8.1 nm, or 16.2 nm depending on wavelength), and $\Delta\lambda$ is the spectral step. Typical correction factors are presented in Table 5.1.2.

Table 5.1.2. Typical Bandwidth correction factor for the VNIIOFI facility.

λ, nm	$k_{BW}(\lambda)$	λ, nm	$k_{BW}(\lambda)$	λ, nm	$k_{BW}(\lambda)$	λ, nm	$k_{BW}(\lambda)$
250	1.0005	340	1.0001	600	1.0000	1500	1.0000
260	1.0005	360	1.0001	700	1.0000	1700	1.0000
270	1.0005	380	1.0001	800	1.0000	2000	1.0000
280	1.0005	400	1.0001	900	1.0000	2200	1.0000
290	1.0005	450	1.0001	1000	1.0000	2300	1.0000
300	1.0004	500	1.0000	1100	1.0000	2400	1.0000
320	1.0003	555	1.0000	1300	1.0000	2500	1.0000

5.1.1.5. Detectors

Four detectors were used:

- In the range 250 nm to 450 nm: PMT of the type Hamamatsu R7446P with voltage of 540 V for 250-300 nm and 330 V for 320-450 nm;
- In the range 450 nm to 1000 nm: Silicon photodiode S1337;
- In the range 1000 nm to 1700 nm: InGaAs photodiode, type Hamamatsu G8370-85;
- In the range 1700 nm to 2500 nm: PbS photoresistor, type Hamamatsu P9217-04.

All detectors were used at room temperature.

PbS was connected directly to the exit slit of the first monochromator. PMT and the photodiodes were connected to exit slit of the second monochromator and were changed manually.

The PMT, Si and InGaAs photodiodes were used with a current-voltage converter amplifier. The PbS photoresistor was used together with an optical chopper (EG&G model 197) at the frequency of 121 Hz. The signal of PbS was detected by a lock-in amplifier, model SR810. The output voltage of the amplifiers was measured by a 6½ digital voltmeter.

5.1.1.6. Alignment

There were three alignment lasers in the facility: two behind the lamps (number 4 in the Fig. 5.1.1) and the third on the translation stage (number 11). The lasers were preliminary aligned against each other, so when the laser 11 stood opposite any of the lasers 4, their beams coincided. Then the laser 11 was used for aligning the blackbody and its aperture. One of the lasers 4 was used for aligning the integrating sphere. Both lasers 4 were then used for aligning each measured lamp. Typical accuracy of positioning the blackbody aperture, integrating sphere and lamps was approximately 0.5 mm.

5.1.1.7. Distance measurement

Distance between the lamp and the sphere, as well as between the blackbody aperture and the sphere, was measured using an extension rod-type micrometer (produced by Mitutoyo). The accuracy of the micrometer is 10 μm. However, the actual uncertainty of the distance measurement

was higher due to backlash of the mounts of the sphere, aperture and lamps. The distance from the sphere to the aperture was approximately 488 mm and was measured with standard uncertainty of 0.07 mm. A lamp was set at the distance of 500.00 mm within the standard uncertainty of 0.05 mm.

5.1.1.8. Lamp current measurement

Each lamp post was equipped with a DC power supply. To measure the lamp current, a precision resistor of 0.1 Ω was connected to the electrical circuit of each post in series with the lamp. The voltage across the resistors was measure by 6½ digital voltmeters. Two other voltmeters were used for measuring lamp voltage.

5.1.1.9. Changing lamp posts

Each lamp was measured at least three times. The lamp post changed every time. No systematic difference between posts was detected.

5.1.1.10. Laboratory conditions

Room temperature in the laboratory was maintained within (20 ± 1) °C for the whole period of the comparison measurements.

5.1.2. Spectral irradiance of the blackbody

The spectral irradiance scale was realised using a high-temperature blackbody of the BB3500M type where the blackbody spectral irradiance $E_{\lambda,\mathrm{BB}}(\lambda,T)$ was calculated from the Planck equation:

$$E_{\lambda,\mathrm{BB}}(\lambda,T) = \frac{A}{l^2}\cdot g\cdot \varepsilon_{\mathrm{eff}}\cdot\frac{c_1}{\pi\lambda^5 n^2}\cdot\frac{1}{\exp\left(\frac{c_2}{\lambda T n}\right)-1} \qquad (5.1.3)$$

where $c_1 = 2\pi hc^2$ = 3,741771852·10^{-16} W m^2 – the first radiation constant,
$c_2 = hc/k$ = 1,438776877·10^{-2} m K – the second radiation constant,
h = 6.626 070 15 × 10^{-34} J s – the Planck constant,
c = 299 792 458 m/s – the speed of light in vacuum,
k = 1.380 649 × 10^{-23} J/K – the Boltzmann constant,
λ – wavelength,
T – thermodynamic temperature of blackbody cavity,
n – refractive index of air,
$\varepsilon_{\mathrm{eff}}$ – effective emissivity of the blackbody,
A – area of the blackbody aperture,
l – distance between the aperture and the entrance of the integrating sphere,
g – geometric correction factor that takes into account non-point sizes of the blackbody aperture and the sphere entrance diaphragm.

The values of air refractive index applied at VNIIOFI are shown in Table 5.1.3

The geometric correction was calculated as:

$$g = 2l^2/\left[r_{\mathrm{A}}^2 + r_{\mathrm{S}}^2 + l^2 + ((r_{\mathrm{A}}^2 + r_{\mathrm{S}}^2 + l^2)^2 - 4r_{\mathrm{A}}^2 r_{\mathrm{S}}^2)^{1/2}\right] \qquad (5.1.4)$$

where r_{A} and r_{S} are radii of the blackbody aperture and the sphere entrance diaphragm, respectively.

Table 5.1.3. Values of refractive index of air applied at VNIIOFI.

λ , nm	$n(\lambda)$	λ , nm	$n(\lambda)$	λ , nm	$n(\lambda)$	λ , nm	$n(\lambda)$
250	1.000295	340	1.000282	600	1.000272	1500	1.000269
260	1.000293	360	1.000281	700	1.000271	1700	1.000268
270	1.000291	380	1.000279	800	1.000270	2000	1.000268
280	1.000290	400	1.000278	900	1.000270	2200	1.000268
290	1.000288	450	1.000276	1000	1.000269	2300	1.000268
300	1.000287	500	1.000274	1100	1.000269	2400	1.000268
320	1.000284	555	1.000273	1300	1.000269	2500	1.000268

5.1.3. Uncertainty budget of scale realisation

Uncertainty components associated with the blackbody:

5.1.3.1. The first and second **radiation constants** c_1 and c_2 of the Planck law are derived from the defining constants of the SI and, therefore, have zero uncertainties.

5.1.3.2. Air **refractive index** (**n**) estimation depends on a model and air conditions such as temperature, pressure and humidity. Humidity has low influence on change of **n**. The temperature in the lab was maintained within ± 1 °C and, therefore, also has low influence. Atmospheric pressure had the main influence. The standard uncertainty of **n** was estimated as $0.5 \cdot 10^{-5}$ in the spectral range from 300 nm to 1700 nm, where the models work well, and as $1 \cdot 10^{-5}$ outside this range. The blackbody spectral irradiance uncertainty associated with **n** was calculated using the Planck law. *Random effect*.

5.1.3.3. Estimation of the blackbody **emissivity** and its uncertainty was based on modeling using the STEEP321 software [13,14]. The emissivity was estimated to be approximately 0.9995 with the standard uncertainty of 0.03 % in visible and IR and 0.06 % in UV. *Systematic effect*.

5.1.3.4. Blackbody temperature measurement uncertainty included four components associated with the following sources: uncertainty of realisation of the Re-C fixed point; the blackbody uniformity; the radiation thermometer stability; and the blackbody stability. The temperature uncertainty components are described below. The associated blackbody spectral irradiance uncertainties were calculated using the Planck law.

5.1.3.4.1. The standard uncertainty of **realisation of the Re-C** fixed point was estimated to be 0.31 K following the CCT recommendations [21]. *Systematic effect*.

5.1.3.4.2. The **blackbody non-uniformity** was estimated on the base of preliminary blackbody mapping. It corresponds to the temperature non-uniformity standard uncertainty of approximately 0.15 K. *Systematic effect*.

5.1.3.4.3. The standard uncertainty associated **with instability of the radiation thermometer** was estimated as 0.09 K from the data of periodical thermometer calibration against the Re-C fixed point. *Random effect*.

5.1.3.4.4. **Blackbody instability** was measured directly during the lamp calibration. The typical temperature instability standard uncertainty was 0.04 K which was combined from a typical drift (0.1K/h divided by 2 and by $3^{1/2}$) and the typical noise (0.02 K). *Random effect*.

5.1.3.5. It is known [22] that radiation of a graphite blackbody suffers from **absorption** of carbon-based molecules (C_2, C_3, CN) at high temperatures. All lamps within this comparison were

measured against the blackbody at the temperature of 2748 K. But the VNIIOFI lamps were additionally measured against the blackbody at 3020 K. The measurement results had systematic differences in UV. The Fig. 5.1.2 shows the average difference Δ_{abs} between the measurements at 3020 K and 2748 K. We think the absorption is the reason of the difference. Although we assume that at 2748 K the absorption is negligible, we introduce an uncertainty component u_c(abs) associated with possible absorption effect. Following the results of [22] we assume that absorption at 2748 K was at least 5 times weaker than at 3020 K. Therefore, the uncertainty was estimated as $u_c(\text{abs}) = \Delta_{abs}/4/3^{1/2}$. *Systematic effect*.

5.1.3.6. Diameter of the blackbody **aperture** was 12.135 mm. Its area was known with standard uncertainty of 0.05 %. *Systematic effect*.

5.1.3.7. Standard uncertainty of the **distance from the blackbody** to the sphere (488 mm) consisted of two components: *Systematic*, 0.06 mm, and *Random*, 0.04 mm. Corresponding spectral irradiance standard uncertainty components are 0.03 % and 0.02 %.

Summary of the uncertainty budget of spectral irradiance realized with the high-temperature blackbody is presented in Table 5.1.4.

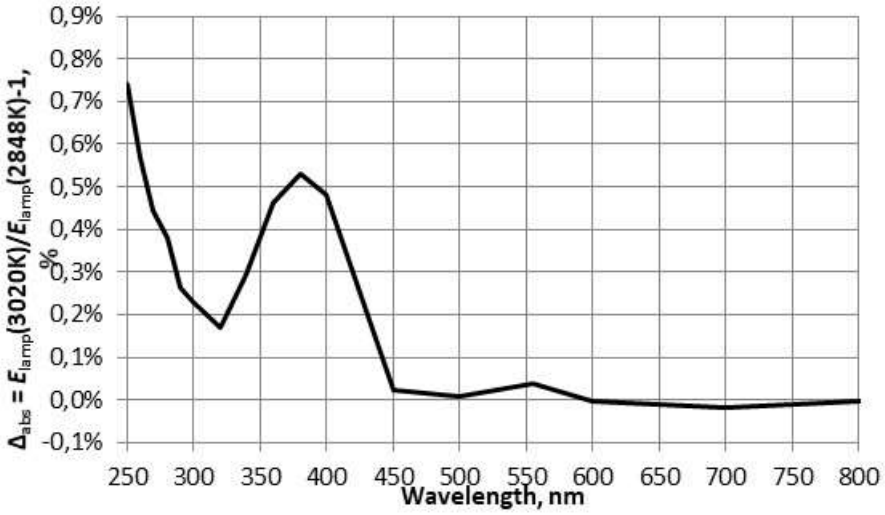

Figure 5.1.2. Average difference Δ_{abs} between spectral irradiances of lamps measured at VNIIOFI against the blackbody at the temperatures of 3020 K and 2748 K.

5.1.4. Uncertainty budget of the traveling lamps

5.1.4.1. Standard uncertainty of a **lamp current measurement** was 0.5 mA. *Systematic effect*.

5.1.4.2. Standard uncertainty of a **lamp current stability** was 0.3 mA. *Random effect*.

5.1.4.3. Standard uncertainty of the **distance from a lamp** to the sphere (500.00 mm) consisted of two components: *Systematic*, 0.03 mm, and *Random*, 0.04 mm. Corresponding spectral irradiance standard uncertainty components are 0.01 % and 0.02 %.

5.1.4.4. **Wavelength accuracy** of the monochromator $\Delta\lambda$ was better than 0.15 nm. Corresponding lamp spectral irradiance standard uncertainty was calculated as

$$u_{wa} = \frac{dR(\lambda)}{R(\lambda)d\lambda} \cdot \Delta\lambda/\sqrt{3} \qquad (5.1.5)$$

where $R(\lambda)$ is the lamp-to-blackbody ratio measured using the spectral comparator. *Systematic effect*.

5.1.4.5. **Wavelength repeatability** was 0.05 nm. Corresponding uncertainty was evaluated using the Eq. 5.1.5 for the wavelength ranges from 250 nm to 300 nm and from 1700 nm to 2500 nm where the ration *R* (*lamp signal / BB signal)* was measured at each wavelength without changing the wavelength. In the range from 320 nm to 1500 nm first the lamp signals were measured by scanning wavelength and then the BB signals were measured. In this range the standard uncertainty was calculated as:

$$u_{wr} = \left(\left(\frac{dS_{\mathrm{BB}}(\lambda)}{S_{\mathrm{BB}}(\lambda) d\lambda} \right)^2 + \left(\frac{dS_{\mathrm{lamp}}(\lambda)}{S_{\mathrm{lamp}}(\lambda) d\lambda} \right)^2 \right)^{1/2} \cdot \Delta\lambda/\sqrt{3} \qquad (5.1.6)$$

where $S_{\mathrm{BB}}(\lambda)$ and $S_{\mathrm{lamp}}(\lambda)$ are signals of the blackbody and lamp, respectively. *Random effect*.

5.1.4.6. **Repeatability of lamp measurement** uncertainty component was estimated as the Type A uncertainty, namely as an average of standard deviations calculated from independent measurements of lamps. Independent measurements were done with total realignment of a lamp and the blackbody aperture.

Summary of the uncertainty budget of a lamp spectral irradiance single measurement is presented in Table 5.1.5.

As a pilot VNIIOFI performed three independent measurements of each participant's lamp. The final spectral irradiance values provided by the pilot were the average of three independent measurement results. The uncertainty budget of the pilot final (average) values of spectral irradiance measurement is presented in Table 5.1.6.

5.1.4.7. **Systematic components** of the pilot average values are the same than that of the single pilot measurement. Therefore, the first component in Table 5.1.6 is the combined systematic uncertainty $u_{\mathrm{VNIIOFI,s}}$ from the Table 5.1.5.

5.1.4.8. The second component u_{r} in Table 5.1.6 is a combined uncertainty of **random** effects. It is equal to the combined random uncertainty of the single measurement ($u_{\mathrm{VNIIOFI,r}}$ in Table 1.5), divided by $\sqrt{3}$, because the final of spectral irradiance value was an average of three independent measurements:

$$u_{\mathrm{r}} = u_{\mathrm{VNIIOFI,r}}/\sqrt{3} \qquad (5.1.7)$$

5.1.4.9. **Stability of pilot measurement.** The final report of CCPR-K1.a.2017 showed that there was a variation of the VNIIOFI spectral irradiance measurement results during the period of the CCPR and COOMET comparison. The variation was interpreted as the pilot measurement stability, which had a random character. The uncertainty, associated with pilot stability, $u_{\mathrm{pilot,stab}}$, is presented the third component in Table 5.1.6.

5.1.4.10. Because of a random effect, the component $u_{\mathrm{pilot,stab}}$ was combined with u_{r} to form the total random uncertainty of the pilot, $u_{\mathrm{pilot,r}}$.

Table 5.1.4. Standard uncertainty components of the blackbody spectral irradiance in % (Uncertainty budget of scale realisation at VNIIOFI)

λ, nm	Air refractive index	Blackbody Emissivity	Blackbody Temperature measurement				Self-absorption of BB radiation	Aperture D=12.135 mm *u*=0.003 mm	Blackbody-to-sphere Distance Systematic *u*=0.06 mm	Blackbody-to-sphere Distance Random *u*=0.04 mm	$u_{BB,s}$ Total systematic	$u_{BB,r}$ Total random	$u_{BB,c}$ combined
			Realisation of Re-C *u*=0.31K	Blackbody Uniformity *u*=0.15K	TSP Stability *u*=0.09K	Blackbody Stability *u*=0.04K							
	Uncorrelated	Correlated	Correlated	Correlated	Corr.	Uncorrelated	Correlated	Correlated	Correlated	Uncorrelated	Correlated	Uncorrelated	
250	0.02	0.06	0.24	0.11	0.07	0.03	0.10	0.05	0.03	0.02	0.29	0.08	0.31
260	0.02	0.06	0.23	0.11	0.07	0.03	0.07	0.05	0.03	0.02	0.28	0.08	0.29
270	0.02	0.06	0.22	0.11	0.06	0.03	0.05	0.05	0.03	0.02	0.26	0.07	0.27
280	0.02	0.06	0.21	0.10	0.06	0.03	0.04	0.05	0.03	0.02	0.25	0.07	0.26
290	0.02	0.06	0.20	0.10	0.06	0.03	0.03	0.05	0.03	0.02	0.24	0.07	0.25
300	0.02	0.06	0.18	0.10	0.06	0.03	0.03	0.05	0.03	0.02	0.24	0.07	0.25
320	0.01	0.06	0.17	0.09	0.05	0.02	0.02	0.05	0.03	0.02	0.22	0.06	0.23
340	0.01	0.06	0.16	0.08	0.05	0.02	0.03	0.05	0.03	0.02	0.21	0.06	0.22
360	0.01	0.06	0.16	0.08	0.05	0.02	0.05	0.05	0.03	0.02	0.20	0.06	0.21
380	0.01	0.06	0.15	0.08	0.05	0.02	0.06	0.05	0.03	0.02	0.21	0.06	0.21
400	0.01	0.03	0.13	0.08	0.04	0.02	0.06	0.05	0.03	0.02	0.19	0.05	0.19
450	0.00	0.03	0.12	0.07	0.04	0.02	0.00	0.05	0.03	0.02	0.16	0.05	0.17
500	0.00	0.03	0.11	0.06	0.03	0.02	0.00	0.05	0.03	0.02	0.15	0.04	0.15
555	0.00	0.03	0.10	0.06	0.03	0.01	0.00	0.05	0.03	0.02	0.14	0.04	0.14
600	0.00	0.03	0.08	0.05	0.03	0.01	0.00	0.05	0.03	0.02	0.13	0.04	0.13
700	0.00	0.03	0.07	0.05	0.02	0.01	0.00	0.05	0.03	0.02	0.11	0.03	0.11
800	0.00	0.03	0.07	0.04	0.02	0.01	0.00	0.05	0.03	0.02	0.10	0.03	0.11
900	0.00	0.03	0.06	0.04	0.02	0.01	0.00	0.05	0.03	0.02	0.10	0.03	0.10
1000	0.00	0.03	0.05	0.03	0.02	0.01	0.00	0.05	0.03	0.02	0.09	0.03	0.10
1100	0.00	0.03	0.05	0.03	0.02	0.01	0.00	0.05	0.03	0.02	0.09	0.03	0.09
1300	0.00	0.03	0.04	0.03	0.01	0.01	0.00	0.05	0.03	0.02	0.08	0.02	0.09
1500	0.00	0.03	0.04	0.02	0.01	0.01	0.00	0.05	0.03	0.02	0.08	0.02	0.08
1700	0.00	0.03	0.03	0.02	0.01	0.01	0.00	0.05	0.03	0.02	0.08	0.02	0.08
2000	0.00	0.03	0.03	0.02	0.01	0.00	0.00	0.05	0.03	0.02	0.07	0.02	0.08
2200	0.00	0.03	0.03	0.02	0.01	0.00	0.00	0.05	0.03	0.02	0.07	0.02	0.08
2300	0.00	0.03	0.03	0.01	0.01	0.00	0.00	0.05	0.03	0.02	0.07	0.02	0.08
2400	0.00	0.03	0.03	0.01	0.01	0.00	0.00	0.05	0.03	0.02	0.07	0.02	0.08
2500	0.00	0.03	0.03	0.01	0.01	0.00	0.00	0.05	0.03	0.02	0.07	0.02	0.08

Table 5.1.5. Standard uncertainty budget of a lamp spectral irradiance measurement at VNIIOFI (single measurement), in %

λ, nm	$u_{BB,s}$ systematic	$u_{BB,r}$ Total random	Lamp current measurement uc=0.5 mA	Lamp current stability uc=0.3 mA	Wavelength accuracy 0.15 nm	Wavelength repeatability 0.05 nm	Distance from lamp Systematic, u(l)=0.03 mm 500 mm	Distance from lamp Random, u(l)=0.04 mm 500 mm	Repeatability of lamp meas-t Type A u_{repeat}	$u_{VNIIOFI,s}$ systematic	$u_{VNIIOFI,r}$ random	**$u_{VNIIOFI,c}$ combined standard**
	Correlated	Uncorrelated	Correlated	Uncorrelated	Correlated	Uncorrelated	Correlated	Uncorrelated	Uncorrelated	Correlated	Uncorrelated	
250	0.29	0.08	0.07	0.04	0.03	0.01	0.01	0.02	0.30	0.30	0.31	**0.43**
260	0.28	0.08	0.07	0.04	0.03	0.01	0.01	0.02	0.22	0.29	0.24	**0.38**
270	0.26	0.07	0.07	0.04	0.03	0.01	0.01	0.02	0.20	0.28	0.22	**0.36**
280	0.25	0.07	0.07	0.04	0.04	0.01	0.01	0.02	0.20	0.26	0.22	**0.34**
290	0.24	0.07	0.06	0.04	0.04	0.01	0.01	0.02	0.18	0.25	0.20	**0.32**
300	0.24	0.07	0.06	0.04	0.04	0.01	0.01	0.02	0.17	0.25	0.19	**0.31**
320	0.22	0.06	0.06	0.03	0.04	0.10	0.01	0.02	0.15	0.25	0.16	**0.30**
340	0.21	0.06	0.05	0.03	0.04	0.10	0.01	0.02	0.14	0.24	0.16	**0.29**
360	0.20	0.06	0.05	0.03	0.03	0.10	0.01	0.02	0.13	0.23	0.15	**0.27**
380	0.21	0.06	0.05	0.03	0.03	0.10	0.01	0.02	0.12	0.24	0.14	**0.28**
400	0.19	0.05	0.04	0.02	0.03	0.10	0.01	0.02	0.11	0.22	0.12	**0.25**
450	0.16	0.05	0.04	0.02	0.02	0.10	0.01	0.02	0.10	0.19	0.12	**0.22**
500	0.15	0.04	0.03	0.02	0.02	0.10	0.01	0.02	0.10	0.18	0.11	**0.21**
555	0.14	0.04	0.03	0.02	0.02	0.05	0.01	0.02	0.10	0.15	0.11	**0.19**
600	0.13	0.04	0.02	0.01	0.01	0.02	0.01	0.02	0.09	0.13	0.10	**0.16**
700	0.11	0.03	0.02	0.01	0.01	0.02	0.01	0.02	0.09	0.12	0.10	**0.16**
800	0.10	0.03	0.02	0.01	0.01	0.02	0.01	0.02	0.09	0.11	0.10	**0.15**
900	0.10	0.03	0.02	0.01	0.01	0.02	0.01	0.02	0.08	0.11	0.09	**0.14**
1000	0.09	0.03	0.01	0.01	0.01	0.02	0.01	0.02	0.08	0.10	0.09	**0.13**
1100	0.09	0.03	0.01	0.01	0.01	0.02	0.01	0.02	0.08	0.09	0.09	**0.13**
1300	0.08	0.02	0.01	0.01	0.01	0.02	0.01	0.02	0.08	0.09	0.09	**0.13**
1500	0.08	0.02	0.01	0.00	0.01	0.02	0.01	0.02	0.08	0.08	0.09	**0.12**
1700	0.08	0.02	0.01	0.00	0.01	0.02	0.01	0.02	0.09	0.08	0.10	**0.13**
2000	0.07	0.02	0.01	0.00	0.01	0.00	0.01	0.02	0.16	0.08	0.16	**0.18**
2200	0.07	0.02	0.01	0.00	0.01	0.00	0.01	0.02	0.18	0.07	0.18	**0.19**
2300	0.07	0.02	0.01	0.00	0.01	0.00	0.01	0.02	0.22	0.07	0.22	**0.23**
2400	0.07	0.02	0.01	0.00	0.01	0.00	0.01	0.02	0.27	0.07	0.27	**0.28**
2500	0.07	0.02	0.01	0.00	0.01	0.00	0.01	0.02	0.33	0.07	0.33	**0.34**

Table 5.1.6. Standard uncertainty of lamp average value of spectral irradiance measured by the pilot, in %

λ, nm	$u_{VNIIOFI,s}$ systematic	$u_r = u_{VNIIOFI,r}/\sqrt{3}$ random	Stability of pilot measurement $u_{pilot,stab}$ random	$u_{pilot,s}$ systematic	$u_{pilot,r}$ random	**$u_{c,pilot}$ combined standard**	**$U_{p,pilot}$ expanded (k=2)**
	Correlated	Uncorrelated	Uncorrelated	Correlated	Uncorrelated		
250	0.30	0.18	0.10	0.30	0.21	**0.37**	**0.74**
260	0.29	0.14	0.10	0.29	0.17	**0.34**	**0.68**
270	0.28	0.13	0.10	0.28	0.16	**0.32**	**0.64**
280	0.26	0.13	0.08	0.26	0.15	**0.30**	**0.60**
290	0.25	0.12	0.08	0.25	0.14	**0.29**	**0.58**
300	0.25	0.11	0.08	0.25	0.14	**0.29**	**0.58**
320	0.25	0.09	0.08	0.25	0.12	**0.28**	**0.56**
340	0.24	0.09	0.08	0.24	0.12	**0.27**	**0.54**
360	0.23	0.09	0.08	0.23	0.12	**0.26**	**0.52**
380	0.24	0.08	0.08	0.24	0.11	**0.26**	**0.52**
400	0.22	0.07	0.08	0.22	0.11	**0.25**	**0.50**
450	0.19	0.07	0.08	0.19	0.11	**0.22**	**0.44**
500	0.18	0.06	0.08	0.18	0.10	**0.21**	**0.42**
555	0.15	0.06	0.08	0.15	0.10	**0.18**	**0.36**
600	0.13	0.06	0.08	0.13	0.10	**0.16**	**0.32**
700	0.12	0.06	0.08	0.12	0.10	**0.16**	**0.32**
800	0.11	0.06	0.08	0.11	0.10	**0.15**	**0.30**
900	0.11	0.05	0.08	0.11	0.09	**0.14**	**0.28**
1000	0.10	0.05	0.07	0.10	0.09	**0.13**	**0.26**
1100	0.09	0.05	0.07	0.09	0.09	**0.13**	**0.26**
1300	0.09	0.05	0.07	0.09	0.09	**0.13**	**0.26**
1500	0.08	0.05	0.07	0.08	0.09	**0.12**	**0.24**
1700	0.08	0.06	0.07	0.08	0.09	**0.12**	**0.24**
2000	0.08	0.09	0.08	0.08	0.12	**0.14**	**0.28**
2200	0.07	0.10	0.10	0.07	0.14	**0.16**	**0.32**
2300	0.07	0.13	0.12	0.07	0.18	**0.19**	**0.38**
2400	0.07	0.16	0.12	0.07	0.20	**0.21**	**0.42**
2500	0.07	0.19	0.12	0.07	0.22	**0.23**	**0.46**

5.2. BelGIM, Belarus

5.2.1. Primary scale realization

Spectral Irradiance scale in the spectral range from 200 nm to 2500 nm was realized using a high-temperature blackbody of the BB3500M type. Emissivity of BB3500M was estimated to be approximately 0.995 with standard uncertainty varied from 0.06% at 350 nm to 0.1% at 200 nm.

$$E_{\mathrm{BB}}(\lambda, T) = \frac{A}{d^2}\varepsilon_{\mathrm{eff}} \cdot \frac{c_1}{\pi\lambda^5 n^2} \cdot \frac{1}{exp\left(\frac{c_2}{\lambda T_{\mathrm{BB}} n}\right)-1} \quad (5.2.1)$$

где c_1 =3,741772·10^{-16} W·m^2;

c_2 =1,438777·10^{-2} K·m;

λ – wavelength in air, m;

T_{BB} – temperature of the blackbody, K;

n – air refractive index;

$\varepsilon_{\mathrm{eff}}$ – effective emissivity of the blackbody;

A – area of the precision blackbody aperture, m^2;

d – distance from the blackbody aperture to the sphere entrance aperture, m.

5.2.2. Measurement facility

The main components of National standard of Belarus of the units of radiant intensity, spectral radiance and irradiance in the spectral range from 0.2 μm to 3.0 μm (NSSRI) are: high-temperature blackbody radiator BB3500M, Linearpyrometer LP5, set-up of the multifunctional spectral facility (MSF), integrating sphere source (ISS), monochromatic radiation source (MRS) and standard lamps. The schematic diagram of NSSRI is shown in Fig.5.2.1.

The high-temperature blackbody radiator BB3500M is used as a base for spectral radiance and irradiance scale in the spectral range from 0.2 μm to 3.0 μm [12]. It was constructed by the All-Russian Institute for Optical and Physical Measurements (VNIIOFI). The radiance temperature of the blackbody is determined with Linearpyrometer LP5 at the distance of 0.7 m. A precision water cooling aperture is placed in front of the blackbody to define the area of uniform radiance.

Spectral radiance of the blackbody is calculated by the Planck's law. Spectral irradiance on a measurement plane is calculated by using the spectral radiance of the blackbody, precision aperture area and distance between the aperture and input aperture of integrating sphere. A special developed water cooling system of the BB3500M black body maintains the temperature of the water in the system with an accuracy of 0.2 ºC.

The set-up of the multifunctional spectroradometrical facility (MSF) consists of two spectral systems, translation table (2.8 m length) and portable radiometric benches. Spectral systems consist of UV-VIS and VIS-NIR double monochromators on the base of MS266 monochromators (SolarLS, Belarus) for ranges 0.20-1.20 μm and 0.35-3.00 μm respectively. The double monochromators have one entrance and three output ports. An entrance optics block for input radiation into the monochromators, based on a toroidal mirror is installed on the input port. At the output ports, detectors are installed.

The spectral irradiance of the lamp is obtained from the ratio of the MSF output signal from the lamp to that of blackbody measured at the entrance aperture of the entrance optics.

As secondary standards of the spectral irradiance in the range from 200 nm up to 400 nm deuterium lamps and 250 nm up to 2500 nm 1000 W FEL-type quartz-halogen lamps are used.

As working standards of the radiant intensity in the spectral range from 250 nm up to 1100 nm filter radiometers based on 3-element trap detectors (Hohenheide OÜ, Estonia) are used.

For measurement of the spectral irradiance on the input optics block an integrating sphere with inside diameter of 50.8 mm is installed. The inner surface of the integrating sphere used as a diffuser is made of PTFE. Its entrance aperture is aligned to radiation sources.

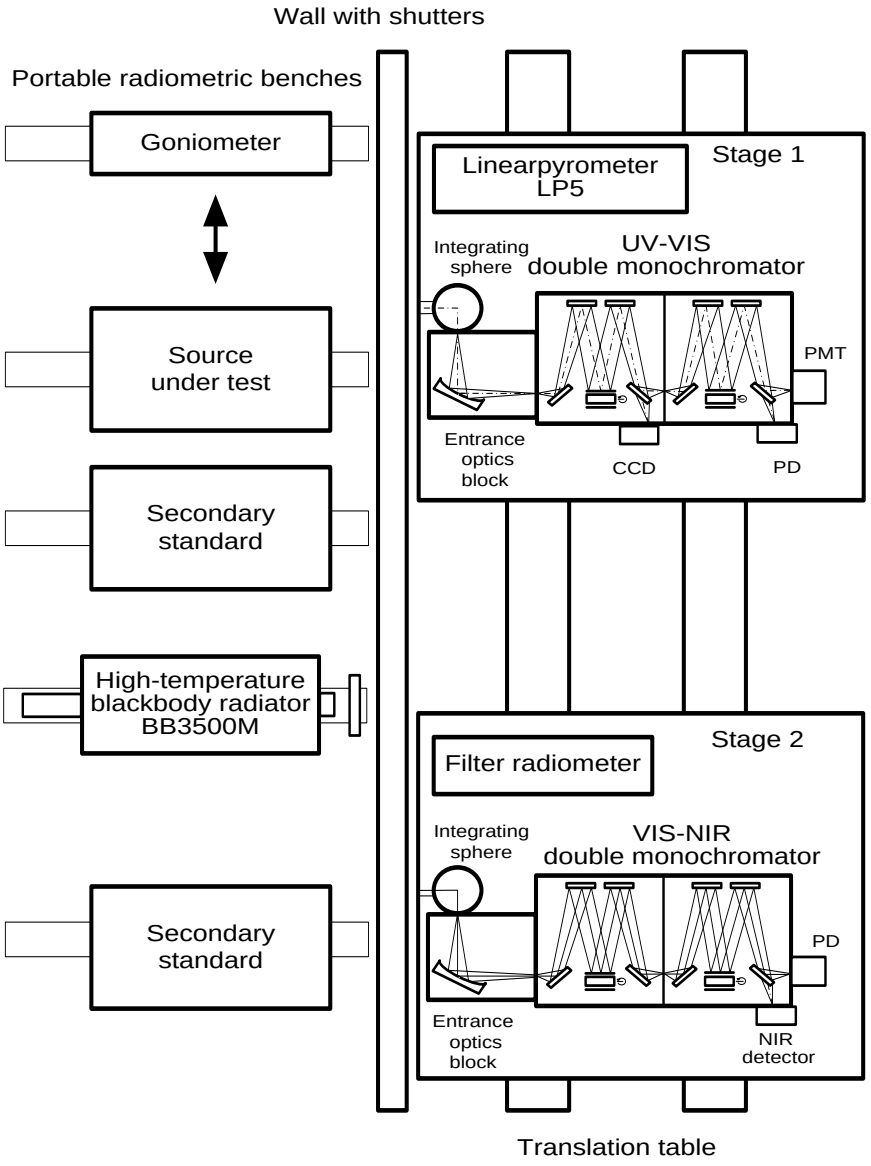

Figure 5.2.1. Schematic diagram of the spectral irradiance facility

The four gratings with different blazed wavelengths are used changing one by one corresponding to wavelengths. The detectors at the exit ports of the monochromator are PMT, Si-photodiode and InAs infrared detector module with built-in preamp are used to measure the output signal from the spectral systems in ranges from 200 nm to 800 nm, from 650 nm to 1200 nm and from 1200 nm to 3000 nm respectively. The InAs detector is operated in combination with chopper and two-phase lock-in amplifier to measure the small signal at long wavelengths.

The design of the spectral irradiance calibration facility allows to measure the spectral irradiance of any radiation sources at distances from 4 mm to 2 m.

The detectors at the exit ports of the monochromator are PMT, Si-photodiode or CCD matrix, InAs infrared detector or InGaAs linear imaging sensor are used to measure the output signal from the spectral

systems in ranges from 350 nm to 800 nm, from 650 nm to 1200 nm, from 350 nm to 1200 nm, from 1200 nm to 3000 nm respectively.

The mainly measurement procedure as follows: the stage 1 moves LP5 to the BB3500M position; LP5 signal is read; the spectral system wavelength is set; the stage moves the spectral system to the lamp position; detector signal is read; shutter is closed; dark signal is read; stage moves the spectral system to the BB3500M position; dark signal is read; shutter is opened; BB3500M signal is read; a ratio lamp/BB3500M is calculated; the signals and ratio are saved into a file.

5.2.2.1. Integrating sphere

The integrating sphere had an inner diameter of 50.8 mm and was covered inside with PTFE. The sphere had two apertures located on orthogonal sides: a circular entrance aperture with diameter of 25,4 mm and an exit circular 12,7mm.

5.2.2.2. Monochromator

The UV-VIS double monochromators on the base of MS266 monochromators (SolarLS, Belarus) for ranges 0.20-1.20 μm. The double monochromators have one entrance and three output ports. An entrance optics block for input radiation into the monochromators, based on a torroidal mirror is installed on the input port. At the output ports, detectors are installed.
The monochromator used with focal length of 284 mm. In the spectral range from 200 nm to 700 nm one pair of gratings was used: 1200 g/mm with dispersion of 3.18 nm/mm. In the spectral range from 700 nm to 1500 nm one pair of gratings was used: 600 g/mm with dispersion of 3.18 nm/mm.
Wavelength accuracy and wavelength repeatability of the monochromator were 0.10 nm and 0.05 nm respectively.

5.2.2.3. Bandwidth correction

Bandwidth correction was applied following the section 5.4.2.1 of the CCPR-K1b final report [20].

5.2.2.4. Detectors

For the present comparison only two detectors were used: room-temperature PMT of the type Hamamatsu 1890-210 and photodiode Hamamatsu S1227-1010BQ (PD) with picoammeter Keitley 6485 or transimpedance amplifier L-1 Model 3300.

5.2.2.5. Distance measurement

Distance between the lamp and the sphere, as well as between the blackbody aperture and the sphere, was measured using an gauge distance 500 mm and set of gauge blocks 1-H2 GOST 9038. Accuracy of the gauge measure from 1 to 20 μm. However, the actual uncertainty of the distance measurement was higher due a play of the mounts of the sphere, aperture and lamps.

5.2.2.6. Measurement sequence

The comparison lamps were measured by means of direct comparison with the blackbody. The comparisons were performed wavelength-by-wavelength, i.e. the measurement sequence was as follows:
– Wavelength is set;
– Translation stage is moved to the position where LP5 stands in front of the blackbody;
– Blackbody temperature is measured and saved;
– Translation stage is moved to the Lamp position;
– Shutter of the Lamp is opened;
– Detector signal is read and average value and its standard deviation are saved;
– Shutter is closed; dark signal is and average value and its standard deviation are saved;
– Translation stage is moved to the blackbody position;
– Shutter of the Blackbody is opened;

– Detector signal is read and average value and its standard deviation are saved;
– Shutter closed; dark signal is read and average value and its standard deviation are saved;
– Translation stage is moved to the position where LP5 stands in front of the blackbody;
– Blackbody temperature is measured and saved;
– Two (sometimes four) Lamp/Blackbody ratios are measured for each wavelength with necessary stage movements;
– New wavelength is set and the measurement cycle is repeated.

5.2.3. Uncertainty budget

5.2.3.1. Uncertainty components associated with the blackbody (scale realization)

5.2.3.1.1. **Radiation constants** c_1 and c_2. The radiation constants c_1 and c_2 for Planck law has negligible small uncertainties. Therefore, these uncertainties were not included in the budget.

5.2.3.1.2. **Air refractive index** *n*. Average value of standard uncertainty of *n* was estimated as 0.00002.

5.2.3.1.3. **Effective emissivity of the blackbody** ε_{eff} . ε_{eff} – approximately equal to 0.995. The spectral irradiance relative uncertainty is spectrally independent from 0.1 % to 0.06 %

5.2.3.1.4. **Blackbody temperature measurement uncertainty** was estimated as 2.0 K.

5.2.3.1.5. **Blackbody non-uniformity** was estimated on the base of preliminary blackbody mapping in 9 points. It corresponds to the temperature non-uniformity standard uncertainty of approximately 0.18 K. The blackbody spectral irradiance uncertainty associated with non-uniformity was calculated using the Planck law.

5.2.3.1.6. **Blackbody instability** was measured directly during the lamp calibration. The typical temperature instability standard uncertainty was not higher than 0.05 K. The blackbody spectral irradiance uncertainty associated with instability was calculated using the Planck law.

5.2.3.1.7. **Blackbody aperture area** This was measured with standard uncertainty of approximately 0.05 μm that corresponds to a spectral irradiance relative uncertainty of 0.02 %

5.2.3.1.8. **Distance from the blackbody aperture to the integration sphere**. It was estimated as 0.05 %.

5.2.3.2. Uncertainty components associated with the measured lamp

5.2.3.2.1. **Lamp current measurement and stability**. This was estimated as 0.8 mA.

Table 5.2.1 presents the uncertainty values submitted to the pilot together with the spectral irradiance values. Uncertainties are the same for all lamps and both rounds.

Table 5.2.1. Uncertainties of BelGIM measurement of spectral irradiance of the FEL lamps. All uncertainties are standard (k=1)

Wavelength, nm	Uncertainties associated with, %		Combined uncertainty
	Uncorrelated effects	Correlated effects	
250	4.00	3.78	5.50
260	2.69	1.33	3.00
270	2.67	1.67	3.15
280	2.58	1.42	2.95
290	1.47	0.30	1.50
300	1.28	0.25	1.30
320	1.12	0.24	1.15
340	1.08	0.23	1.10
360	1.03	0.22	1.05
380	0.93	0.21	0.95
400	0.88	0.20	0.90
450	0.83	0.19	0.85
500	0.80	0.19	0.82
555	0.78	0.19	0.80
600	0.80	0.19	0.82
700	0.83	0.19	0.85
800	0.86	0.19	0.88
900	0.88	0.19	0.90
1000	1.01	0.21	1.03
1100	1.24	0.17	1.25

5.3. NSC IM, Ukraine

5.3.1. Description of measurement equipment

5.3.1.1 Artifacts

For the comparisons NSC IM used three FEL-type tungsten halogen lamps with the nominal power, voltage and current of 1000 W, 120 V and 8.2 A, respectively. The serial numbers of the lamps were No.3224, No.3225 and No.7-3112. The lamps were manufactured by OSRAM-Sylvania, but mounted and pre-aged by the company Newport (USA). The lamps were equipped with a holder and alignment jig similar to that required by the technical protocol. The NSC IM lamp is shown in Figure 4.2.

The lamps were used with the DC power supply ORIEL OPS-Q1000, shown in Figure 5.3.1.

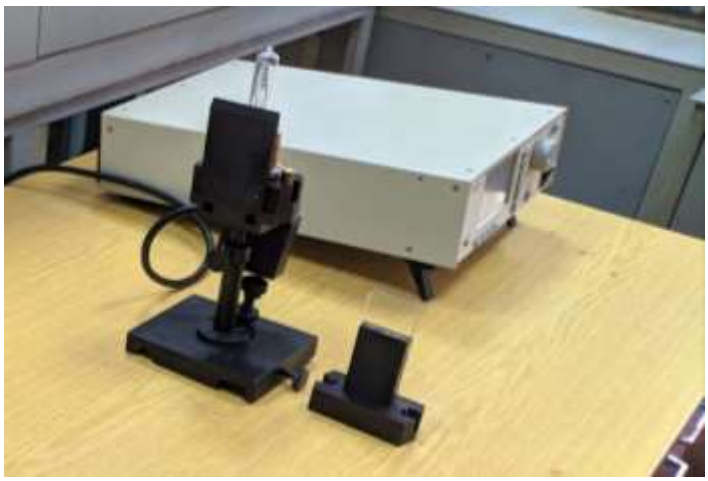

Figure 5.3.1. The NSC IM lamp in a special holder in front of the power supply ORIEL OPS-Q1000

5.3.1.2 Equipment for measuring relative spectral irradiance of the FEL lamps

To measure the relative spectral irradiance of FEL lamps, NSC IM developed the spectrometer based on the double monochromator MSA-130 and detectors Hamamatsu 1337-1010 BQ (250 nm – 1100 nm) and Hamamatsu G12183-010K (1100 nm – 2500 nm). The facility is shown in Figure 5.3.2 (photos) and Figure 5.3.3 (diagram).

The relative spectral responsivity of the spectrometer was calibrated by the National standard of spectral irradiance DETU 11-06-06 using a high-temperature Black Body.

Stabilized current of 8.2 A was supplied to the using the power supply ORIEL OPS-Q1000 from the NEWPORT company. The photodiode signal of the spectrometer was measured using a Keithley 6485 picoammeter.

5.3.1.3 Equipment for measuring absolute spectral irradiance of FEL lamps at wavelength of 900 nm

To measure the value of the absolute spectral irradiance of the FEL lamps, the filter radiometer based on the trap-detector with photodiodes Hamamatsu 1337-1010 BR and Newport Optical Filter Mounts with bandpass filter at 900 nm and aperture of 4.3 mm was developed in NSC IM. The filter radiometer is shown in Figure 5.3.4.

Figure 5.3.2. Facility for measuring relative spectral irradiance of FEL lamps

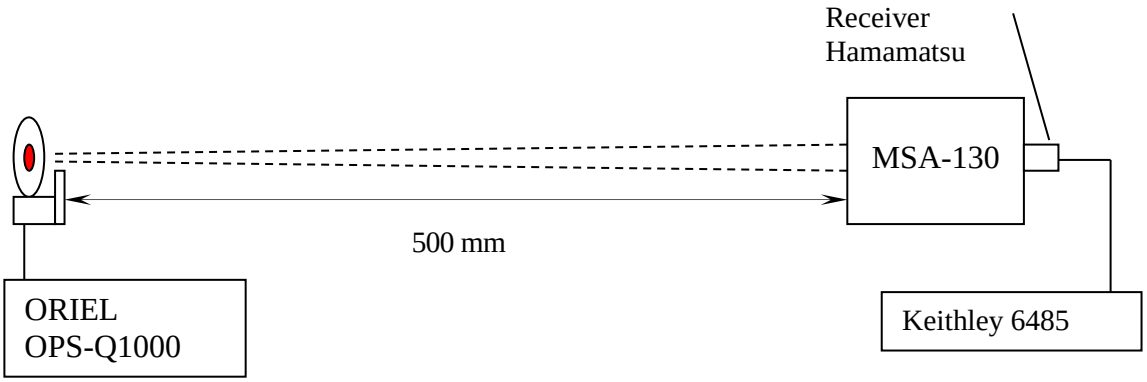

Figure 5.3.3. Diagram of the facility for measuring relative spectral irradiance of FEL lamps

Figure 5.3.4. Filter radiometer at wavelength of 900 nm

The Figures 5.3.5 shows the photo and diagram of the installation where the absolute spectral irradiance of the lamp was measured by the radiometer.

The spectral responsivity of the trap detector was measured at the National standard DETU 11-06-06. The spectral transmittance of the 900 nm filter was measured at the National standard DETU 11-09-08 in conditions close to those stated in the technical protocol of comparisons.

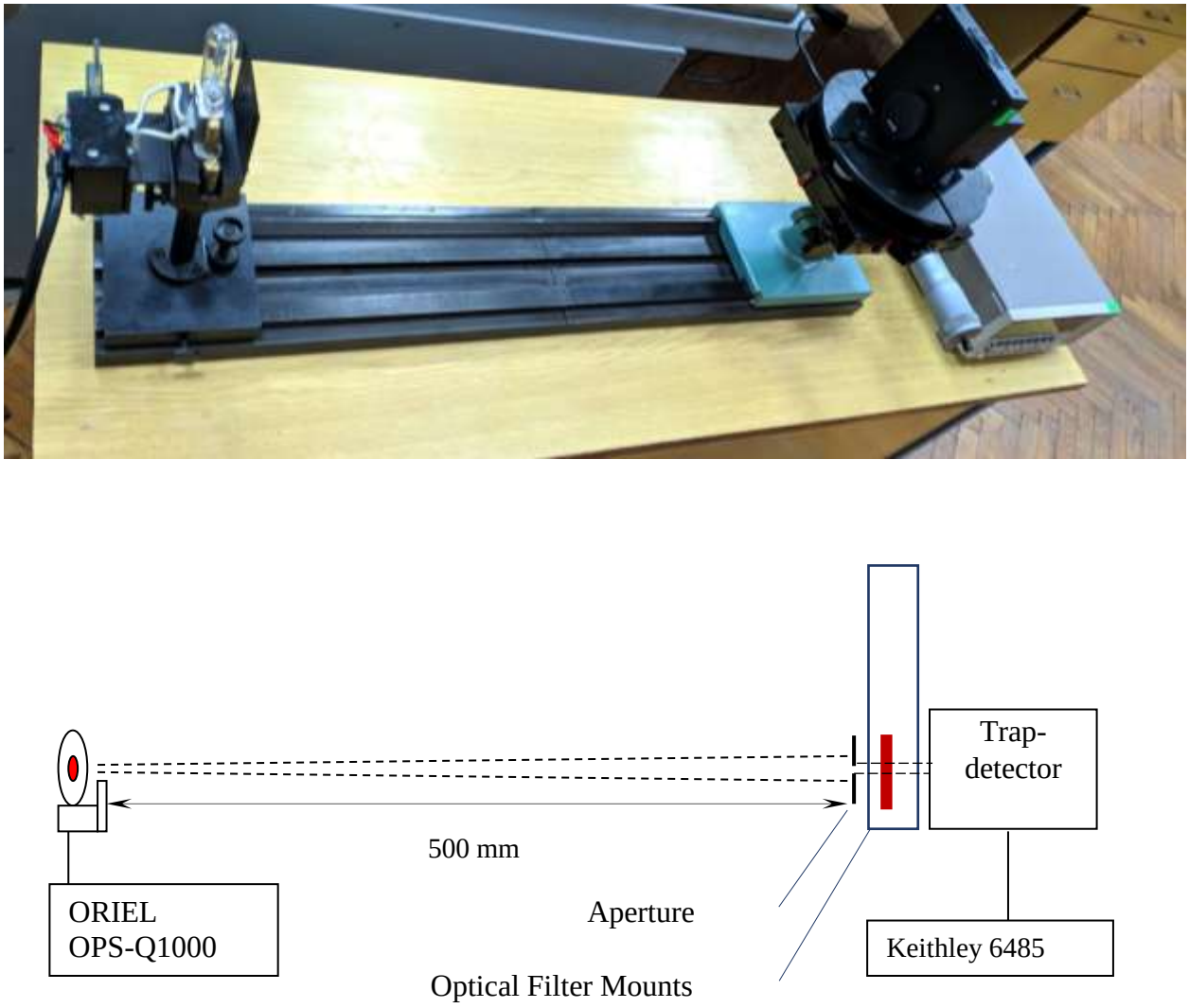

Figure 5.3.5. Photo (top) and the diagram (bottom) of the installation for measuring absolute spectral irradiance of the FEL lamp by the filter radiometer at the wavelength of 900 nm

5.3.2. Measurements

5.3.2.1 Measurement of relative spectral irradiance of FEL lamps at the distance of 500 mm.

The measurements were performed on the facility shown in Figures 5.3.2 and 5.3.3. Five measurements were performed in each round of comparisons. The average spectra of relative spectral irradiance are shown graphically in Figure 5.3.6.

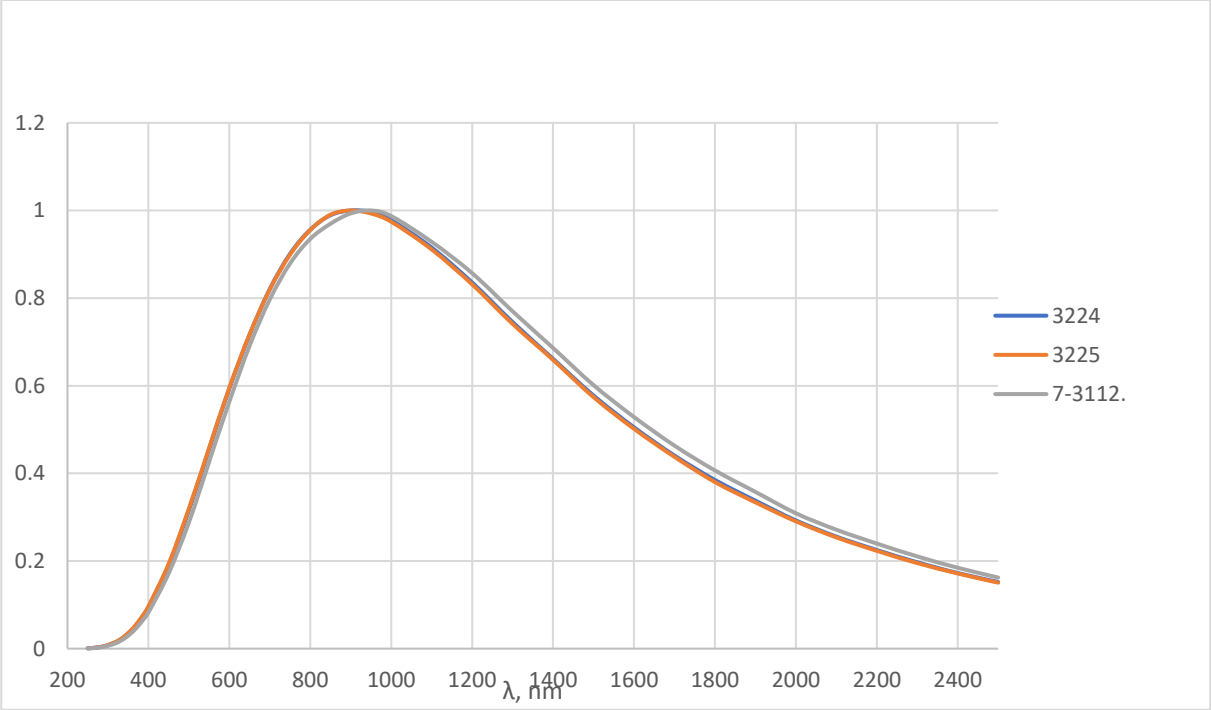

Figure 5.3.6. Spectra of relative spectral irradiance of NSC IM traveling lamps

5.3.2.2 Calibration of the filter radiometer

The spectrum of the FEL lamp in the wavelength range from 840 nm to 940 nm is the flattest. Thus, the wavelength of 900 nm is the most appropriate for the filter radiometer to measure the absolute value of the spectral irradiance. This significantly reduces the measurement uncertainty associated with wavelengths accuracy and slit width of the monochromator when measuring the spectral responsivity of the filter radiometer.

The diagram of the setup to measure the filter spectral transmittance is shown in Figure 5.3.7. The monochromator MDR-41, equipped with a halogen lamp and a mirror condenser, forms a monochromatic radiation beam, which illuminates an aperture of the filter radiometer. Between the aperture and the trap detector there is a filter mount with two positions: first, when the 900 nm filter is in the light beam and second, when the filter is out of beam.

The ratio of monochromatic fluxes with and without a filter was measured using a trap detector. Due to the fact that the radiation was almost completely absorbed in the trap detector, there was no uncertainty associated with multiple reflections between the detector and the filter.

Measurements were performed with a step of 1 nm and a slit width of 0.5 nm.

The spectral responsivity of the trap detector was measured separately with the National standard DETU 11-06-06. The resulting spectral responsivity of the filter radiometer is shown in Figure 5.3.8.

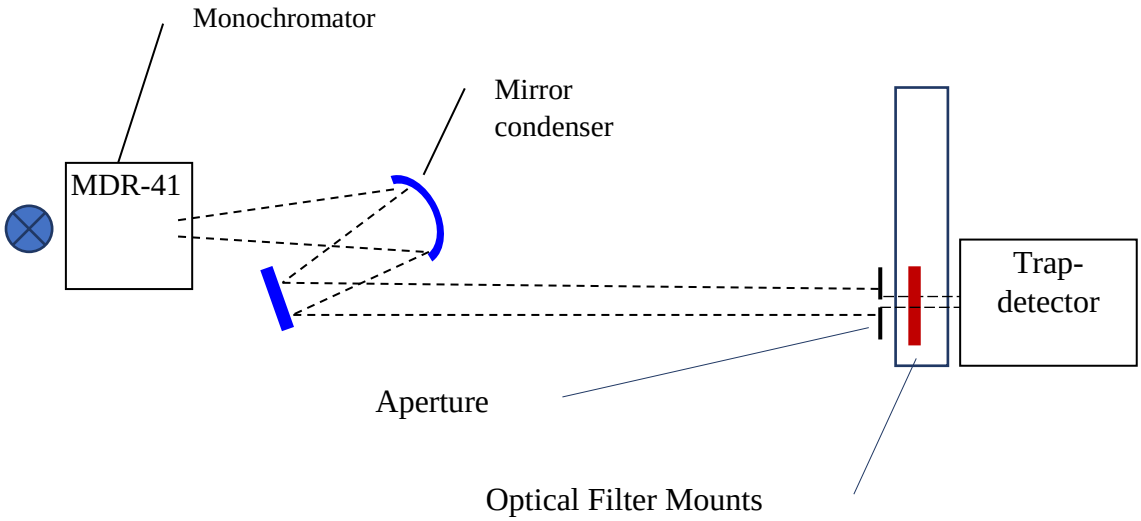

Figure 5.3.7. Setup for measuring the spectral transmittance of the bandpass filter at 900 nm

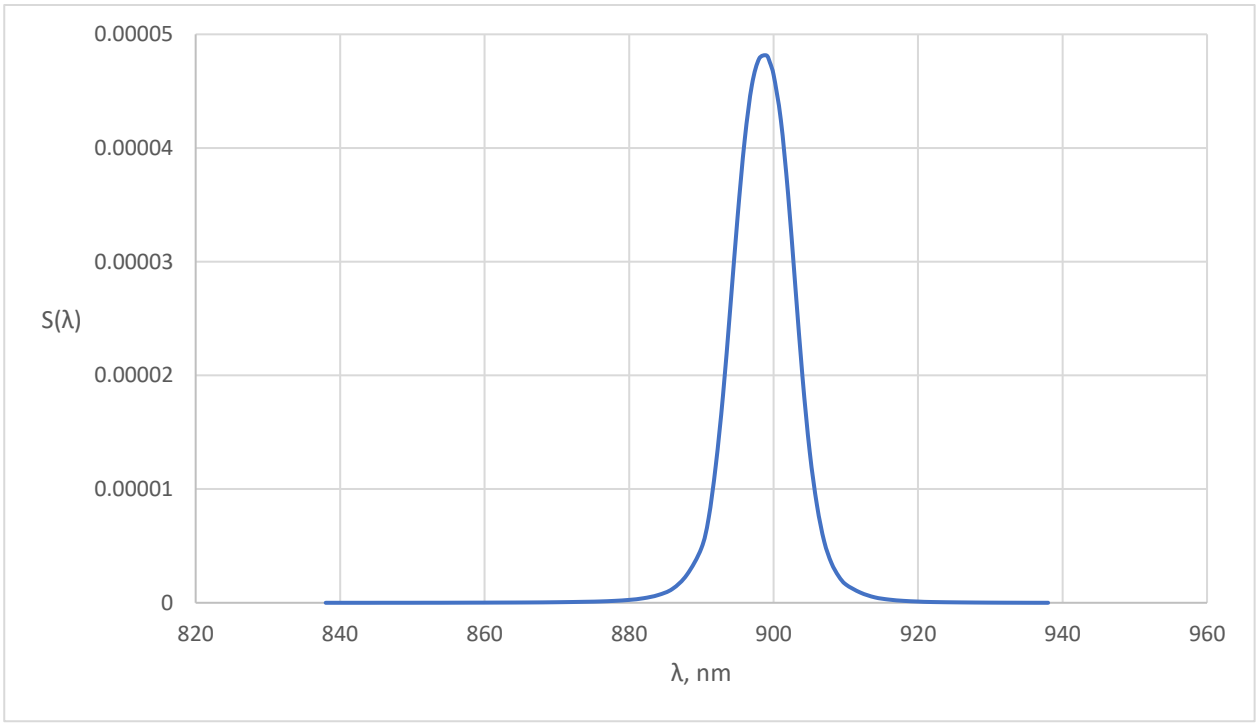

Figure 5.3.8. Spectral responsivity (A×cm^2/mW) of the filter radiometer

5.3.2.3 Measuring the filter radiometer signal and calculating the absolute spectral irradiance.

The signal of the filter radiometer was measured when it was in front of the lamp as it is shown in Figure 5.3.5 at the distance of 500 mm.

The calculation the maximum value of the spectral irradiance of the FEL lamps was performed according to the formulas:

$$I = \int_0^\infty E_{max} \cdot E(\lambda)_{rel} \cdot S(\lambda) d\lambda \,, \tag{5.3.1}$$

$$E_{max} = \frac{I}{\int_0^\infty E(\lambda)_{rel} \cdot S(\lambda) d\lambda} \,, \tag{5.3.2}$$

where I is the signal (current, A) of the filter radiometer, E_{max} is the maximum value of the spectral irradiance of the FEL lamps, $E(\lambda)_{rel}$ is the relative spectral irradiance of the FEL lamps, $S(\lambda)$ is the spectral responsivity of the filter radiometer.

The spectral irradiance of the FEL lamps was calculated from the formula:

$$E(\lambda) = E_{max} \cdot E(\lambda)_{rel} \tag{5.3.3}$$

The values of the spectral irradiance were measured 5 times in each round of the comparisons. The average results are shown in Figure 5.3.9.

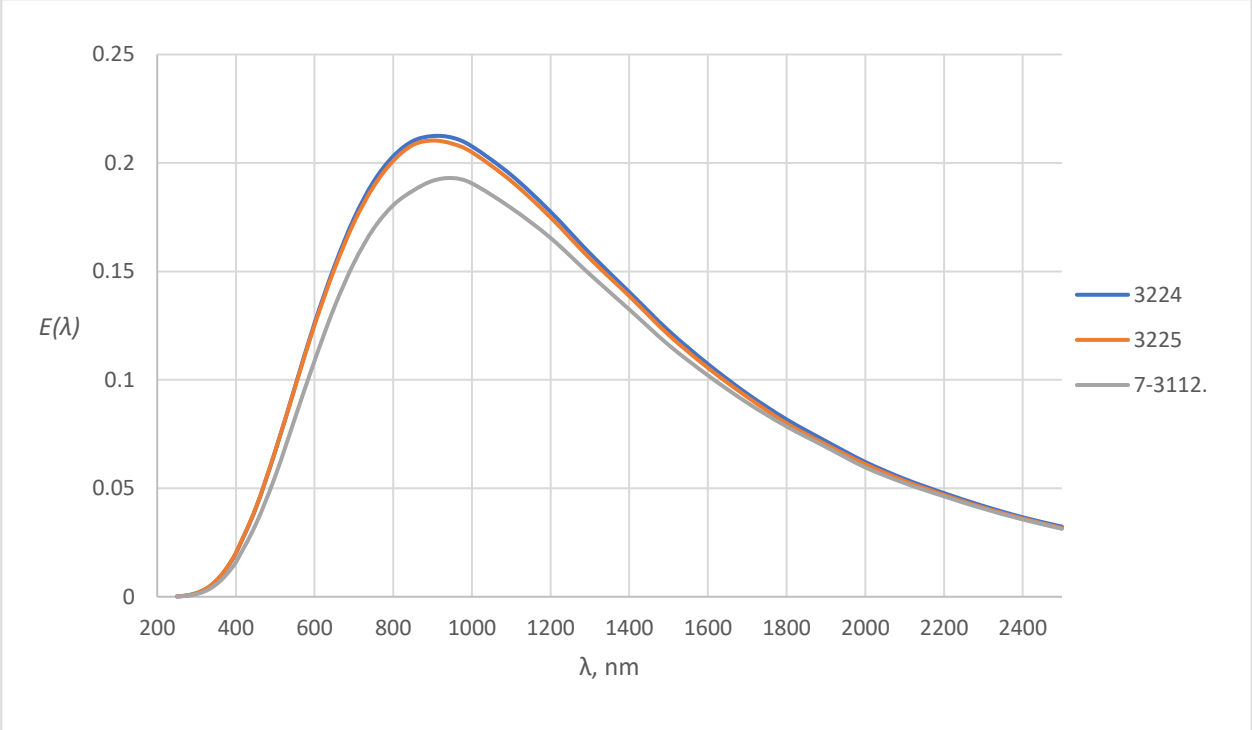

Figure 5.3.9. Graph of spectral irradiance (W/m^2×nm) of the NSC IM lamps

5.3.3. Uncertainty budget

5.3.3.1. Uncertainty budget of the filter radiometer spectral responsivity measurement

The total standard uncertainty of measuring the spectral responsivity of the filter radiometer consists of the components given in Table 5.3.1.

Table 5.3.1. The uncertainty budget of the filter radiometer spectral responsivity measurements

Source of uncertainty	Value, %
Uncertainty of spectral transmittance measurements of the bandpass filter with a nominal value of 900 nm in the range from 838 nm to 938 nm	0.05
Uncertainty of trap-detector calibration measurements in the range from 838 nm to 938 nm	0.10
Uncertainty of measuring the aperture area of the filter radiometer	0.14
Total standard uncertainty	**0.18**

5.3.3.2. Uncertainty budget of FEL lamp spectral irradiance measurement

Table 5.3.2 lists the sources of the relative standard uncertainty of spectral irradiance measurement of the traveling FEL lamps. The Table 5.3.3. presents the type B uncertainty components.

Table 5.3.2. Sources of relative standard uncertainty of spectral irradiance measurements of FEL lamps

Number	Sources of relative standard uncertainty
1	Standard uncertainty of lamp current setting
2	Standard uncertainty of calibration of relative responsivity of the spectrometer
3	Standard uncertainty of spectrometer wavelength setting
4	Stability of the relative spectral responsivity of the spectrometer
5	Standard uncertainty of measurements of relative spectral irradiance in the spectral range of responsivity of the filter radiometer at determination of E_{max}
6	Standard uncertainty of spectral responsivity of the filter radiometer
7	Stability of FEL lamps
8	Standard uncertainty of spectrometer signal measurement
9	Standard uncertainty of filter radiometer signal measurement
10	Standard uncertainty of setting the distance between the aperture of the filter radiometer and the lamp

Table 5.3.3. Type B relative standard uncertainty of FEL lamp spectral irradiance measurement, in %. The numbers in the first line correspond to the sources specified in Table 5.3.2.

λ, nm	**1**	**2**	**3**	**4**	**5**	**6**	**7**	**8**	**9**	**10**	u_B, %
250	0.03	2.051	0.498	0.647	0.01	0.18	0.002	0.023	0.023	0.12	**2.218**
260	0.03	2.031	0.562	0.327	0.01	0.18	0.002	0.023	0.023	0.12	**2.144**
270	0.03	2.028	0.448	0.208	0.01	0.18	0.002	0.023	0.023	0.12	**2.099**
280	0.03	1.519	0.442	0.087	0.01	0.18	0.002	0.023	0.023	0.12	**1.600**
290	0.03	1.019	0.400	0.023	0.01	0.18	0.002	0.023	0.023	0.12	**1.117**
300	0.03	0.448	0.368	0.126	0.01	0.18	0.002	0.023	0.023	0.12	**0.633**
320	0.03	0.493	0.296	0.055	0.01	0.18	0.002	0.023	0.023	0.12	**0.619**
340	0.03	0.458	0.266	0.170	0.01	0.18	0.002	0.023	0.023	0.12	**0.598**
360	0.03	0.458	0.222	0.095	0.01	0.18	0.002	0.023	0.023	0.12	**0.563**
380	0.03	0.542	0.189	0.059	0.01	0.18	0.002	0.023	0.023	0.12	**0.618**
400	0.03	0.486	0.168	0.064	0.01	0.18	0.002	0.023	0.023	0.12	**0.563**
450	0.03	0.406	0.118	0.043	0.01	0.18	0.002	0.023	0.023	0.12	**0.479**
500	0.03	0.367	0.086	0.049	0.01	0.18	0.002	0.023	0.023	0.12	**0.439**
555	0.03	0.372	0.060	0.049	0.01	0.18	0.002	0.023	0.023	0.12	**0.439**
600	0.03	0.306	0.044	0.056	0.01	0.18	0.002	0.023	0.023	0.12	**0.384**
700	0.03	0.254	0.023	0.070	0.01	0.18	0.002	0.023	0.023	0.12	**0.344**
800	0.03	0.238	0.009	0.056	0.01	0.18	0.002	0.023	0.023	0.12	**0.329**
900	0.03	0.195	0.001	0.110	0.01	0.18	0.002	0.023	0.023	0.12	**0.315**
1000	0.03	0.255	0.005	0.109	0.01	0.18	0.002	0.023	0.023	0.12	**0.355**
1100	0.03	0.171	0.008	0.138	0.01	0.18	0.002	0.023	0.023	0.12	**0.312**
1300	0.03	0.225	0.012	0.211	0.01	0.18	0.002	0.023	0.023	0.12	**0.379**
1500	0.03	0.174	0.014	0.231	0.01	0.18	0.002	0.023	0.023	0.12	**0.364**
1700	0.03	0.077	0.014	0.224	0.01	0.18	0.002	0.023	0.023	0.12	**0.324**
2000	0.03	0.165	0.014	0.213	0.01	0.18	0.002	0.023	0.023	0.12	**0.349**
2200	0.03	0.235	0.013	0.234	0.01	0.18	0.002	0.023	0.023	0.12	**0.399**
2300	0.03	0.344	0.013	0.267	0.01	0.18	0.002	0.023	0.023	0.12	**0.489**
2400	0.03	0.389	0.013	0.397	0.01	0.18	0.002	0.023	0.023	0.12	**0.598**
2500	0.03	3.168	0.012	0.569	0.01	0.18	0.002	0.023	0.023	0.12	**3.226**

Uncertainty values type A u_A, % (Uncorrelated effects), type B u_B, % (Correlated effects) and the total standard uncertainty u_c, % (Combined uncertainty, k = 1) are presented in Tables 5.3.4-5.3.6 (the form of the Appendix A.3 of the Technical protocol) separately for each lamp No 3224, No 3225 and No 7-3112, and for each round of measurements.

Table 5.3.4. Uncertainties of measurement of spectral irradiance of the lamp No3224. All uncertainties are standard (k=1)

Wavelength, nm	Round 1			Round 2		
	Uncertainties associated with, %		Combined uncertainty	Uncertainties associated with, %		Combined uncertainty
	Uncorrelated effects	Correlated effects		Uncorrelated effects	Correlated effects	
250	0.106	2.218	2.221	0.114	2.218	2.221
260	0.097	2.144	2.146	0.132	2.144	2.148
270	0.093	2.099	2.101	0.099	2.099	2.101
280	0.095	1.600	1.603	0.085	1.600	1.602
290	0.085	1.117	1.120	0.083	1.117	1.120
300	0.075	0.633	0.638	0.087	0.633	0.639
320	0.070	0.619	0.622	0.079	0.619	0.624
340	0.068	0.598	0.602	0.071	0.598	0.603
360	0.063	0.563	0.567	0.068	0.563	0.567
380	0.065	0.618	0.622	0.067	0.618	0.622
400	0.062	0.563	0.567	0.069	0.563	0.568
450	0.060	0.479	0.483	0.067	0.479	0.484
500	0.064	0.439	0.444	0.068	0.439	0.444
555	0.057	0.439	0.443	0.062	0.439	0.444
600	0.060	0.384	0.389	0.063	0.384	0.389
700	0.075	0.344	0.352	0.075	0.344	0.352
800	0.091	0.329	0.342	0.054	0.329	0.334
900	0.095	0.315	0.329	0.086	0.315	0.326
1000	0.093	0.355	0.367	0.087	0.355	0.365
1100	0.087	0.312	0.324	0.093	0.312	0.326
1300	0.085	0.379	0.389	0.091	0.379	0.390
1500	0.084	0.364	0.374	0.084	0.364	0.374
1700	0.092	0.324	0.337	0.081	0.324	0.334
2000	0.115	0.349	0.367	0.098	0.349	0.362
2200	0.135	0.399	0.421	0.107	0.399	0.413
2300	0.145	0.489	0.510	0.115	0.489	0.502
2400	0.155	0.598	0.618	0.134	0.598	0.613
2500	0.160	3.226	3.230	0.139	3.226	3.229

Table 5.3.5. Uncertainties of measurement of spectral irradiance of the lamp No3225 All uncertainties are standard (k=1)

Wavelength, nm	Round 1			Round 2		
	Uncertainties associated with, %		Combined uncertainty	Uncertainties associated with, %		Combined uncertainty
	Uncorrelated effects	Correlated effects		Uncorrelated effects	Correlated effects	
250	0.118	2.218	2.221	0.121	2.218	2.222
260	0.106	2.144	2.146	0.112	2.144	2.146
270	0.099	2.099	2.101	0.011	2.099	2.099
280	0.098	1.600	1.603	0.093	1.600	1.603
290	0.089	1.117	1.120	0.089	1.117	1.120
300	0.081	0.633	0.639	0.088	0.633	0.640
320	0.078	0.619	0.623	0.086	0.619	0.624
340	0.071	0.598	0.603	0.079	0.598	0.604
360	0.069	0.563	0.568	0.071	0.563	0.568
380	0.072	0.618	0.622	0.070	0.618	0.622
400	0.067	0.563	0.567	0.067	0.563	0.567
450	0.070	0.479	0.484	0.073	0.479	0.485
500	0.066	0.439	0.444	0.078	0.439	0.446
555	0.065	0.439	0.444	0.077	0.439	0.446
600	0.068	0.384	0.390	0.076	0.384	0.392
700	0.065	0.344	0.350	0.069	0.344	0.351
800	0.089	0.329	0.341	0.063	0.329	0.335
900	0.091	0.315	0.327	0.075	0.315	0.323
1000	0.098	0.355	0.368	0.081	0.355	0.364
1100	0.101	0.312	0.328	0.093	0.312	0.326
1300	0.093	0.379	0.391	0.087	0.379	0.389
1500	0.089	0.364	0.375	0.078	0.364	0.373
1700	0.087	0.324	0.336	0.091	0.324	0.337
2000	0.097	0.349	0.362	0.093	0.349	0.361
2200	0.115	0.399	0.415	0.098	0.399	0.411
2300	0.128	0.489	0.505	0.105	0.489	0.500
2400	0.136	0.598	0.613	0.112	0.598	0.609
2500	0.151	3.226	3.230	0.127	3.226	3.229

Table 5.3.6. Uncertainties of measurement of spectral irradiance of the lamp 7-3112 All uncertainties are standard (k=1)

Wavelength, nm	Round 1			Round 2		
	Uncertainties associated with, %		Combined uncertainty	Uncertainties associated with, %		Combined uncertainty
	Uncorrelated effects	Correlated effects		Uncorrelated effects	Correlated effects	
250	0.131	2.218	2.222	0.139	2.218	2.223
260	0.126	2.144	2.147	0.135	2.144	2.148
270	0.117	2.099	2.102	0.127	2.099	2.103
280	0.111	1.600	1.604	0.111	1.600	1.604
290	0.105	1.117	1.122	0.098	1.117	1.121
300	0.101	0.633	0.641	0.093	0.633	0.640
320	0.104	0.619	0.627	0.089	0.619	0.625
340	0.980	0.598	1.148	0.085	0.598	0.604
360	0.087	0.563	0.570	0.093	0.563	0.571
380	0.085	0.618	0.624	0.085	0.618	0.624
400	0.089	0.563	0.570	0.078	0.563	0.569
450	0.084	0.479	0.486	0.083	0.479	0.486
500	0.079	0.439	0.446	0.081	0.439	0.447
555	0.077	0.439	0.446	0.085	0.439	0.447
600	0.076	0.384	0.392	0.085	0.384	0.394
700	0.068	0.344	0.351	0.068	0.344	0.351
800	0.083	0.329	0.340	0.075	0.329	0.338
900	0.084	0.315	0.326	0.089	0.315	0.327
1000	0.089	0.355	0.366	0.078	0.355	0.363
1100	0.100	0.312	0.328	0.089	0.312	0.324
1300	0.097	0.379	0.392	0.094	0.379	0.391
1500	0.093	0.364	0.376	0.085	0.364	0.374
1700	0.086	0.324	0.336	0.099	0.324	0.339
2000	0.094	0.349	0.361	0.088	0.349	0.360
2200	0.106	0.399	0.413	0.104	0.399	0.412
2300	0.118	0.489	0.503	0.123	0.489	0.504
2400	0.127	0.598	0.612	0.138	0.598	0.614
2500	0.143	3.226	3.229	0.141	3.226	3.229

5.4. TÜBİTAK UME. Türkiye

5.4.1. Description of scale realization

The scale was realized with the absolute radiometer (AR) approach. An absolute trap detector, which is traceable to the absolute cryogenic radiometer based optical power scale of TÜBİTAK UME [21-25], is used as a reference detector in order to measure spectral optical power at the output of a double-monochromator system (Bentham DTMc300) equipped with a quartz tungsten halogen lamp (QTH) and a deuterium lamp. Spectral optical power measurements are performed by collimating the output monochromatic radiation via different set optical mirrors and apertures to the trap detector (Figure 5.4.1). A calibrated aperture (0.1 cm^2) is used in front of the trap detector input in order to realize spectral irradiance.

Details of the used double-monochromator and uncertainty budget of the realization are given in Tables 5.4.1 and 5.4.3, respectively. Similar technique is used for calibrating spectral irradiance responsivity of the developed spectroradiometer [26, 27].

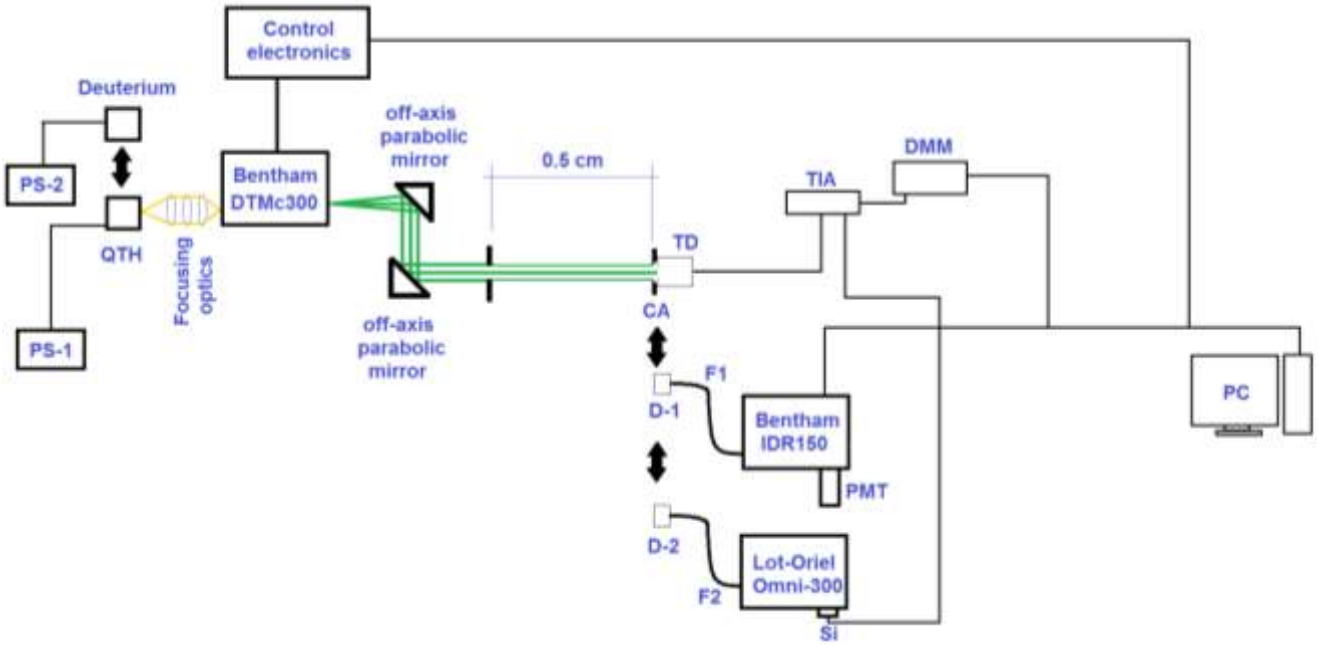

Figure 5.4.1. Realization of detector-based spectral irradiance scale at TÜBİTAK UME. PS-1 and PS-2 are power supplies. QTH is the tungsten halogen lamp (250 W). TD is the trap detector. CA is the calibrated aperture. D-1 and D-2 are end-on precision cosine-corrected diffusers (Bentham - DIFFD7). F1 and F2 are UV grade fused silica fiber bundles (Bentham - FOP-UV-4-1000). PMT is the photomultiplier tube. Si is the UV enhanced silicon detector. TIA is the transimpedance amplifier. DMM is the digital multimeter and PC is the personal computer

Table 5.4.1. Double-monochromator used for realization of spectral irradiance scale at TÜBİTAK UME.

Type	Aperture ratio:	Slit width & height:	Grating 1 spectral range:	Grating 2 spectral range:	Grating 3 spectral range:
Bentham-DTMc300	f/4.1	10µm-10mm (W) x 20mm (H)	(200 - 600) nm. Ruled. 2400 g/mm. blaze at 250 nm	(300 - 1200) nm Ruled. 1200 g/mm. blaze@500 nm	(600 - 1800) nm Ruled. 830 g/mm. blaze@1200 nm

Then the trap detector and aperture removed from the measurement setup and transfer standard spectroradiometers (UV and VIS-NIR) are placed in turn in order to obtain their spectral irradiance responsivities (Figure 5.4.1). Spectroradiometers are equipped with end-on precision cosine-corrected diffusers (Bentham - DIFFD7) and UV grade fused silica fiber bundle (Bentham - FOP-UV-4-1000). Details of the used spectroradiometers and uncertainty budget of the calibration of transfer standards are given in Table 5.4.2 and 5.4.4. respectively.

Table 5.4.2. Transfer standard spectroradiometers.

Spectro-radiometer	Type	Aperture ratio:	Slit width & height:	Grating 1 spectral range:	Grating 2 spectral range:
1	Bentham IDR150	f/4	10µm-10mm (W) x 20mm (H)	(200 - 600) nm. Ruled. 2400 g/mm. blaze at 300 nm	
2	Lot-Oriel Omni-300	f/4	10µm-10mm (W) x 20mm (H)	(200 - 1100) nm. Ruled. 1200 g/mm. blaze at 440 nm	(650 - 2200) nm. Ruled. 600 g/mm. blaze at 1000 nm

5.4.2. Description of measurement facility and procedure

The measurement facility diagram and photo are shown below in Figure 5.4.2 and Figure 5.4.3, respectively.

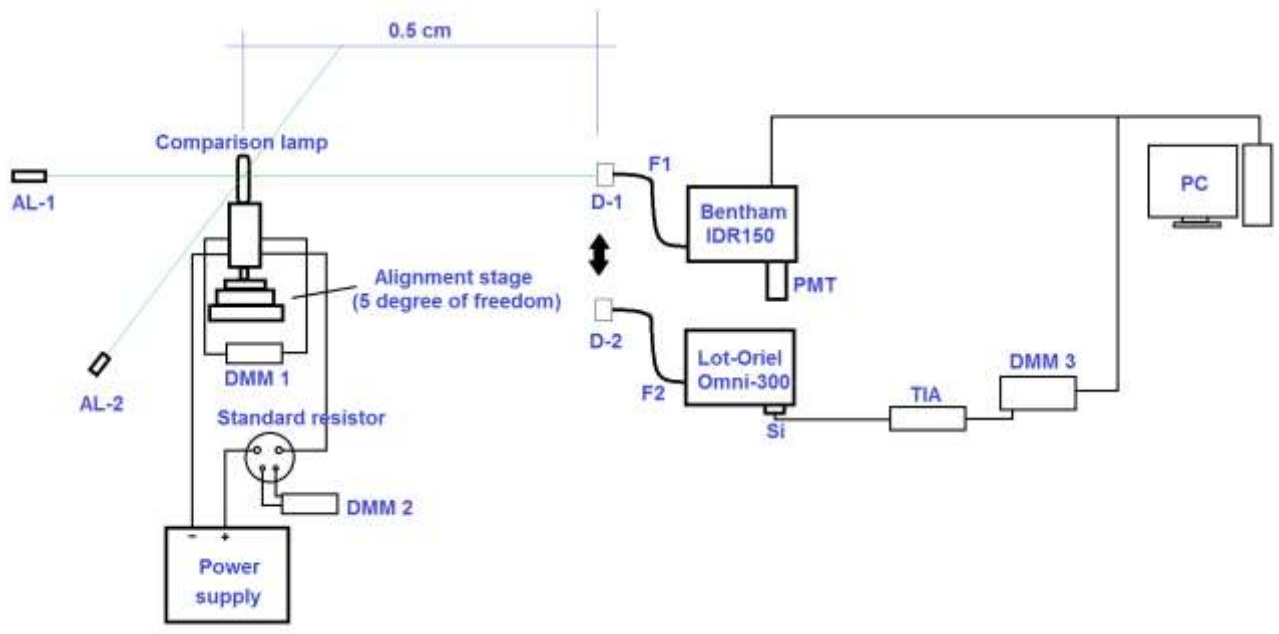

Figure 5.4.2. Lamp spectral irradiance measurement setup

Each of lamp (LAMP 352, LAMP 351 and LAMP 349) was fixed to the lamp holder, which had 5 degrees of freedom alignment capability. Two laser diodes were used in order to align vertical and horizontal positions of lamp filament according to the comparison protocol. The alignment process is shown in Figure 5.4.4.

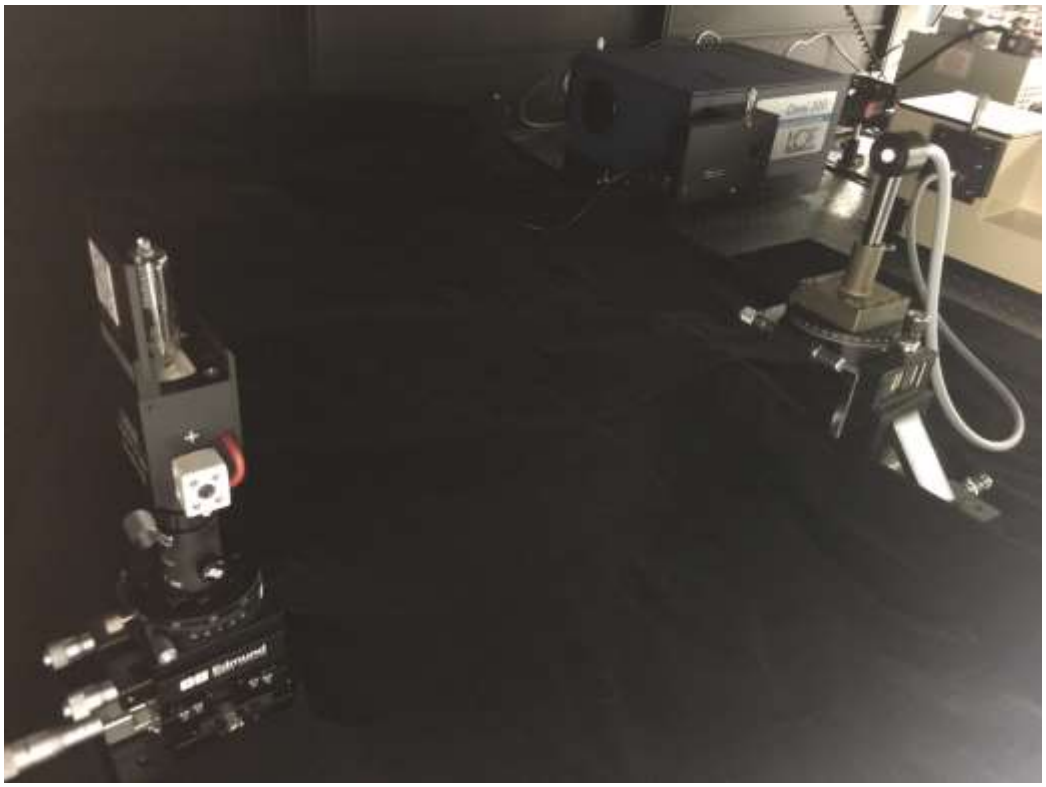

Figure 5.4.3. A photograph showing the lamp measurement setup

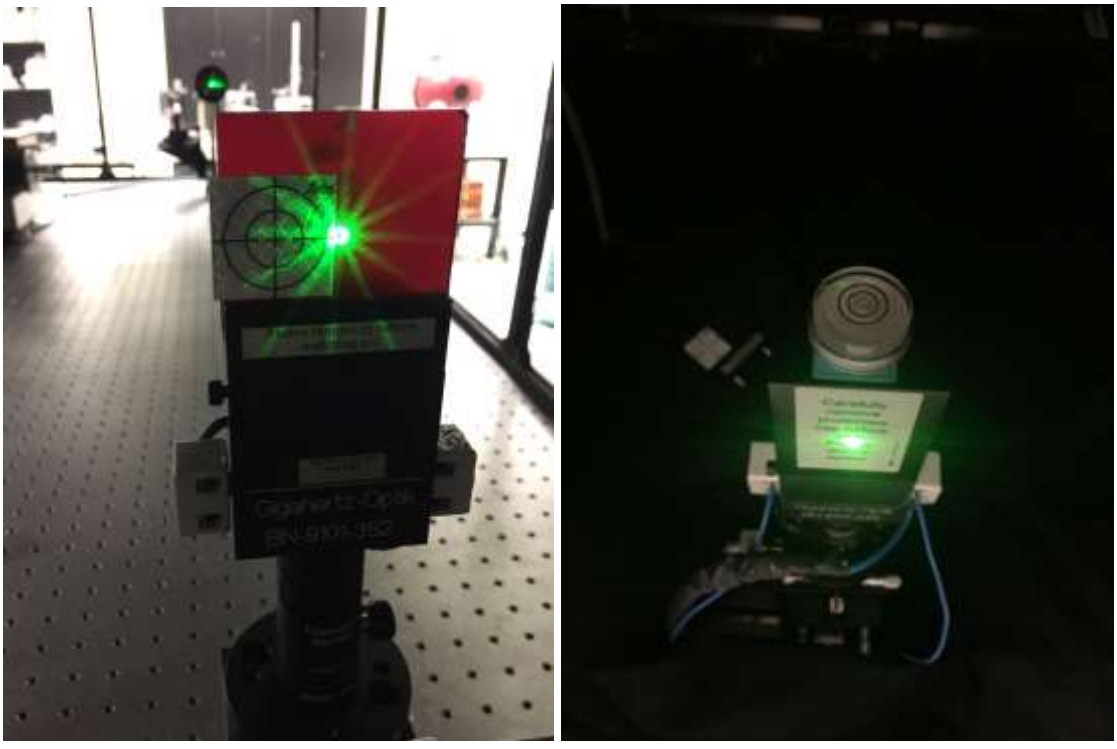

Figure 5.4.4. Photographs showing the alignment of the lamp filament

The distance between the reference plane of the diffuser and the lamp was aligned to 0.5 m with a calibrated distance measurement instrument (Figure 5.4.5).

Figure 5.4.5. Photographs showing the distance measurement

Electrical connection of the lamp was performed according to the comparison protocol. A DC power supply (Heizinger PTN55. 250-10) was used to operate the lamps. A calibrated shunt resistor (Guildline. 9230/100) and digital multimeters (Agilent. 3458A) were used for obtaining the lamp current and voltage. Each lamp was operated at the same fixed electrical current of 8.100 A. The spectral irradiance measurement of each lamp was performed after warm-up time (approx. 15 min).

5.4.3. Uncertainty budget

Uncertainty budget of spectral irradiance the comparison lamp measurements, performed at TÜBİTAK UME, is given in Table 5.4.5. Table 5.4.3 and Table 5.4.4 present the uncertainty budgets of the scale realisation and the uncertainty budget of calibration of the transfer standard spectroradiometers, respectively.

Table 5.4.6 presents the uncertainty values submitted to the pilot together with the spectral irradiance values. Uncertainties are the same for all lamps and both rounds.

Table 5.4.3. Uncertainty budget of the realization of spectral irradiance scale at TÜBİTAK UME

		Relative standard uncertainty, %																			
		at wavelengths																			
	Source of uncertainty	**250**	**260**	**270**	**280**	**290**	**300**	**320**	**340**	**360**	**380**	**400**	**450**	**500**	**555**	**600**	**700**	**800**	**900**	**1000**	**1100**
1	trap detector responsivity	1.25	1.25	1.25	1.25	1.25	1.05	1.05	1.05	0.75	0.75	0.75	0.75	0.75	0.75	0.75	0.75	0.75	0.75	0.75	0.75
2	aperture area	0.01	0.01	0.01	0.01	0.01	0.01	0.01	0.01	0.01	0.01	0.01	0.01	0.01	0.01	0.01	0.01	0.01	0.01	0.01	0.01
3	transimpedance amplifier	0.005	0.005	0.005	0.005	0.005	0.005	0.005	0.005	0.005	0.005	0.005	0.005	0.005	0.005	0.005	0.005	0.005	0.005	0.005	0.005
4	digital multimeter	0.0004	0.0004	0.0004	0.0004	0.0004	0.0004	0.0004	0.0004	0.0004	0.0004	0.0004	0.0004	0.0004	0.0004	0.0004	0.0004	0.0004	0.0004	0.0004	0.0004
5	photocurrent measurements	0.35	0.32	0.31	0.31	0.31	0.27	0.27	0.25	0.23	0.22	0.19	0.19	0.16	0.16	0.16	0.16	0.17	0.19	0.19	0.19
6	interreflections	0.35	0.32	0.29	0.26	0.21	0.18	0.16	0.13	0.12	0.12	0.03	0.02	0.02	0.02	0.02	0.02	0.02	0.02	0.02	0.02
7	alignment repeatability	0.25	0.25	0.25	0.25	0.25	0.25	0.25	0.25	0.25	0.25	0.25	0.25	0.25	0.25	0.25	0.25	0.25	0.25	0.25	0.25
8	repeatability	0.12	0.12	0.12	0.12	0.12	0.12	0.12	0.12	0.12	0.12	0.12	0.12	0.12	0.12	0.12	0.12	0.12	0.12	0.12	0.12
9	wavelength	0.04	0.04	0.04	0.04	0.03	0.03	0.03	0.03	0.03	0.03	0.03	0.02	0.02	0.02	0.02	0.01	0.01	0.01	0.01	0.01
10	straylight	0.01	0.01	0.01	0.01	0.01	0.01	0.01	0.01	0.01	0.01	0.01	0.01	0.01	0.01	0.01	0.01	0.01	0.01	0.01	0.01
11	diffraction	0.03	0.03	0.03	0.03	0.03	0.03	0.03	0.03	0.03	0.03	0.03	0.03	0.03	0.03	0.03	0.03	0.03	0.03	0.03	0.03
	combined standard uncertainty	**1.37**	**1.36**	**1.35**	**1.34**	**1.33**	**1.13**	**1.13**	**1.12**	**0.84**	**0.84**	**0.82**	**0.82**	**0.82**	**0.82**	**0.82**	**0.82**	**0.82**	**0.82**	**0.82**	**0.82**
	expanded uncertainty (k=2)	**2.7**	**2.7**	**2.7**	**2.7**	**2.7**	**2.3**	**2.3**	**2.2**	**1.7**	**1.7**	**1.6**	**1.6**	**1.6**	**1.6**	**1.6**	**1.6**	**1.6**	**1.6**	**1.6**	**1.6**

Table 5.4.4. Uncertainty budget of calibration of transfer standard spectroradiometers at TÜBİTAK UME

		Relative standard uncertainty, %																		
		at wavelengths																		
	Source of uncertainty	**250**	**260**	**270**	**280**	**290**	**300**	**320**	**340**	**360**	**380**	**400**	**450**	**500**	**555**	**600**	**700**	**800**	**900**	**1000**	**1100**
1	spectral irradiance scale	1.37	1.36	1.35	1.34	1.33	1.13	1.13	1.12	0.84	0.84	0.82	0.82	0.82	0.82	0.82	0.82	0.82	0.82	0.82	0.82
2	reference signal	0.35	0.32	0.31	0.31	0.31	0.27	0.27	0.25	0.23	0.22	0.19	0.19	0.16	0.16	0.16	0.16	0.17	0.19	0.19	0.19
3	transfer standard signal	0.38	0.35	0.33	0.33	0.33	0.29	0.29	0.27	0.25	0.24	0.21	0.21	0.17	0.17	0.17	0.17	0.18	0.21	0.21	0.21
4	reference plane alignment	0.23	0.23	0.23	0.23	0.23	0.23	0.23	0.23	0.23	0.23	0.23	0.23	0.23	0.23	0.23	0.23	0.23	0.23	0.23	0.23
5	alignment repeatability	0.25	0.25	0.25	0.25	0.25	0.25	0.25	0.25	0.25	0.25	0.25	0.25	0.25	0.25	0.25	0.25	0.25	0.25	0.25	0.25
6	measurement repeatability	0.13	0.13	0.13	0.13	0.13	0.13	0.13	0.13	0.13	0.13	0.13	0.13	0.13	0.13	0.13	0.13	0.13	0.13	0.13	0.13
7	wavelength	0.04	0.04	0.04	0.04	0.03	0.03	0.03	0.03	0.03	0.03	0.03	0.02	0.02	0.02	0.02	0.01	0.01	0.01	0.01	0.01
8	straylight	0.01	0.01	0.01	0.01	0.01	0.01	0.01	0.01	0.01	0.01	0.01	0.01	0.01	0.01	0.01	0.01	0.01	0.01	0.01	0.01
	combined standard uncertainty	**1.51**	**1.48**	**1.47**	**1.47**	**1.46**	**1.26**	**1.25**	**1.24**	**0.98**	**0.97**	**0.94**	**0.94**	**0.92**	**0.92**	**0.92**	**0.92**	**0.93**	**0.94**	**0.94**	**0.94**
	expanded uncertainty (k=2)	**3.0**	**3.0**	**2.9**	**2.9**	**2.9**	**2.5**	**2.5**	**2.5**	**2.0**	**1.9**	**1.9**	**1.9**	**1.8**	**1.8**	**1.8**	**1.8**	**1.9**	**1.9**	**1.9**	**1.9**

Table 5.4.5. Uncertainty budget of spectral irradiance comparison lamps measurements performed at TÜBİTAK UME

		Relative standard uncertainty, %																			
		at wavelengths																			
	Source of uncertainty	250	260	270	280	290	300	320	340	360	380	400	450	500	555	600	700	800	900	1000	1100
1	spectral irradiance scale	1.51	1.48	1.47	1.47	1.46	1.26	1.25	1.24	0.98	0.97	0.94	0.94	0.92	0.92	0.92	0.92	0.93	0.94	0.94	0.94
2	distance (50 cm)	0.05	0.05	0.05	0.05	0.05	0.05	0.05	0.05	0.05	0.05	0.05	0.05	0.05	0.05	0.05	0.05	0.05	0.05	0.05	0.05
3	lamp current stability	0.035	0.035	0.035	0.035	0.035	0.035	0.035	0.035	0.035	0.035	0.035	0.035	0.035	0.035	0.035	0.035	0.035	0.035	0.035	0.035
4	signal measurement	0.38	0.35	0.34	0.33	0.33	0.29	0.29	0.27	0.24	0.23	0.20	0.20	0.17	0.17	0.17	0.17	0.18	0.20	0.20	0.20
5	alignment repeatability	0.30	0.30	0.30	0.30	0.30	0.30	0.30	0.30	0.30	0.30	0.30	0.30	0.30	0.30	0.30	0.30	0.30	0.30	0.30	0.30
6	measurement repeatability	0.36	0.35	0.35	0.33	0.34	0.33	0.30	0.30	0.30	0.30	0.28	0.28	0.28	0.28	0.28	0.28	0.28	0.28	0.28	0.28
	Uncorrelated	**0.61**	**0.58**	**0.57**	**0.56**	**0.56**	**0.53**	**0.51**	**0.50**	**0.49**	**0.48**	**0.46**	**0.46**	**0.44**	**0.44**	**0.44**	**0.44**	**0.45**	**0.46**	**0.46**	**0.46**
	Correlated	**1.51**	**1.48**	**1.47**	**1.47**	**1.46**	**1.26**	**1.25**	**1.24**	**0.98**	**0.97**	**0.94**	**0.94**	**0.93**	**0.93**	**0.93**	**0.93**	**0.93**	**0.94**	**0.94**	**0.94**
	combined standard uncertainty	**1.63**	**1.59**	**1.58**	**1.57**	**1.56**	**1.36**	**1.36**	**1.34**	**1.09**	**1.09**	**1.05**	**1.05**	**1.03**	**1.03**	**1.03**	**1.03**	**1.03**	**1.05**	**1.05**	**1.05**
	expanded uncertainty (k=2)	**3.3**	**3.2**	**3.2**	**3.1**	**3.1**	**2.7**	**2.7**	**2.7**	**2.2**	**2.2**	**2.1**	**2.1**	**2.1**	**2.1**	**2.1**	**2.1**	**2.1**	**2.1**	**2.1**	**2.1**

Table 5.4.6. Uncertainties of TÜBİTAK UME measurement of spectral irradiance of the FEL lamps. All uncertainties are standard (k=1)

Wavelength. nm	Uncertainties associated with. %		Combined uncertainty
	Uncorrelated effects	Correlated effects	
250	0.61	1.51	1.63
260	0.58	1.48	1.59
270	0.57	1.47	1.58
280	0.56	1.47	1.57
290	0.56	1.46	1.56
300	0.53	1.26	1.37
320	0.51	1.25	1.35
340	0.50	1.24	1.34
360	0.49	0.98	1.10
380	0.48	0.97	1.08
400	0.46	0.94	1.05
450	0.46	0.94	1.05
500	0.44	0.93	1.03
555	0.44	0.93	1.03
600	0.44	0.93	1.03
700	0.44	0.93	1.03
800	0.45	0.93	1.03
900	0.46	0.94	1.05
1000	0.46	0.94	1.05
1100	0.46	0.94	1.05

6. Measurement results

This section presents Spectral Irradiance values, reported by participants for their lamps and that obtained by the pilot.

6.1. BelGIM lamps data

BelGIM calibrated three traveling lamps: BN-9101-674 BN-9101-675 and BN-9101-692.

BelGIM was able to calibrate the lamps in a limited spectral range: from 250 nm to 1000 nm in the Round 1 and from 250 nm to 1100 nm in the Round 2.

Table 6.1.1. Spectral Irradiance of BelGIM lamp **BN-9101-674**

Wave-length, nm	BelGIM Data						Pilot Data
	Round 1			Round 2			
	Spectral Irradiance $E_{\mathrm{Bel},674,1}$ W m^{-2} nm^{-1}	Correlated uncertainty $u_{\mathrm{corr}}(E_{\mathrm{Bel},674,1})$ %	Uncorrelated uncertainty $u_{\mathrm{uncorr}}(E_{\mathrm{Bel},674,1})$ %	Spectral Irradiance $(E_{\mathrm{Bel},674,2})$ W m^{-2} nm^{-1}	Correlated uncertainty $u_{\mathrm{corr}}(E_{\mathrm{Bel},674,2})$ %	Uncorrelated uncertainty $u_{\mathrm{uncorr}}(E_{\mathrm{Bel},674,2})$ %	Spectral Irradiance $E_{\mathrm{p},674}$ W m^{-2} nm^{-1}
250	2.196E-04	3.78	4.00	2.207E-04	3.78	4.00	2.220E-04
260	3.869E-04	1.33	2.69	3.869E-04	1.33	2.69	3.862E-04
270	6.227E-04	1.67	2.67	6.270E-04	1.67	2.67	6.344E-04
280	1.002E-03	1.42	2.58	9.901E-04	1.42	2.58	9.887E-04
290	1.483E-03	0.30	1.47	1.478E-03	0.30	1.47	1.475E-03
300	2.119E-03	0.25	1.28	2.120E-03	0.25	1.28	2.123E-03
320	4.028E-03	0.24	1.12	4.031E-03	0.24	1.12	4.035E-03
340	6.916E-03	0.23	1.08	6.919E-03	0.23	1.08	6.933E-03
360	1.096E-02	0.22	1.03	1.097E-02	0.22	1.03	1.102E-02
380	1.640E-02	0.21	0.93	1.639E-02	0.21	0.93	1.643E-02
400	2.320E-02	0.20	0.88	2.319E-02	0.20	0.88	2.321E-02
450	4.554E-02	0.19	0.83	4.558E-02	0.19	0.83	4.562E-02
500	7.367E-02	0.19	0.80	7.374E-02	0.19	0.80	7.386E-02
555	1.038E-01	0.19	0.78	1.039E-01	0.19	0.78	1.076E-01
600	1.340E-01	0.19	0.80	1.338E-01	0.19	0.80	1.342E-01
700	1.813E-01	0.19	0.83	1.813E-01	0.19	0.83	1.818E-01
800	2.060E-01	0.19	0.86	2.061E-01	0.19	0.86	2.082E-01
900	2.140E-01	0.19	0.88	2.141E-01	0.19	0.88	2.155E-01
1000	2.134E-01	0.21	1.01	2.107E-01	0.21	1.01	2.093E-01
1100		0.17	1.24	2.074E-01	0.17	1.24	1.956E-01

Table 6.1.2. Spectral Irradiance of BelGIM lamp **BN-9101-675**

Wave-length, nm	BelGIM Data						Pilot Data
	Round 1			Round 2			
	Spectral Irradiance $E_{\mathrm{Bel},675,1}$ W m^{-2} nm^{-1}	Correlated uncertainty $u_{\mathrm{corr}}(E_{\mathrm{Bel},675,1})$ %	Uncorrelated uncertainty $u_{\mathrm{uncorr}}(E_{\mathrm{Bel},675,1})$ %	Spectral Irradiance $(E_{\mathrm{Bel},675,2})$ W m^{-2} nm^{-1}	Correlated uncertainty $u_{\mathrm{corr}}(E_{\mathrm{Bel},675,2})$ %	Uncorrelated uncertainty $u_{\mathrm{uncorr}}(E_{\mathrm{Bel},675,2})$ %	Spectral Irradiance $E_{\mathrm{p},675}$ W m^{-2} nm^{-1}
250	1.920E-04	3.78	4.00	1.929E-04	3.78	4.00	1.944E-04
260	3.377E-04	1.33	2.69	3.376E-04	1.33	2.69	3.398E-04
270	5.498E-04	1.67	2.67	5.535E-04	1.67	2.67	5.587E-04
280	8.807E-04	1.42	2.58	8.704E-04	1.42	2.58	8.709E-04
290	1.306E-03	0.30	1.47	1.301E-03	0.30	1.47	1.303E-03
300	1.882E-03	0.25	1.28	1.883E-03	0.25	1.28	1.887E-03
320	3.602E-03	0.24	1.12	3.605E-03	0.24	1.12	3.608E-03
340	6.265E-03	0.23	1.08	6.267E-03	0.23	1.08	6.257E-03
360	9.988E-03	0.22	1.03	9.988E-03	0.22	1.03	1.002E-02
380	1.501E-02	0.21	0.93	1.500E-02	0.21	0.93	1.504E-02
400	2.132E-02	0.20	0.88	2.131E-02	0.20	0.88	2.136E-02
450	4.228E-02	0.19	0.83	4.232E-02	0.19	0.83	4.261E-02
500	6.955E-02	0.19	0.80	6.961E-02	0.19	0.80	6.980E-02
555	9.925E-02	0.19	0.78	9.930E-02	0.19	0.78	1.028E-01
600	1.288E-01	0.19	0.80	1.287E-01	0.19	0.80	1.293E-01
700	1.770E-01	0.19	0.83	1.769E-01	0.19	0.83	1.774E-01
800	1.985E-01	0.19	0.86	1.965E-01	0.19	0.86	2.052E-01
900	2.124E-01	0.19	0.88	2.123E-01	0.19	0.88	2.139E-01
1000	2.019E-01	0.21	1.01	2.005E-01	0.21	1.01	2.088E-01
1100		0.17	1.24	1.975E-01	0.17	1.24	1.957E-01

Table 6.1.3. Spectral Irradiance of BelGIM lamp **BN-9101-692**

Wave-length, nm	BelGIM Data						Pilot Data
	Round 1			Round 2			
	Spectral Irradiance $E_{\mathrm{Bel},692,1}$ W m^{-2} nm^{-1}	Correlated uncertainty $u_{\mathrm{corr}}\left(E_{\mathrm{Bel},692,1}\right)$ %	Uncorrelated uncertainty $u_{\mathrm{uncorr}}\left(E_{\mathrm{Bel},692,1}\right)$ %	Spectral Irradiance $\left(E_{\mathrm{Bel},692,2}\right)$ W m^{-2} nm^{-1}	Correlated uncertainty $u_{\mathrm{corr}}\left(E_{\mathrm{Bel},692,2}\right)$ %	Uncorrelated uncertainty $u_{\mathrm{uncorr}}\left(E_{\mathrm{Bel},692,2}\right)$ %	Spectral Irradiance $E_{\mathrm{p},692}$ W m^{-2} nm^{-1}
250	1.354E-04	3.78	4.00	1.361E-04	3.78	4.00	1.401E-04
260	2.431E-04	1.33	2.69	2.431E-04	1.33	2.69	2.496E-04
270	4.118E-04	1.67	2.67	4.145E-04	1.67	2.67	4.191E-04
280	6.583E-04	1.42	2.58	6.596E-04	1.42	2.58	6.539E-04
290	1.007E-03	0.30	1.47	1.004E-03	0.30	1.47	1.008E-03
300	1.465E-03	0.25	1.28	1.466E-03	0.25	1.28	1.476E-03
320	2.865E-03	0.24	1.12	2.866E-03	0.24	1.12	2.885E-03
340	5.057E-03	0.23	1.08	5.059E-03	0.23	1.08	5.095E-03
360	8.239E-03	0.22	1.03	8.243E-03	0.22	1.03	8.298E-03
380	1.261E-02	0.21	0.93	1.260E-02	0.21	0.93	1.265E-02
400	1.817E-02	0.20	0.88	1.816E-02	0.20	0.88	1.821E-02
450	3.716E-02	0.19	0.83	3.719E-02	0.19	0.83	3.734E-02
500	6.225E-02	0.19	0.80	6.230E-02	0.19	0.80	6.258E-02
555	9.041E-02	0.19	0.78	9.043E-02	0.19	0.78	9.394E-02
600	1.190E-01	0.19	0.80	1.189E-01	0.19	0.80	1.196E-01
700	1.664E-01	0.19	0.83	1.666E-01	0.19	0.83	1.675E-01
800	1.942E-01	0.19	0.86	1.944E-01	0.19	0.86	1.963E-01
900	2.051E-01	0.19	0.88	2.052E-01	0.19	0.88	2.063E-01
1000	2.006E-01	0.21	1.01	2.009E-01	0.21	1.01	2.022E-01
1100		0.17	1.24	1.940E-01	0.17	1.24	1.901E-01

6.2. NSC IM lamps data

NSC IM traveling lamps: BN-9101-639, BN-9101-640 and BN-9101-641.

Table 6.2.1. Spectral Irradiance of NSC IM lamp **No 3224**

Wave-length, nm	NSC IM Data						Pilot Data
	Round 1			Round 2			
	Spectral Irradiance $E_{\mathrm{IM},3224,1}$ W m^{-2} nm^{-1}	Correlated uncertainty $u_{\mathrm{corr}}(E_{\mathrm{IM},3224,1})$ %	Uncorrelated uncertainty $u_{\mathrm{uncorr}}(E_{\mathrm{IM},3224,1})$ %	Spectral Irradiance $E_{\mathrm{IM},3224,2}$ W m^{-2} nm^{-1}	Correlated uncertainty $u_{\mathrm{corr}}(E_{\mathrm{IM},3224,2})$ %	Uncorrelated uncertainty $u_{\mathrm{uncorr}}(E_{\mathrm{IM},3224,2})$ %	Spectral Irradiance $E_{\mathrm{p},3224}$ W m^{-2} nm^{-1}
250	1.668E-04	2.22	0.11	1.695E-04	2.22	0.11	1.842E-04
260	2.926E-04	2.14	0.10	2.971E-04	2.14	0.13	3.187E-04
270	4.860E-04	2.10	0.09	4.929E-04	2.10	0.10	5.242E-04
280	7.488E-04	1.60	0.10	7.572E-04	1.60	0.09	8.017E-04
290	1.154E-03	1.12	0.09	1.165E-03	1.12	0.08	1.230E-03
300	1.681E-03	0.63	0.08	1.695E-03	0.63	0.09	1.786E-03
320	3.222E-03	0.62	0.07	3.248E-03	0.62	0.08	3.447E-03
340	5.689E-03	0.60	0.07	5.735E-03	0.60	0.07	6.008E-03
360	9.258E-03	0.56	0.06	9.325E-03	0.56	0.07	9.677E-03
380	1.402E-02	0.62	0.07	1.412E-02	0.62	0.07	1.458E-02
400	1.998E-02	0.56	0.06	2.011E-02	0.56	0.07	2.082E-02
450	4.037E-02	0.48	0.06	4.065E-02	0.48	0.07	4.183E-02
500	6.685E-02	0.44	0.06	6.730E-02	0.44	0.07	6.896E-02
555	9.939E-02	0.44	0.06	9.999E-02	0.44	0.06	1.021E-01
600	1.258E-01	0.38	0.06	1.265E-01	0.38	0.06	1.286E-01
700	1.740E-01	0.34	0.08	1.747E-01	0.34	0.08	1.772E-01
800	2.027E-01	0.33	0.09	2.035E-01	0.33	0.05	2.050E-01
900	2.120E-01	0.32	0.10	2.127E-01	0.32	0.09	2.135E-01
1000	2.073E-01	0.36	0.09	2.080E-01	0.36	0.09	2.079E-01
1100	1.941E-01	0.31	0.09	1.947E-01	0.31	0.09	1.942E-01
1300	1.580E-01	0.38	0.09	1.586E-01	0.38	0.09	1.577E-01
1500	1.225E-01	0.36	0.08	1.229E-01	0.36	0.08	1.222E-01
1700	9.346E-02	0.32	0.09	9.372E-02	0.32	0.08	9.311E-02
2000	6.206E-02	0.35	0.12	6.224E-02	0.35	0.10	6.176E-02
2200	4.772E-02	0.40	0.14	4.789E-02	0.40	0.11	4.727E-02
2300	4.178E-02	0.49	0.15	4.194E-02	0.49	0.12	4.147E-02
2400	3.660E-02	0.60	0.16	3.670E-02	0.60	0.13	3.635E-02
2500	3.225E-02	3.23	0.16	3.239E-02	3.23	0.14	3.220E-02

Table 6.2.2. Spectral Irradiance of NSC IM lamp **No 3225**

Wave-length, nm	NSC IM Data						Pilot Data
	Round 1			Round 2			
	Spectral Irradiance $E_{\mathrm{IM},3225,1}$ W m^{-2} nm^{-1}	Correlated uncertainty $u_{\mathrm{corr}}(E_{\mathrm{IM},3225,1})$ %	Uncorrelated uncertainty $u_{\mathrm{uncorr}}(E_{\mathrm{IM},3225,1})$ %	Spectral Irradiance $E_{\mathrm{IM},3225,2}$ W m^{-2} nm^{-1}	Correlated uncertainty $u_{\mathrm{corr}}(E_{\mathrm{IM},3225,2})$ %	Uncorrelated uncertainty $u_{\mathrm{uncorr}}(E_{\mathrm{IM},3225,2})$ %	Spectral Irradiance $E_{\mathrm{p},3225}$ W m^{-2} nm^{-1}
250	1.654E-04	2.22	0.12	1.684E-04	2.22	0.12	1.840E-04
260	2.959E-04	2.14	0.11	3.011E-04	2.14	0.11	3.250E-04
270	4.947E-04	2.10	0.10	5.023E-04	2.10	0.01	5.398E-04
280	7.452E-04	1.60	0.10	7.540E-04	1.60	0.09	8.054E-04
290	1.177E-03	1.12	0.09	1.188E-03	1.12	0.09	1.269E-03
300	1.713E-03	0.63	0.08	1.730E-03	0.63	0.09	1.845E-03
320	3.278E-03	0.62	0.08	3.308E-03	0.62	0.09	3.549E-03
340	5.777E-03	0.60	0.07	5.826E-03	0.60	0.08	6.170E-03
360	9.377E-03	0.56	0.07	9.452E-03	0.56	0.07	9.907E-03
380	1.416E-02	0.62	0.07	1.427E-02	0.62	0.07	1.491E-02
400	2.016E-02	0.56	0.07	2.032E-02	0.56	0.07	2.122E-02
450	4.052E-02	0.48	0.07	4.083E-02	0.48	0.07	4.244E-02
500	6.695E-02	0.44	0.07	6.744E-02	0.44	0.08	6.965E-02
555	9.903E-02	0.44	0.07	9.971E-02	0.44	0.08	1.027E-01
600	1.248E-01	0.38	0.07	1.256E-01	0.38	0.08	1.291E-01
700	1.721E-01	0.34	0.07	1.729E-01	0.34	0.07	1.770E-01
800	2.005E-01	0.33	0.09	2.014E-01	0.33	0.06	2.041E-01
900	2.099E-01	0.32	0.09	2.107E-01	0.32	0.08	2.119E-01
1000	2.046E-01	0.36	0.10	2.053E-01	0.36	0.08	2.060E-01
1100	1.913E-01	0.31	0.10	1.920E-01	0.31	0.09	1.921E-01
1300	1.556E-01	0.38	0.09	1.562E-01	0.38	0.09	1.554E-01
1500	1.205E-01	0.36	0.09	1.210E-01	0.36	0.08	1.202E-01
1700	9.194E-02	0.32	0.09	9.224E-02	0.32	0.09	9.141E-02
2000	6.099E-02	0.35	0.10	6.123E-02	0.35	0.09	6.064E-02
2200	4.687E-02	0.40	0.12	4.705E-02	0.40	0.10	4.636E-02
2300	4.101E-02	0.49	0.13	4.117E-02	0.49	0.11	4.071E-02
2400	3.603E-02	0.60	0.14	3.616E-02	0.60	0.11	3.574E-02
2500	3.158E-02	3.23	0.15	3.177E-02	3.23	0.13	3.133E-02

Table 6.2.3. Spectral Irradiance of NSC IM lamp **No 7-3112**

Wave-length, nm	NSC IM Data						Pilot Data
	Round 1			Round 2			
	Spectral Irradiance $E_{\mathrm{IM,7\ 3112,1}}$ W m^{-2} nm^{-1}	Correlated uncertainty $u_{\mathrm{corr}}\left(E_{\mathrm{IM,7\ 3112,1}}\right)$ %	Uncorrelated uncertainty $u_{\mathrm{uncorr}}\left(E_{\mathrm{IM,7\ 3112,1}}\right)$ %	Spectral Irradiance $E_{\mathrm{IM,7\ 3112,2}}$ W m^{-2} nm^{-1}	Correlated uncertainty $u_{\mathrm{corr}}\left(E_{\mathrm{IM,7\ 3112,2}}\right)$ %	Uncorrelated uncertainty $u_{\mathrm{uncorr}}\left(E_{\mathrm{IM,7\ 3112,2}}\right)$ %	Spectral Irradiance $E_{\mathrm{p,7\ 3112}}$ W m^{-2} nm^{-1}
250	1.138E-04	2.22	0.13	1.141E-04	2.22	0.14	1.248E-04
260	2.024E-04	2.14	0.13	2.061E-04	2.14	0.14	2.219E-04
270	3.466E-04	2.10	0.12	3.529E-04	2.10	0.13	3.740E-04
280	5.530E-04	1.60	0.11	5.617E-04	1.60	0.11	5.944E-04
290	8.506E-04	1.12	0.11	8.597E-04	1.12	0.10	9.028E-04
300	1.248E-03	0.63	0.10	1.262E-03	0.63	0.09	1.323E-03
320	2.431E-03	0.62	0.10	2.454E-03	0.62	0.09	2.603E-03
340	4.364E-03	0.60	0.98	4.404E-03	0.60	0.09	4.601E-03
360	7.202E-03	0.56	0.09	7.272E-03	0.56	0.09	7.522E-03
380	1.107E-02	0.62	0.09	1.116E-02	0.62	0.09	1.149E-02
400	1.584E-02	0.56	0.09	1.598E-02	0.56	0.08	1.658E-02
450	3.301E-02	0.48	0.08	3.328E-02	0.48	0.08	3.417E-02
500	5.537E-02	0.44	0.08	5.576E-02	0.44	0.08	5.748E-02
555	8.471E-02	0.44	0.08	8.529E-02	0.44	0.09	8.663E-02
600	1.084E-01	0.38	0.08	1.092E-01	0.38	0.09	1.106E-01
700	1.534E-01	0.34	0.07	1.544E-01	0.34	0.07	1.556E-01
800	1.800E-01	0.33	0.08	1.810E-01	0.33	0.08	1.830E-01
900	1.913E-01	0.32	0.08	1.922E-01	0.32	0.09	1.929E-01
1000	1.902E-01	0.36	0.09	1.910E-01	0.36	0.08	1.897E-01
1100	1.789E-01	0.31	0.10	1.796E-01	0.31	0.09	1.786E-01
1300	1.483E-01	0.38	0.10	1.489E-01	0.38	0.09	1.466E-01
1500	1.158E-01	0.36	0.09	1.164E-01	0.36	0.09	1.144E-01
1700	8.928E-02	0.32	0.09	8.961E-02	0.32	0.10	8.748E-02
2000	5.956E-02	0.35	0.09	5.974E-02	0.35	0.09	5.839E-02
2200	4.619E-02	0.40	0.11	4.641E-02	0.40	0.10	4.487E-02
2300	4.055E-02	0.49	0.12	4.072E-02	0.49	0.12	3.951E-02
2400	3.557E-02	0.60	0.13	3.571E-02	0.60	0.14	3.477E-02
2500	3.124E-02	3.23	0.14	3.140E-02	3.23	0.14	3.047E-02

6.3. TÜBİTAK UME lamps data

Three lamps were measured at TÜBİTAK UME: BN-9101-349, BN-9101-351 and BN-9101-352 in the spectral range from 250 nm to 1100 nm.

Table 6.3.1. Spectral Irradiance of TÜBİTAK UME lamp **BN-9101-349**

Wave-length, nm	TÜBİTAK UME Data						Pilot Data
	Round 1			Round 2			
	Spectral Irradiance $E_{\mathrm{UME},349,1}$ W m^{-2} nm^{-1}	Correlated uncertainty $u_{\mathrm{corr}}(E_{\mathrm{UME},349,1})$ %	Uncorrelated uncertainty $u_{\mathrm{uncorr}}(E_{\mathrm{UME},349,1})$ %	Spectral Irradiance $(E_{\mathrm{UME},349,2})$ W m^{-2} nm^{-1}	Correlated uncertainty $u_{\mathrm{corr}}(E_{\mathrm{UME},349,2})$ %	Uncorrelated uncertainty $u_{\mathrm{uncorr}}(E_{\mathrm{UME},349,2})$ %	Spectral Irradiance $E_{\mathrm{p},349}$ W m^{-2} nm^{-1}
250	2.625E-04	1.51	0.61	2.632E-04	1.51	0.61	2.669E-04
260	4.511E-04	1.48	0.58	4.515E-04	1.48	0.58	4.581E-04
270	7.319E-04	1.47	0.57	7.324E-04	1.47	0.57	7.429E-04
280	1.127E-03	1.47	0.56	1.131E-03	1.47	0.56	1.145E-03
290	1.672E-03	1.46	0.56	1.676E-03	1.46	0.56	1.696E-03
300	2.392E-03	1.26	0.53	2.398E-03	1.26	0.53	2.425E-03
320	4.508E-03	1.25	0.51	4.513E-03	1.25	0.51	4.565E-03
340	7.699E-03	1.24	0.50	7.691E-03	1.24	0.50	7.785E-03
360	1.219E-02	0.98	0.49	1.217E-02	0.98	0.49	1.230E-02
380	1.807E-02	0.97	0.48	1.809E-02	0.97	0.48	1.824E-02
400	2.543E-02	0.94	0.46	2.540E-02	0.94	0.46	2.564E-02
450	4.954E-02	0.94	0.46	4.949E-02	0.94	0.46	4.995E-02
500	7.971E-02	0.93	0.44	7.965E-02	0.93	0.44	8.040E-02
555	1.162E-01	0.93	0.44	1.164E-01	0.93	0.44	1.165E-01
600	1.445E-01	0.93	0.44	1.451E-01	0.93	0.44	1.449E-01
700	1.944E-01	0.93	0.44	1.948E-01	0.93	0.44	1.952E-01
800	2.219E-01	0.93	0.45	2.223E-01	0.93	0.45	2.227E-01
900	2.283E-01	0.94	0.46	2.286E-01	0.94	0.46	2.300E-01
1000	2.216E-01	0.94	0.46	2.214E-01	0.94	0.46	2.231E-01
1100	2.064E-01	0.94	0.46	2.068E-01	0.94	0.46	2.082E-01

Table 6.3.2. Spectral Irradiance of TÜBİTAK UME lamp **BN-9101-351**

Wave-length, nm	TÜBİTAK UME Data						Pilot Data
	Round 1			Round 2			
	Spectral Irradiance $E_{\mathrm{UME},351,1}$ W m^{-2} nm^{-1}	Correlated uncertainty $u_{\mathrm{corr}}\left(E_{\mathrm{UME},351,1}\right)$ %	Uncorrelated uncertainty $u_{\mathrm{uncorr}}\left(E_{\mathrm{UME},351,1}\right)$ %	Spectral Irradiance $\left(E_{\mathrm{UME},351,2}\right)$ W m^{-2} nm^{-1}	Correlated uncertainty $u_{\mathrm{corr}}\left(E_{\mathrm{UME},351,2}\right)$ %	Uncorrelated uncertainty $u_{\mathrm{uncorr}}\left(E_{\mathrm{UME},351,2}\right)$ %	Spectral Irradiance $E_{\mathrm{p},351}$ W m^{-2} nm^{-1}
250	2.626E-04	1.51	0.61	2.631E-04	1.51	0.61	2.672E-04
260	4.506E-04	1.48	0.58	4.508E-04	1.48	0.58	4.582E-04
270	7.366E-04	1.47	0.57	7.372E-04	1.47	0.57	7.488E-04
280	1.135E-03	1.47	0.56	1.138E-03	1.47	0.56	1.154E-03
290	1.687E-03	1.46	0.56	1.691E-03	1.46	0.56	1.714E-03
300	2.415E-03	1.26	0.53	2.420E-03	1.26	0.53	2.453E-03
320	4.540E-03	1.25	0.51	4.543E-03	1.25	0.51	4.607E-03
340	7.752E-03	1.24	0.50	7.747E-03	1.24	0.50	7.858E-03
360	1.227E-02	0.98	0.49	1.226E-02	0.98	0.49	1.241E-02
380	1.820E-02	0.97	0.48	1.818E-02	0.97	0.48	1.840E-02
400	2.565E-02	0.94	0.46	2.559E-02	0.94	0.46	2.586E-02
450	4.992E-02	0.94	0.46	4.987E-02	0.94	0.46	5.034E-02
500	8.031E-02	0.93	0.44	8.027E-02	0.93	0.44	8.095E-02
555	1.168E-01	0.93	0.44	1.171E-01	0.93	0.44	1.173E-01
600	1.456E-01	0.93	0.44	1.460E-01	0.93	0.44	1.458E-01
700	1.953E-01	0.93	0.44	1.955E-01	0.93	0.44	1.962E-01
800	2.227E-01	0.93	0.45	2.234E-01	0.93	0.45	2.237E-01
900	2.294E-01	0.94	0.46	2.297E-01	0.94	0.46	2.309E-01
1000	2.217E-01	0.94	0.46	2.222E-01	0.94	0.46	2.236E-01
1100	2.064E-01	0.94	0.46	2.071E-01	0.94	0.46	2.084E-01

Table 6.3.3. Spectral Irradiance of TÜBİTAK UME lamp **BN-9101-352**

Wave-length, nm	TÜBİTAK UME Data						Pilot Data
	Round 1			Round 2			
	Spectral Irradiance $E_{\mathrm{UME},352,1}$ W m^{-2} nm^{-1}	Correlated uncertainty $u_{\mathrm{corr}}(E_{\mathrm{UME},352,1})$ %	Uncorrelated uncertainty $u_{\mathrm{uncorr}}(E_{\mathrm{UME},352,1})$ %	Spectral Irradiance $(E_{\mathrm{UME},352,2})$ W m^{-2} nm^{-1}	Correlated uncertainty $u_{\mathrm{corr}}(E_{\mathrm{UME},352,2})$ %	Uncorrelated uncertainty $u_{\mathrm{uncorr}}(E_{\mathrm{UME},352,2})$ %	Spectral Irradiance $E_{\mathrm{p},352}$ W m^{-2} nm^{-1}
250	1.644E-04	1.51	0.61	1.649E-04	1.51	0.61	1.671E-04
260	2.881E-04	1.48	0.58	2.886E-04	1.48	0.58	2.926E-04
270	4.802E-04	1.47	0.57	4.815E-04	1.47	0.57	4.878E-04
280	7.496E-04	1.47	0.56	7.507E-04	1.47	0.56	7.609E-04
290	1.138E-03	1.46	0.56	1.145E-03	1.46	0.56	1.157E-03
300	1.660E-03	1.26	0.53	1.668E-03	1.26	0.53	1.685E-03
320	3.238E-03	1.25	0.51	3.237E-03	1.25	0.51	3.273E-03
340	5.683E-03	1.24	0.50	5.648E-03	1.24	0.50	5.729E-03
360	9.161E-03	0.98	0.49	9.168E-03	0.98	0.49	9.256E-03
380	1.388E-02	0.97	0.48	1.389E-02	0.97	0.48	1.402E-02
400	1.997E-02	0.94	0.46	1.995E-02	0.94	0.46	2.008E-02
450	4.027E-02	0.94	0.46	4.021E-02	0.94	0.46	4.062E-02
500	6.681E-02	0.93	0.44	6.688E-02	0.93	0.44	6.730E-02
555	9.991E-02	0.93	0.44	9.995E-02	0.93	0.44	1.001E-01
600	1.265E-01	0.93	0.44	1.268E-01	0.93	0.44	1.266E-01
700	1.746E-01	0.93	0.44	1.749E-01	0.93	0.44	1.754E-01
800	2.031E-01	0.93	0.45	2.035E-01	0.93	0.45	2.037E-01
900	2.116E-01	0.94	0.46	2.119E-01	0.94	0.46	2.128E-01
1000	2.064E-01	0.94	0.46	2.059E-01	0.94	0.46	2.077E-01
1100	1.932E-01	0.94	0.46	1.928E-01	0.94	0.46	1.944E-01

7. Pre-Draft A procedure

The following Pre-Draft A processes were carried out:

- Pre-Draft-A Process 1: Verification of reported results;
- Pre-Draft-A Process 2: Review of uncertainty budgets and descriptions of measurement techniques and facilities;
- Pre-Draft-A Process 3: Review of Relative Data;

Relative Data were calculated separately for each lamp & round combination by the equation:

$$Rel.Data = \left(\frac{E_{NMI,j,R}(\lambda)}{E_{p,j}(\lambda)} - 1\right) - \frac{1}{N_L N_R}\sum_{j,R}\left(\frac{E_{NMI,j,R}(\lambda)}{E_{p,j}(\lambda)} - 1\right)$$

where:

$E_{NMI,j,R}(\lambda)$ – value of spectral irradiance of the lamp j reported by participating NMI for the round R at the wavelength λ;

$E_{p,j}(\lambda)$ – value of spectral irradiance reported by the pilot for the same lamp and wavelength;

N_L – total number of lamps used by the participating NMI (usually 3);

$N_R = 2$ – number rounds.

The relative data are presented in graphic form in Appendix A.

7.1. Data Corrections at the Pre-Draft A stage

NO any data were withdrawn or corrected at the Pre-Draft stage.

8. Comparison data analysis

8.1. Method of comparison data analysis

The comparison COOMET.PR-K1.a.2018 was considered as a set of three independent bilateral comparisons with the same pilot/link laboratory. Therefore, the analysis of each bilateral comparison was performed independently.

The analysis follows the approach described in the Appendix B of the Guidelines for CCPR and RMO Bilateral Key Comparisons CCPR-G5 [5]. The approach is based on the work of Ojanen [28].

Analysis of the comparison data was done independently for each wavelength.

For each non-linked NMI, for each lamp *j*, the Spectral Irradiance values measured by this NMI in two rounds, $E_{\mathrm{nl},j,R}$, where R = 1,2, are averaged:

$$E_{\mathrm{nl},j}(\lambda) = \frac{1}{2}\sum_{R=1}^{2} E_{\mathrm{nl},j,R}\,(\lambda) \tag{8.1}$$

Note: BelGIM has not submitted the first-round data for the wavelength of 1100 nm. Therefore, $E_{\mathrm{BelGIM},j}(1100) = E_{\mathrm{BelGIM},j,2}\,(1100)$.

The standard uncertainty of $E_{\mathrm{nl},j}(\lambda)$ is given by:

$$u\left(E_{\mathrm{nl},j}(\lambda)\right) = \sqrt{\left(\frac{1}{2}\sum_{R=1}^{2} u_{\mathrm{corr}}\left(E_{\mathrm{nl},j,R}(\lambda)\right)\right)^{2} + \frac{1}{4}\sum_{R=1}^{2} u^{2}_{\mathrm{uncorr}}\left(E_{\mathrm{nl},j,R}(\lambda)\right)} \tag{8.2}$$

where $u_{\mathrm{corr}}\left(E_{\mathrm{nl},j,R}(\lambda)\right)$ and $u_{\mathrm{uncorr}}\left(E_{\mathrm{nl},j,R}(\lambda)\right)$ are reported total correlated and uncorrelated components of standard uncertainty.

The standard uncertainty of the average spectral irradiance measurement results of the non-link NMI is calculated by averaging $u\left(E_{\mathrm{nl},j}(\lambda)\right)$ of all lamps:

$$u\left(E_{\mathrm{nl}}(\lambda)\right) = \frac{1}{m}\sum_{j=1}^{3} u\left(E_{\mathrm{nl},j}(\lambda)\right), \tag{8.3}$$

where *m* is a number of lamps: *m*=3.

For each lamp *j*, the relative difference between the non-link NMI measurement and the pilot measurement is given by

$$\Delta_{\mathrm{nl},j}(\lambda) = \frac{E_{\mathrm{nl},j}(\lambda)}{E_{\mathrm{p},j}(\lambda)} - 1\,, \tag{8.4}$$

where $E_{\mathrm{p},j}(\lambda)$ is the spectral irradiance of the lamp *j* measured by the pilot.

The final difference between the non-link NMI and the pilot measurement results is obtained by averaging the differences $\Delta_{\mathrm{nl},j}(\lambda)$ of all lamps:

$$\Delta_{\mathrm{nl}}(\lambda) = \frac{1}{m}\sum_{j=1}^{3} \Delta_{\mathrm{nl},j}(\lambda)\,. \tag{8.5}$$

The unilateral degree of equivalence (DoE), the deviation from KCRV, of the non-link NMI, $D_{\mathrm{nl}}(\lambda)$, is calculated by:

$$D_{\mathrm{nl}}(\lambda) = \Delta_{\mathrm{nl}}(\lambda) + D_{\mathrm{p}}(\lambda), \tag{8.6}$$

where $D_{\mathrm{p}}(\lambda)$ is the DoE of the pilot taken from the final report of CCPR-K1.a.2017 [1]. The values of $D_{\mathrm{p}}(\lambda)$ are repeated here in Table 8.1.

Table 8.1. Values of DoE of pilot/link laboratory, VNIIOFI.

λ , nm	$D_{\mathrm{p}}(\lambda)$, %	λ , nm	$D_{\mathrm{p}}(\lambda)$, %	λ , nm	$D_{\mathrm{p}}(\lambda)$, %	λ , nm	$D_{\mathrm{p}}(\lambda)$, %
250	-0.42	340	-0.32	600	0.04	1500	-0.06
260	-0.29	360	-0.35	700	0.06	1700	-0.07
270	-0.25	380	-0.37	800	-0.07	2000	0.03
280	-0.12	400	-0.20	900	0.02	2200	0.12
290	-0.24	450	-0.03	1000	-0.05	2300	-0.17
300	-0.36	500	0.01	1100	0.04	2400	-0.10
320	-0.19	555	-0.01	1300	-0.10	2500	-0.07

The uncertainty of the non-link DoE is given as an expanded uncertainty:

$$U\big(D_{\mathrm{nl}}(\lambda)\big) = 2u\big(D_{\mathrm{nl}}(\lambda)\big), \tag{8.7}$$

Where the standard uncertainty is calculated as

$$u^2\big(D_{\mathrm{nl}}(\lambda)\big) = u^2\big(E_{\mathrm{nl}}(\lambda)\big) + u^2\big(\Delta_{\mathrm{KCRV}}(\lambda)\big) + \Big(1 - 2w_{\mathrm{p}}(\lambda)\Big)\, s_{\mathrm{KC}}^2(\lambda) + u_{\mathrm{p,uncorr,KC}}^2(\lambda) + u_{\mathrm{p,uncorr,BC}}^2(\lambda) + u_{\mathrm{p,st}}^2(\lambda), \tag{8.8}$$

were

$u\big(\Delta_{\mathrm{KCRV}}(\lambda)\big)$is the standard uncertainty of KCRV;

$w_{\mathrm{p}}(\lambda)$ is the weight of the pilot (VNIIOFI) when calculated KCRV in CCPR-K1.a.2017;

$s_{\mathrm{KC}}(\lambda)$ is the additional *s* term added during a Mandel-Paule approach in obtaining consistency in CCPR-K1.a.2017;

$u_{\mathrm{p,uncorr,KC}}(\lambda)$ and $u_{\mathrm{p,uncorr,BC}}(\lambda)$ are the standard uncertainties associated with uncorrelated effects (random uncertainty) of the pilot/link laboratory (VNIIOFI) during CCPR-K1.a.2017 and COOMET.PR-K1.a.2018, respectively;

$u_{\mathrm{p,st}}(\lambda)$ is the standard uncertainty associated with stability of the pilot scale between CCPR-K1.a.2017 and COOMET.PR-K1.a.2018.

Values of $u\big(\Delta_{\mathrm{KCRV}}(\lambda)\big)$, $s_{\mathrm{KC}}(\lambda)$ and $w_{\mathrm{p}}(\lambda)$ are available in [1].

Values of $u_{\mathrm{p,uncorr,KC}}(\lambda)$ are presented in Table 5.1.5 of this report in the second from end column labelled as "$u_{\mathrm{VNIIOFI,r}}$ random".

Values of $u_{\mathrm{p,st}}(\lambda)$ and $u_{\mathrm{p,uncorr,BC}}(\lambda)$ are presented in Table 5.1.6 of the present report in the forth and sixth columns, respectively, and labelled as "Stability of pilot measurement $u_{\mathrm{pilot,stab}}$ random" and "$u_{\mathrm{pilot,r}}$ random", respectively.

The values of $u\big(\Delta_{\mathrm{KCRV}}(\lambda)\big)$, $w_{\mathrm{p}}(\lambda)$, $s_{\mathrm{KC}}(\lambda)$, $u_{\mathrm{p,uncorr,KC}}(\lambda)$, $u_{\mathrm{p,uncorr,BC}}(\lambda)$ and $u_{\mathrm{p,st}}(\lambda)$ are collected in Table 8.2 below.

In the equation (8.8), combine all component related to the pilot/link to one, $u_{\mathrm{link}}(\lambda)$. Therefore, the standard uncertainty $u\big(D_{\mathrm{nl}}(\lambda)\big)$ is presented as

$$u\big(D_{\mathrm{nl}}(\lambda)\big) = \sqrt{u^2\big(E_{\mathrm{nl}}(\lambda)\big) + u^2\big(\Delta_{\mathrm{KCRV}}(\lambda)\big) + u_{\mathrm{link}}^2(\lambda)} \tag{8.9}$$

where

$$u_{\mathrm{link}}^2(\lambda) = \big(1 - 2w_{\mathrm{p}}(\lambda)\big)\, s_{\mathrm{KC}}^2(\lambda) + u_{\mathrm{p,uncorr,KC}}^2(\lambda) + u_{\mathrm{p,uncorr,BC}}^2(\lambda) + u_{\mathrm{p,st}}^2(\lambda) \tag{8.10}$$

The values of $u_{\mathrm{link}}(\lambda)$ are presented in the last column of Table 8.2.

Table 8.2. Values of variables of Equations (8.8) and (8.9) except $u\big(E_{\mathrm{nl}}(\lambda)\big)$

λ, nm	$u\big(\Delta_{\mathrm{KCRV}}(\lambda)\big)$, %	$w_{\mathrm{p}}(\lambda)$	$s_{\mathrm{KC}}(\lambda)$, %	$u_{\mathrm{p,uncorr,KC}}(\lambda)$, %	$u_{\mathrm{p,uncorr,BC}}(\lambda)$, %	$u_{\mathrm{p,st}}(\lambda)$, %	$u_{\mathrm{link}}(\lambda)$, %
250	0.28	0.149	0.00	0.31	0.21	0.10	0.39
260	0.25	0.143	0.00	0.24	0.17	0.10	0.31
270	0.23	0.139	0.00	0.22	0.16	0.10	0.29
280	0.22	0.136	0.00	0.22	0.15	0.08	0.28
290	0.20	0.133	0.00	0.20	0.14	0.08	0.26
300	0.19	0.139	0.00	0.19	0.14	0.08	0.25
320	0.18	0.137	0.00	0.16	0.12	0.08	0.22
340	0.17	0.137	0.00	0.16	0.12	0.08	0.22
360	0.16	0.137	0.00	0.15	0.12	0.08	0.21
380	0.15	0.134	0.11	0.14	0.11	0.08	0.22
400	0.14	0.134	0.15	0.12	0.11	0.08	0.22
450	0.12	0.130	0.00	0.12	0.11	0.08	0.18
500	0.11	0.128	0.00	0.11	0.10	0.08	0.17
555	0.10	0.126	0.00	0.11	0.10	0.08	0.17
600	0.10	0.125	0.00	0.10	0.10	0.08	0.16
700	0.09	0.135	0.00	0.10	0.10	0.08	0.16
800	0.09	0.141	0.00	0.10	0.10	0.08	0.16
900	0.08	0.144	0.00	0.09	0.09	0.08	0.15
1000	0.08	0.132	0.02	0.09	0.09	0.07	0.15
1100	0.08	0.151	0.00	0.09	0.09	0.07	0.15
1300	0.08	0.135	0.21	0.09	0.09	0.07	0.23
1500	0.08	0.136	0.23	0.09	0.09	0.07	0.24
1700	0.09	0.145	0.31	0.10	0.09	0.07	0.30
2000	0.10	0.155	0.28	0.16	0.12	0.08	0.32
2200	0.12	0.140	0.57	0.18	0.14	0.10	0.54
2300	0.13	0.139	0.58	0.22	0.18	0.12	0.58
2400	0.16	0.130	0.89	0.27	0.20	0.12	0.84
2500	0.20	0.212	0.00	0.33	0.22	0.12	0.41

9. Comparison results

This section presents the values of Degrees of Equivalence (DoEs) of the non-link laboratories, i.e. deviations from KCRV, $D_{\mathrm{nl}}(\lambda)$, and their associated expanded uncertainties, $U\left(D_{\mathrm{nl}}(\lambda)\right)$.

9.1. BelGIM results

DoEs of BelGIM were calculate by the equations (8.1) – (8.9), where the subscript "nl" should replace with "Bel".

Table 9.1.1 presents the values of spectral irradiance, measured by BelGIM (averaged over rounds by equation (8.1)) and by the pilot/link laboratory (VNIIOFI) for all three lamps of BelGIM, as well as the relative differences between BelGIM and the pilot measurement results, $\Delta_{\mathrm{Bel}}(\lambda)$, calculated by the equation (8.4) and (8.5).

Deviations of BelGIM results from KCRV, $D_{\mathrm{Bel}}(\lambda)$, were calculated by equation (8.6) using the values of Δ_{Bel} from the last column of the Table 9.2.1 and the values of $D_{\mathrm{p}}(\lambda)$ from the Table 8.1. The values of $D_{\mathrm{Bel}}(\lambda)$ are presented in Table 9.1.3.

Table 9.1.1. Values of spectral irradiance, measured by BelGIM (averaged over rounds by equation 8.1) and pilot, and relative differences between BelGIM and pilot results (equation 8.5).

λ, nm	Spectral Irradiance, W m^{-2} nm^{-1}						Difference of BelGIM from pilot $\Delta_{\mathrm{Bel}}(\lambda)$, %
	Lamp BN-9101-674		Lamp BN-9101-675		Lamp BN-9101-692		
	BelGIM	Pilot	BelGIM	Pilot	BelGIM	Pilot	
	$E_{\mathrm{Bel},674}$	$E_{\mathrm{p},674}$	$E_{\mathrm{Bel},675}$	$E_{\mathrm{p},675}$	$E_{\mathrm{Bel},692}$	$E_{\mathrm{p},692}$	
250	2.202E-04	2.220E-04	1.925E-04	1.944E-04	1.358E-04	1.401E-04	-1.65
260	3.869E-04	3.862E-04	3.377E-04	3.398E-04	2.431E-04	2.496E-04	-1.02
270	6.249E-04	6.344E-04	5.517E-04	5.587E-04	4.132E-04	4.191E-04	-1.40
280	9.961E-04	9.887E-04	8.756E-04	8.709E-04	6.590E-04	6.539E-04	0.68
290	1.481E-03	1.475E-03	1.304E-03	1.303E-03	1.006E-03	1.007E-03	0.06
300	2.120E-03	2.123E-03	1.883E-03	1.887E-03	1.466E-03	1.476E-03	-0.37
320	4.030E-03	4.035E-03	3.604E-03	3.608E-03	2.866E-03	2.885E-03	-0.31
340	6.918E-03	6.933E-03	6.266E-03	6.257E-03	5.058E-03	5.095E-03	-0.27
360	1.097E-02	1.102E-02	9.988E-03	1.002E-02	8.241E-03	8.298E-03	-0.51
380	1.640E-02	1.643E-02	1.501E-02	1.504E-02	1.261E-02	1.265E-02	-0.26
400	2.320E-02	2.321E-02	2.132E-02	2.136E-02	1.817E-02	1.821E-02	-0.18
450	4.556E-02	4.562E-02	4.230E-02	4.261E-02	3.718E-02	3.734E-02	-0.44
500	7.371E-02	7.386E-02	6.958E-02	6.980E-02	6.228E-02	6.258E-02	-0.33
555	1.039E-01	1.076E-01	9.928E-02	1.028E-01	9.042E-02	9.394E-02	-3.56
600	1.339E-01	1.342E-01	1.288E-01	1.293E-01	1.190E-01	1.196E-01	-0.36
700	1.813E-01	1.818E-01	1.770E-01	1.774E-01	1.665E-01	1.675E-01	-0.37
800	2.061E-01	2.082E-01	1.975E-01	2.052E-01	1.943E-01	1.963E-01	-1.92
900	2.141E-01	2.155E-01	2.124E-01	2.139E-01	2.052E-01	2.063E-01	-0.64
1000	2.121E-01	2.093E-01	2.012E-01	2.088E-01	2.008E-01	2.022E-01	-1.02
1100	2.074E-01	1.956E-01	1.975E-01	1.957E-01	1.940E-01	1.901E-01	3.02

Table 9.1.2 presents the values of the combined standard uncertainty of the deviation of BelGIM from KCRV, $u\left(D_{\mathrm{Bel}}(\lambda)\right)$, and its components, including: the uncertainty of BelGIM measurements, $u\left(E_{\mathrm{Bel}}(\lambda)\right)$, calculated by the equations (8.2) and (8.3); the uncertainty of KCRV, $u\left(\Delta_{\mathrm{KCRV}}(\lambda)\right)$; and the uncertainty of link quality, $u_{\mathrm{link}}(\lambda)$, calculated by the equation (8.10).

Table 9.1.2. Combined standard uncertainty of BelGIM DoEs, $u\left(D_{\mathrm{Bel}}(\lambda)\right)$, and its components: uncertainty of BelGIM measurements, $u\left(E_{\mathrm{Bel}}(\lambda)\right)$, uncertainty of KCRV, $u\left(\Delta_{\mathrm{KCRV}}(\lambda)\right)$; and uncertainty of link quality, $u_{\mathrm{link}}(\lambda)$.

λ, nm	$u\left(E_{\mathrm{Bel}}(\lambda)\right)$, %	$u\left(\Delta_{\mathrm{KCRV}}(\lambda)\right)$, %	$u_{\mathrm{link}}(\lambda)$, %	$u\left(D_{\mathrm{Bel}}(\lambda)\right)$, %
250	4.72	0.28	0.39	4.75
260	2.32	0.25	0.31	2.35
270	2.52	0.23	0.29	2.55
280	2.31	0.22	0.28	2.34
290	1.08	0.20	0.26	1.13
300	0.94	0.19	0.25	0.99
320	0.83	0.18	0.22	0.87
340	0.80	0.17	0.22	0.84
360	0.76	0.16	0.21	0.80
380	0.69	0.15	0.22	0.74
400	0.65	0.14	0.22	0.70
450	0.62	0.12	0.18	0.65
500	0.60	0.11	0.17	0.63
555	0.58	0.10	0.17	0.62
600	0.60	0.10	0.16	0.63
700	0.62	0.09	0.16	0.64
800	0.64	0.09	0.16	0.66
900	0.65	0.08	0.15	0.67
1000	0.74	0.08	0.15	0.76
1100	0.89	0.08	0.15	0.91

9.1.2. DoE of BelGIM

Table 9.1.3 summarizes the DoEs of BelGIM: differences from KCRV, $D_{\mathrm{Bel}}(\lambda)$, its standard uncertainty, $u\left(D_{\mathrm{Bel}}(\lambda)\right)$, and its expanded uncertainty, $U\left(D_{\mathrm{Bel}}(\lambda)\right)$, calculated by equation (8.7). The BelGIM DoEs are also presented in Figure 9.1.1.

Table 9.1.3. Summary of DoEs of BelGIM: differences from KCRV, $D_{\mathrm{Bel}}(\lambda)$, its standard uncertainty, $u\left(D_{\mathrm{Bel}}(\lambda)\right)$, and its expanded uncertainty, $U\left(D_{\mathrm{Bel}}(\lambda)\right)$.

λ, nm	$D_{\mathrm{Bel}}(\lambda)$, %	$u\left(D_{\mathrm{Bel}}(\lambda)\right)$, %	$U\left(D_{\mathrm{Bel}}(\lambda)\right)$, % ($k$=2)
250	-2.07	4.75	9.49
260	-1.31	2.35	4.71
270	-1.65	2.55	5.10
280	0.56	2.34	4.68
290	-0.18	1.13	2.26
300	-0.73	0.99	1.98
320	-0.50	0.87	1.75
340	-0.59	0.84	1.69
360	-0.86	0.80	1.61
380	-0.63	0.74	1.48
400	-0.38	0.70	1.41
450	-0.47	0.65	1.31
500	-0.32	0.63	1.26
555	-3.57	0.62	1.23
600	-0.32	0.63	1.25
700	-0.31	0.64	1.29
800	-1.99	0.66	1.33
900	-0.62	0.67	1.35
1000	-1.07	0.76	1.53
1100	3.06	0.91	1.82

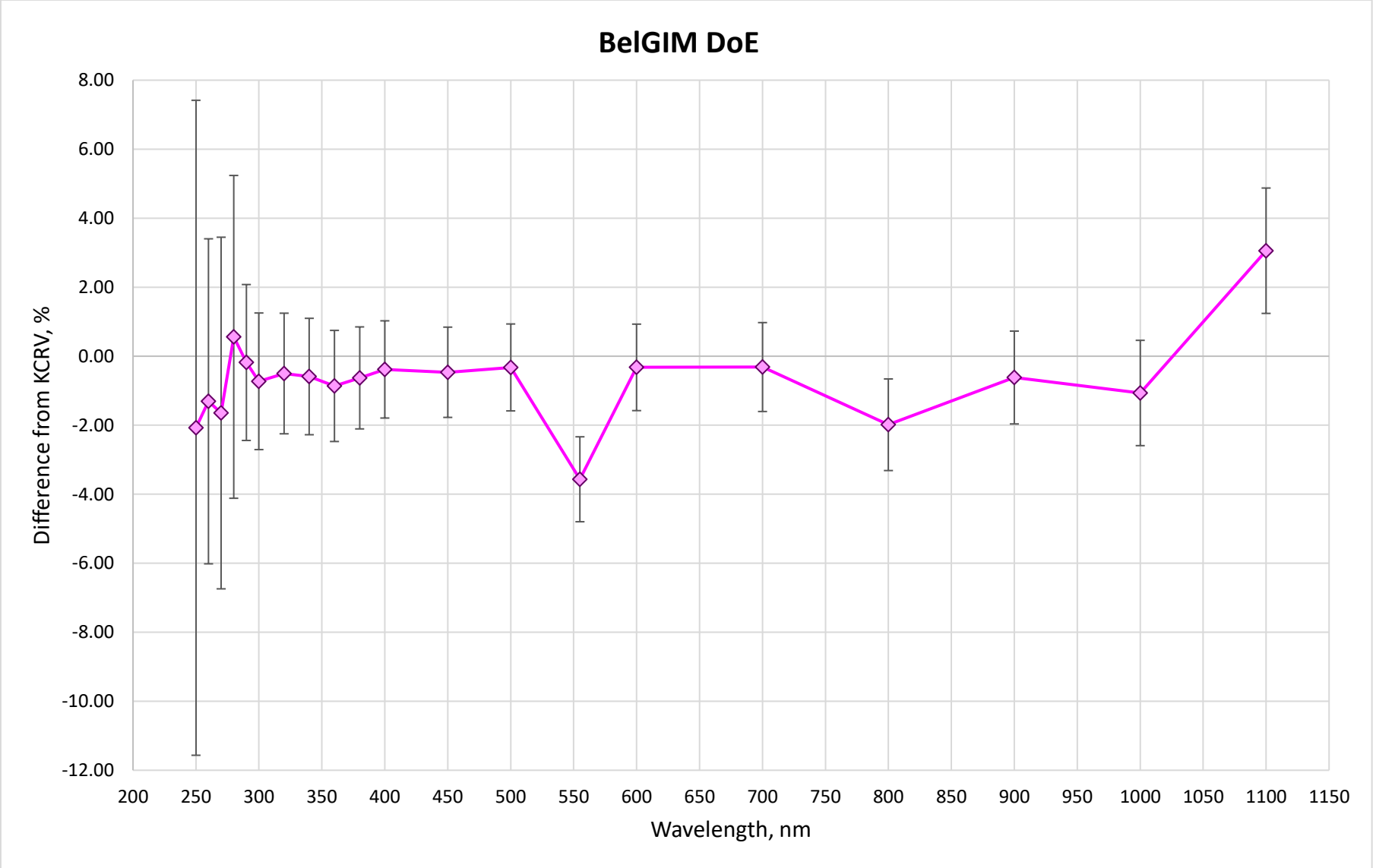

Figure 9.1.1. DoEs of BelGIM

9.2. NSC IM results

DoEs of NSC IM were calculate by the equations (8.1) – (8.9), where the subscript "nl" should replace with "IM".

Table 9.2.1 presents the values of spectral irradiance, measured by NSC IM (averaged over rounds by equation (8.1)) and by the pilot/link laboratory (VNIIOFI) for all three lamps of NSC IM, as well as the relative differences between NSC IM and the pilot measurement results, Δ_{IM}, calculated by the equation (8.4) and (8.5).

Deviations of NSC IM results from KCRV, $D_{\mathrm{IM}}(\lambda)$, were calculated by equation (8.6) using the values of Δ_{IM} from the last column of the Table 9.1.1 and the values of $D_{\mathrm{p}}(\lambda)$ from the Table 8.1. The values of $D_{\mathrm{IM}}(\lambda)$ are presented in Table 9.2.3.

Table 9.2.2 presents the values of the combined standard uncertainty of the deviation of NSC IM from KCRV, $u\big(D_{\mathrm{IM}}(\lambda)\big)$, and its components, including: the uncertainty of NSC IM measurements, $u\big(E_{\mathrm{IM}}(\lambda)\big)$, calculated by the equations (8.2) and (8.3); the uncertainty of KCRV, $u\big(\Delta_{\mathrm{KCRV}}(\lambda)\big)$; and the uncertainty of link quality, $u_{\mathrm{link}}(\lambda)$, calculated by the equation (8.10).

Table 9.2.1. Values of spectral irradiance, measured by NSC IM (averaged over rounds by equation 8.1) and pilot, and relative differences between NSC IM and pilot results (equation 8.5).

Wave-length, nm	Spectral Irradiance, W m^{-2} nm^{-1}						Difference of NSC IM from pilot
	Lamp 3224		Lamp 3225		Lamp 7-3112		
	NSC IM	Pilot	NSC IM	Pilot	NSC IM	Pilot	
	$E_{\mathrm{IM},3224}$	$E_{\mathrm{p},3224}$	$E_{\mathrm{IM},3225}$	$E_{\mathrm{p},3225}$	$E_{\mathrm{IM},7\ 3112}$	$E_{\mathrm{p},7\ 3112}$	Δ_{IM}, %
250	1.682E-04	1.842E-04	1.669E-04	1.840E-04	1.140E-04	1.248E-04	-8.90
260	2.949E-04	3.187E-04	2.985E-04	3.250E-04	2.043E-04	2.219E-04	-7.87
270	4.895E-04	5.242E-04	4.985E-04	5.398E-04	3.498E-04	3.740E-04	-6.92
280	7.530E-04	8.017E-04	7.496E-04	8.054E-04	5.574E-04	5.944E-04	-6.42
290	1.160E-03	1.230E-03	1.182E-03	1.269E-03	8.552E-04	9.028E-04	-5.93
300	1.688E-03	1.786E-03	1.721E-03	1.845E-03	1.255E-03	1.323E-03	-5.76
320	3.235E-03	3.447E-03	3.293E-03	3.549E-03	2.442E-03	2.603E-03	-6.51
340	5.712E-03	6.008E-03	5.801E-03	6.170E-03	4.384E-03	4.601E-03	-5.21
360	9.292E-03	9.677E-03	9.415E-03	9.907E-03	7.237E-03	7.522E-03	-4.25
380	1.407E-02	1.458E-02	1.422E-02	1.491E-02	1.112E-02	1.149E-02	-3.81
400	2.005E-02	2.082E-02	2.024E-02	2.122E-02	1.591E-02	1.658E-02	-4.13
450	4.051E-02	4.183E-02	4.067E-02	4.244E-02	3.314E-02	3.417E-02	-3.45
500	6.707E-02	6.896E-02	6.720E-02	6.965E-02	5.557E-02	5.748E-02	-3.20
555	9.969E-02	1.021E-01	9.937E-02	1.027E-01	8.500E-02	8.663E-02	-2.49
600	1.262E-01	1.286E-01	1.252E-01	1.291E-01	1.088E-01	1.106E-01	-2.18
700	1.743E-01	1.772E-01	1.725E-01	1.770E-01	1.539E-01	1.556E-01	-1.78
800	2.031E-01	2.050E-01	2.010E-01	2.041E-01	1.805E-01	1.830E-01	-1.28
900	2.124E-01	2.135E-01	2.103E-01	2.119E-01	1.917E-01	1.929E-01	-0.62
1000	2.077E-01	2.079E-01	2.049E-01	2.060E-01	1.906E-01	1.897E-01	-0.06

1100	1.944E-01	1.942E-01	1.916E-01	1.921E-01	1.792E-01	1.786E-01	0.06
1300	1.583E-01	1.577E-01	1.559E-01	1.554E-01	1.486E-01	1.466E-01	0.69
1500	1.227E-01	1.222E-01	1.208E-01	1.202E-01	1.161E-01	1.144E-01	0.78
1700	9.359E-02	9.311E-02	9.209E-02	9.141E-02	8.944E-02	8.748E-02	1.17
2000	6.215E-02	6.176E-02	6.111E-02	6.064E-02	5.965E-02	5.839E-02	1.19
2200	4.780E-02	4.727E-02	4.696E-02	4.636E-02	4.630E-02	4.487E-02	1.87
2300	4.186E-02	4.147E-02	4.109E-02	4.071E-02	4.063E-02	3.951E-02	1.57
2400	3.665E-02	3.635E-02	3.610E-02	3.574E-02	3.564E-02	3.477E-02	1.44
2500	3.232E-02	3.220E-02	3.168E-02	3.133E-02	3.132E-02	3.047E-02	1.42

Table 9.2.2. Combined standard uncertainty of NSC IM DoEs, $u(D_{\mathrm{IM}})$, and its components: uncertainty of NSC IM measurements, $u(E_{\mathrm{IM}})$, uncertainty of KCRV, $u(\Delta_{\mathrm{KCRV}})$; and uncertainty of link quality, u_{link}.

λ, nm	$u(E_{\mathrm{IM}})$ %	$u(\Delta_{\mathrm{KCRV}})$ %	u_{link} %	$u(D_{\mathrm{IM}})$ %	λ, nλ, nm m	$u(E_{\mathrm{IM}})$ %	$u(\Delta_{\mathrm{KCRV}})$ %	u_{link} %	$u(D_{\mathrm{IM}})$ %
250	2.22	0.28	0.39	2.27	600	0.39	0.10	0.16	0.43
260	2.15	0.25	0.31	2.18	700	0.35	0.09	0.16	0.39
270	2.10	0.23	0.29	2.13	800	0.33	0.09	0.16	0.38
280	1.60	0.22	0.28	1.64	900	0.32	0.08	0.15	0.36
290	1.12	0.20	0.26	1.17	1000	0.36	0.08	0.15	0.40
300	0.64	0.19	0.25	0.71	1100	0.32	0.08	0.15	0.36
320	0.62	0.18	0.22	0.68	1300	0.38	0.08	0.23	0.46
340	0.66	0.17	0.22	0.71	1500	0.37	0.08	0.24	0.45
360	0.57	0.16	0.21	0.62	1700	0.33	0.09	0.30	0.46
380	0.62	0.15	0.22	0.67	2000	0.36	0.10	0.32	0.49
400	0.57	0.14	0.22	0.62	2200	0.41	0.12	0.54	0.69
450	0.48	0.12	0.18	0.53	2300	0.50	0.13	0.58	0.78
500	0.44	0.11	0.17	0.49	2400	0.61	0.16	0.84	1.05
555	0.44	0.10	0.17	0.48	2500	3.23	0.20	0.41	3.26

9.2.2. DoE of NSC IM

Table 9.2.3 summarizes the DoEs of NSC IM: differences from KCRV, $D_{\mathrm{IM}}(\lambda)$, its standard uncertainty, $u\left(D_{\mathrm{IM}}(\lambda)\right)$, and its expanded uncertainty, $U\left(D_{\mathrm{IM}}(\lambda)\right)$, calculated by equation (8.7). The NSC IM DoEs are also presented in Figure 9.2.1.

Table 9.2.3. Summary of DoEs of NSC IM: differences from KCRV, $D_{\mathrm{IM}}(\lambda)$, its standard uncertainty, $u\left(D_{\mathrm{IM}}(\lambda)\right)$, and its expanded uncertainty, $U\left(D_{\mathrm{IM}}(\lambda)\right)$.

λ, nm	$D_{\mathrm{IM}}(\lambda)$, %	$u\left(D_{\mathrm{IM}}(\lambda)\right)$, %	$U\left(D_{\mathrm{IM}}(\lambda)\right)$, % ($k$=2)
250	-9.32	2.27	4.54
260	-8.16	2.18	4.36
270	-7.17	2.13	4.26
280	-6.54	1.64	3.28
290	-6.17	1.17	2.33
300	-6.12	0.71	1.42
320	-6.70	0.68	1.36
340	-5.53	0.71	1.43
360	-4.60	0.62	1.25
380	-4.18	0.67	1.35
400	-4.33	0.62	1.25
450	-3.48	0.53	1.06
500	-3.19	0.49	0.97
555	-2.50	0.48	0.97
600	-2.14	0.43	0.86
700	-1.72	0.39	0.79
800	-1.35	0.38	0.76
900	-0.60	0.36	0.73
1000	-0.11	0.40	0.79
1100	0.10	0.36	0.72
1300	0.59	0.46	0.91
1500	0.72	0.45	0.90
1700	1.10	0.46	0.91
2000	1.22	0.49	0.97
2200	1.99	0.69	1.38
2300	1.40	0.78	1.55
2400	1.34	1.05	2.10
2500	1.35	3.26	6.52

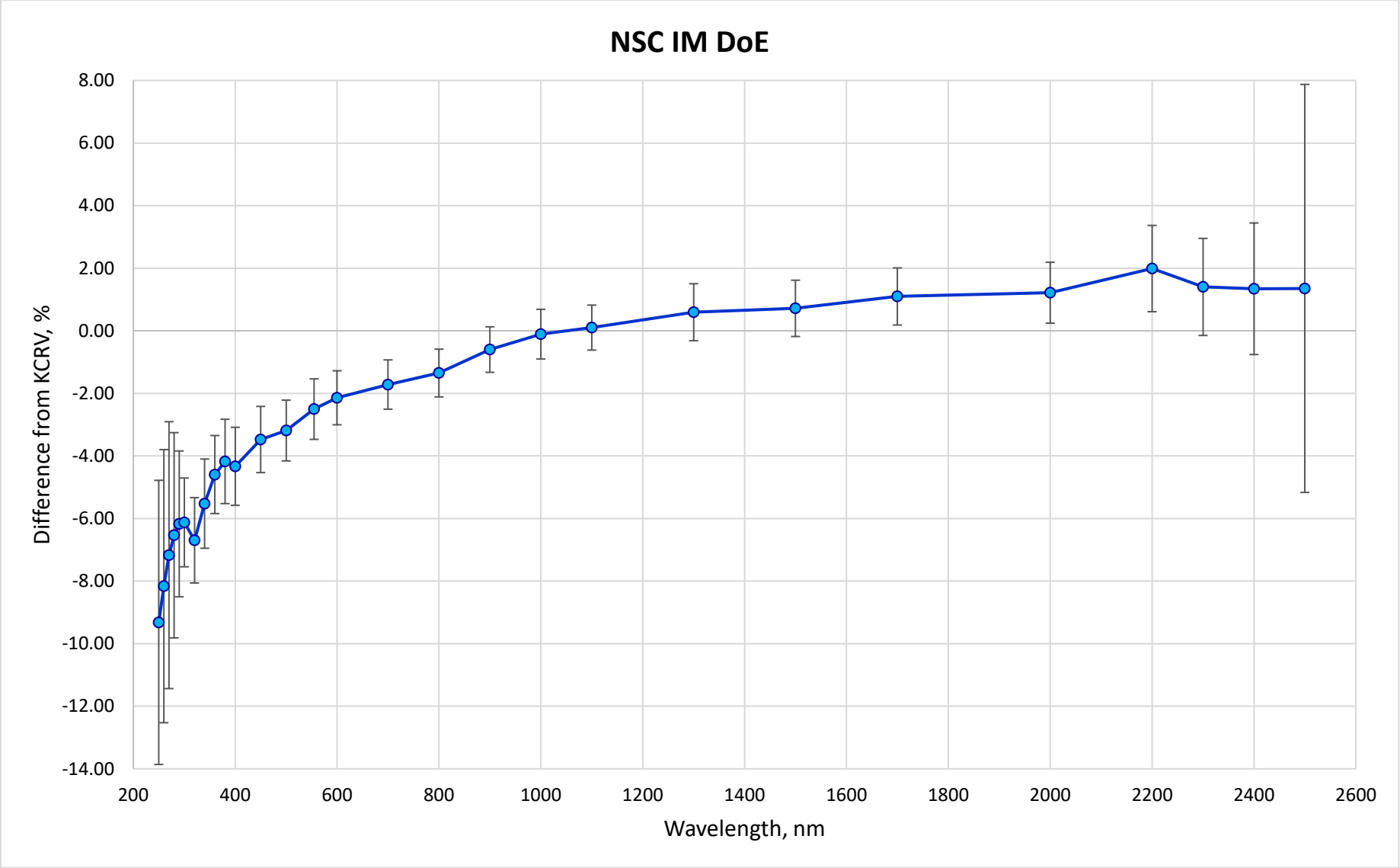

Figure 9.2.1. DoEs of NSC IM

9.3. TÜBİTAK UME results

DoEs of TÜBİTAK UME were calculate by the equations (8.1) – (8.9), where the subscript "nl" should replace with "UME".

Table 9.3.1 presents the values of spectral irradiance, measured by TÜBİTAK UME (averaged over rounds by equation (8.1)) and by the pilot/link laboratory (VNIIOFI) for all three lamps of TÜBİTAK UME, as well as the relative differences between TÜBİTAK UME and the pilot measurement results, $\Delta_{\mathrm{UME}}(\lambda)$, calculated by the equation (8.4) and (8.5).

Deviations of TÜBİTAK UME results from KCRV, $D_{\mathrm{UME}}(\lambda)$, were calculated by equation (8.6) using the values of Δ_{Bel} from the last column of the Table 9.3.1 and the values of $D_{\mathrm{p}}(\lambda)$ from the Table 8.1. The values of $D_{\mathrm{UME}}(\lambda)$ are presented in Table 9.3.3.

Table 9.3.2 presents the values of the combined standard uncertainty of the deviation of TÜBİTAK UME from KCRV, $u\left(D_{\mathrm{UME}}(\lambda)\right)$, and its components, including: the uncertainty of TÜBİTAK UME measurements, $u\left(E_{\mathrm{UME}}(\lambda)\right)$, calculated by the equations (8.2) and (8.3); the uncertainty of KCRV, $u\left(\Delta_{\mathrm{KCRV}}(\lambda)\right)$; and the uncertainty of link quality, $u_{\mathrm{link}}(\lambda)$, calculated by (8.10).

Table 9.3.1. Values of spectral irradiance, measured by TÜBİTAK UME (averaged over rounds by equation 8.1) and pilot, and relative differences between TÜBİTAK UME and pilot results (equation 8.5).

λ, nm	Spectral Irradiance, W m^{-2} nm^{-1}						Difference of UME from pilot $\Delta_{\mathrm{UME}}(\lambda)$, %
	Lamp BN-9101-349		Lamp BN-9101-351		Lamp BN-9101-352		
	UME	Pilot	UME	Pilot	UME	Pilot	
	$E_{\mathrm{UME,349}}$	$E_{\mathrm{p,349}}$	$E_{\mathrm{UME,351}}$	$E_{\mathrm{p,351}}$	$E_{\mathrm{UME,352}}$	$E_{\mathrm{p,352}}$	
250	2.629E-04	2.669E-04	2.629E-04	2.672E-04	1.647E-04	1.671E-04	-1.54
260	4.513E-04	4.581E-04	4.507E-04	4.582E-04	2.884E-04	2.926E-04	-1.53
270	7.322E-04	7.429E-04	7.369E-04	7.488E-04	4.809E-04	4.878E-04	-1.49
280	1.129E-03	1.145E-03	1.137E-03	1.154E-03	7.502E-04	7.609E-04	-1.44
290	1.674E-03	1.696E-03	1.689E-03	1.714E-03	1.142E-03	1.157E-03	-1.38
300	2.395E-03	2.425E-03	2.418E-03	2.452E-03	1.664E-03	1.685E-03	-1.30
320	4.511E-03	4.565E-03	4.542E-03	4.607E-03	3.238E-03	3.273E-03	-1.22
340	7.695E-03	7.785E-03	7.750E-03	7.858E-03	5.666E-03	5.729E-03	-1.22
360	1.218E-02	1.230E-02	1.227E-02	1.241E-02	9.165E-03	9.256E-03	-1.05
380	1.808E-02	1.824E-02	1.819E-02	1.840E-02	1.389E-02	1.402E-02	-1.00
400	2.542E-02	2.564E-02	2.562E-02	2.586E-02	1.996E-02	2.008E-02	-0.80
450	4.952E-02	4.995E-02	4.990E-02	5.034E-02	4.024E-02	4.062E-02	-0.89
500	7.968E-02	8.039E-02	8.029E-02	8.095E-02	6.685E-02	6.730E-02	-0.79
555	1.163E-01	1.165E-01	1.170E-01	1.173E-01	9.993E-02	1.001E-01	-0.22
600	1.448E-01	1.449E-01	1.458E-01	1.458E-01	1.267E-01	1.266E-01	0.00
700	1.946E-01	1.952E-01	1.954E-01	1.962E-01	1.748E-01	1.754E-01	-0.35
800	2.221E-01	2.227E-01	2.231E-01	2.237E-01	2.033E-01	2.037E-01	-0.26
900	2.285E-01	2.300E-01	2.296E-01	2.309E-01	2.118E-01	2.128E-01	-0.58
1000	2.215E-01	2.231E-01	2.220E-01	2.236E-01	2.062E-01	2.077E-01	-0.73
1100	2.066E-01	2.082E-01	2.068E-01	2.084E-01	1.930E-01	1.944E-01	-0.75

Table 9.3.2. Combined standard uncertainty of TÜBİTAK UME DoEs, $u\left(D_{\mathrm{UME}}(\lambda)\right)$, and its components: uncertainty of TÜBİTAK UME measurements, $u\left(E_{\mathrm{UME}}(\lambda)\right)$, uncertainty of KCRV, $u\left(\Delta_{\mathrm{KCRV}}(\lambda)\right)$; and uncertainty of link quality, $u_{\mathrm{link}}(\lambda)$.

λ, nm	$u\left(E_{\mathrm{UME}}(\lambda)\right)$, %	$u\left(\Delta_{\mathrm{KCRV}}(\lambda)\right)$, %	$u_{\mathrm{link}}(\lambda)$, %	$u\left(D_{\mathrm{UME}}(\lambda)\right)$, %
250	1.57	0.28	0.39	1.64
260	1.54	0.25	0.31	1.59
270	1.52	0.23	0.29	1.57
280	1.52	0.22	0.28	1.56
290	1.51	0.20	0.26	1.55
300	1.31	0.19	0.25	1.35
320	1.30	0.18	0.22	1.33
340	1.29	0.17	0.22	1.32
360	1.04	0.16	0.21	1.07
380	1.03	0.15	0.22	1.06
400	0.99	0.14	0.22	1.03
450	0.99	0.12	0.18	1.02
500	0.98	0.11	0.17	1.00
555	0.98	0.10	0.17	1.00
600	0.98	0.10	0.16	1.00
700	0.98	0.09	0.16	1.00
800	0.98	0.09	0.16	1.00
900	0.99	0.08	0.15	1.01
1000	0.99	0.08	0.15	1.01
1100	0.99	0.08	0.15	1.01

9.3.2. DoE of TÜBİTAK UME

Table 9.2.3 summarizes the DoEs of TÜBİTAK UME: differences from KCRV, $D_{\mathrm{UME}}(\lambda)$, its standard uncertainty, $u\left(D_{\mathrm{UME}}(\lambda)\right)$, and its expanded uncertainty, $U\left(D_{\mathrm{UME}}(\lambda)\right)$, calculated by equation (8.7). The TÜBİTAK UME DoEs are also presented in Figure 9.2.1.

Table 9.3.3. Summary of DoEs of TÜBİTAK UME: differences from KCRV, $D_{\mathrm{UME}}(\lambda)$, its standard uncertainty, $u\left(D_{\mathrm{UME}}(\lambda)\right)$, and its expanded uncertainty, $U\left(D_{\mathrm{UME}}(\lambda)\right)$.

λ, nm	$D_{\mathrm{UME}}(\lambda)$, %	$u\left(D_{\mathrm{UME}}(\lambda)\right)$, %	$U\left(D_{\mathrm{UME}}(\lambda)\right)$, % ($k$=2)
250	-1.96	1.64	3.28
260	-1.82	1.59	3.17
270	-1.74	1.57	3.14
280	-1.56	1.56	3.12
290	-1.62	1.55	3.09
300	-1.66	1.35	2.70
320	-1.41	1.33	2.66
340	-1.54	1.32	2.64
360	-1.40	1.07	2.14
380	-1.37	1.06	2.12
400	-1.00	1.03	2.06
450	-0.92	1.02	2.04
500	-0.78	1.00	2.00
555	-0.23	1.00	2.00
600	0.04	1.00	2.00
700	-0.29	1.00	2.00
800	-0.33	1.00	2.00
900	-0.56	1.01	2.02
1000	-0.78	1.01	2.02
1100	-0.71	1.01	2.02

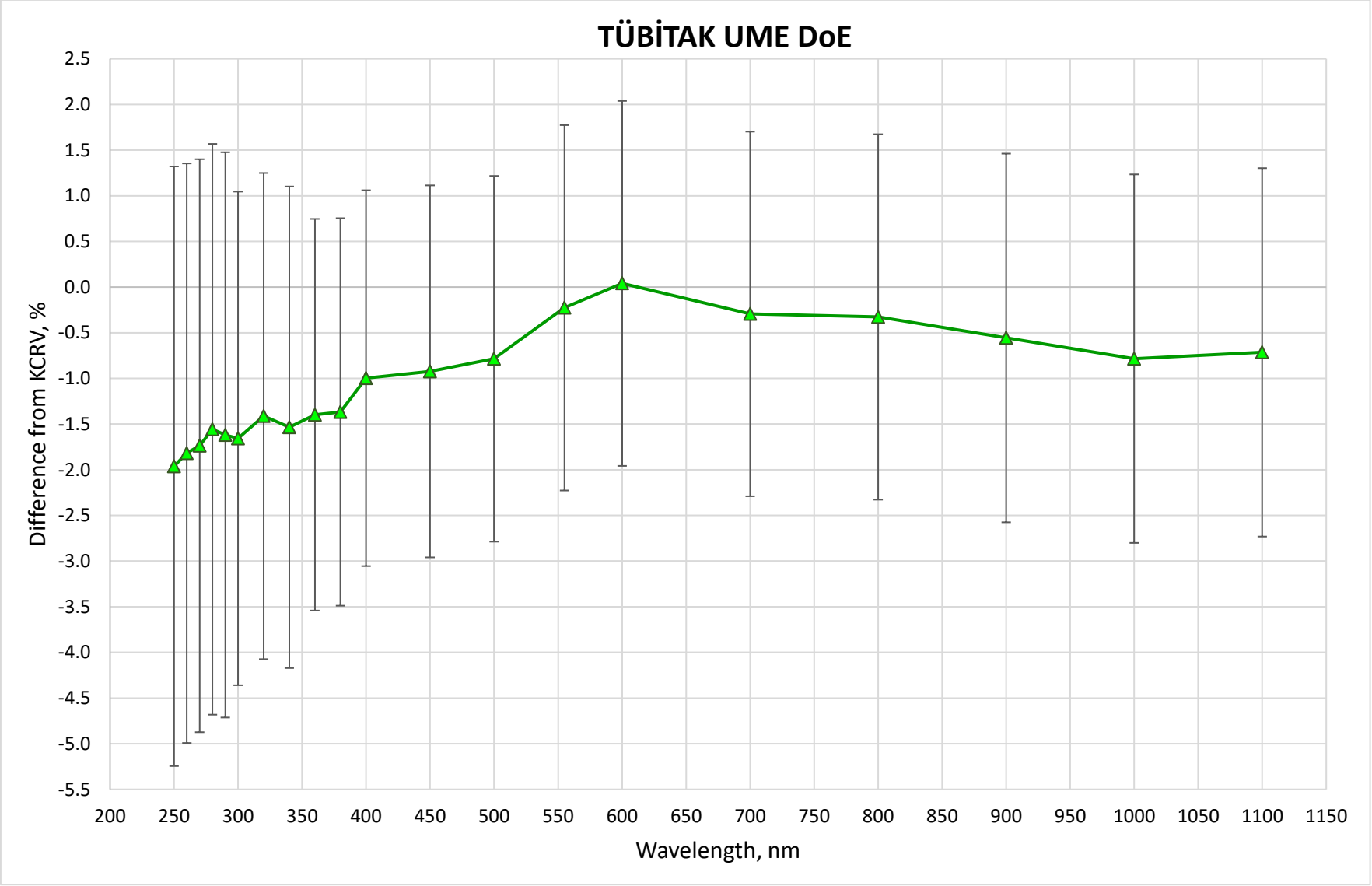

Figure 9.3.1. DoEs of TÜBİTAK UME

10. REFERENCES

[1] CIPM Mutual Recognition Arrangement, available from https://www.bipm.org/en/cipm-mra

[2] Emma R Woolliams, Nigel P Fox, Maurice G Cox, Peter M Harris and Neil J Harrison, Final report on CCPR K1-a: Spectral irradiance from 250 nm to 2500 nm, *Metrologia*, 2006, **43**, Tech. Suppl., 02003.

[3] B.B. Khlevnoy , CIPM key comparison CCPR-K1.a.2017 for spectral irradiance 250 nm to 2500 nm. Final report, *Metrologia*, 2023, **60**, Tech. Suppl., 02002, DOI 10.1088/0026-1394/60/1A/02002.

[4] Measurement Comparisons in the CIPM MRA, ***CIPM MRA-G-11***, Version 1.1, January 2021, available from www.bipm.org.

[5] Guidelines for CCPR and RMO Bilateral Key Comparisons, ***CCPR-G5***, October 2014, available from www.bipm.org

[6] Guidelines for RMO PR Key Comparisons, ***CCPR-G6***, October 2014, available from www.bipm.org.

[7] Dong-Joo Shin, Chul-Woung Park, Svetlana S Kolesnikova and Boris B Khlevnoy , Final report on bilateral comparison APMP.PR-K1.a.1-2008 between KRISS (Korea) and VNIIOFI (Russia): Spectral irradiance from 250 nm to 2500 nm, *Metrologia*, 2010, **47**, Tech. Suppl., 02005.

[8] Frank Wilkinson, Gan Xu and Yuanjie Liu, Final report on CCPR-K1.a.1: Bilateral comparison of spectral irradiance between NMIA (Australia) and SPRING (Singapore), *Metrologia*, 2006, **43**, Tech. Suppl., 02002.

[9] Teresa Goodman, William Servantes, Emma Woolliams, Peter Sperfeld, Mihai Simionescu, Peter Blattner, Stefan Källberg, Boris Khlevnoy and Paul Dekker, Final report on the EURAMET.PR-K1.a-2009 comparison of spectral irradiance 250 nm—2500 nm, *Metrologia*, 2015, **52**, Tech. Suppl., 02003.

[10] M Ojanen, M Shpak, P Kärhä, R Leecharoen and E Ikonen, Report of the spectral irradiance comparison EURAMET.PR-K1.a.1 between MIKES (Finland) and NIMT (Thailand), *Metrologia*, 2009, **46**, Tech. Suppl., 02001.

[11] Guidelines for CCPR Key Comparison Report Preparation, ***CCPR-G2***, January 2019, available from www.bipm.org.

[12] Sapritsky V. I., Khlevnoy B. B., Khromchenko V. B., Lisiansky B. E., Mekhontsev S. N., Melenevsky U. A., Morozova S. P., Prokhorov A. V., Samoilov L. N., Shapoval V. I., Sudarev K. A., Zelener M. F., *Appl. Opt.*, 1997, 36, 5403-5408.

[13] Prokhorov A, 2020, VIRIAL International. Scientific and Engineering Services and Software for Optical Radiometry and Radiation Thermometry. STEEP321, available at: www.virial.com/steep321.html

[14] Prokhorov A., Effective emissivities of isothermal blackbody cavities calculated by the Monte Carlo method using the three-component BRDF Model, *Appl. Opt.*, 2012, V. 51, No.13, 2322-2332.

[15] Samoylov M. L., Ogarev S. A., Khlevnoy B. B., Khromchenko V. B., Mekhontsev S. N., Sapritsky V. I., High Accuracy Radiation TSP-type Thermometers for Radiometric Scale Realization in Temperature Range from 600 to 3200 °C, *Temperature: It´s Measurement and Control in Science and Industry: Proc. 8th Symposium on Temperature*, 2003, V. 7, 583–588.

[16] Woolliams E. R., Anhalt K., Ballico M., Bloembergen P., Bourson F., Briaudeau S., Campos J., Cox M. G., Campo D., Dong W., Dury M. R., Gavrilov V., Grigoryeva I., Hernanz M. L., Jahan F., Khlevnoy B., Khromchenko V., Lowe D. H., Lu X., Machin G.,

Mantilla J. M., Martin M. J., McEvoy H. C., Rougié B., Sadli M., Salim S. G. R., Sasajima N., Taubert D. R., Todd A. D. W., Van den Bossche R., Van der Ham E., Wang T., Whittam A., Wilthan B., Woods D. J., Woodward J. T., Yamada Y., Yamaguchi Y., Yoon H. W. and Yuan Z., Thermodynamic temperature assignment to the point of inflection of the melting curve of high-temperature fixed points, *Phil.Trans.R.Soc.A* **374**: 20150044

[17] B.B. Khlevnoy, I.A. Grigoryeva, D.A. Otryaskin, Development and investigation of WC–C fixed-point cells, *Metrologia* **49**, S59 (2012).

[18] B. B. Khlevnoy and I. A. Grigoryeva, Long-Term Stability of WC-C Peritectic Fixed Point, *Int J Thermophys* (2015) **36**:367–373

[19] I. A. Grigoryeva, B. B. Khlevnoy and M. V. Solodilov, Reproducibility of WC–C High-Temperature Fixed Point, *Int J Thermophys* (2017) **38**:69, DOI 10.1007/s10765-017-2203-0

[20] P. Sperfeld, Final report on the CIPM key comparison CCPR-K1.b: Spectral irradiance 200 nm to 350 nm, *Metrologia*, 2008, **45**, *Tech. Suppl*., 02002, DOI 10.1088/0026-1394/45/ 1A/02002.

[21] A.D.W. Todd, K. Anhalt, P. Bloembergen, B.B. Khlevnoy, D.H. Lowe, G. Machin, M. Sadli, N. Sasajima and P. Saunders, On the uncertainties in the realization of the kelvin based on thermodynamic temperatures of high-temperature fixed-point cells, *Metrologia* **58,** 035007

[22] P. Sperfeld, S. Pape, B. Khlevnoy and A. Burdakin, Performance limitations of carbon-cavity blackbodies due to absorption bands at the highest temperatures, *Metrologia*, **46** (2009) S170–S173.

[17] C. Carreras and A. Corróns, Absolute spectroradiometric and photometric scales based on an electrically calibrated pyroelectric radiometer, *Appl. Opt*., 1981, 20.

[18] P. Corredera, A. Corróns, A. Pons and J. Campos, Absolute spectral irradiance scale in the 700-2400 nm spectral range, *Appl. Opt*., 1990, 29.

[19] S.N. Park, C.W. Park, D.H. Lee, and B.H. Kim, "Consistency of the Temperature Scales above the Silver Freezing Point Realized at Four Different Spectral Bands", *SICE-ICASE International Joint Conference* 2006 Oct., 18-21, 2006 in Bexco, Busan, Korea (2006).

[20] Preston-Thomas H., "The International Scale of 1990 (ITS-90)", Metrologia, 1990, 27, 3-10.

[21] Bazkır O., Samedov F. "Charecterization of silicon photodiode based trap detectors and establishment of spectral responsivity scale". Optics and Lasers in Engineering. 43(2). 131-141. 2005.

[22] Bazkir O., Ugur S., Samedov F., Esendemir A., "High-accuracy optical power measurements by using electrical - substitution cryogenic radiometer". Optical Engineering. 44(1). 016401(1)-016401(6). 2005.

[23] Durak M., Samedov F., "Realization of a filter radiometer based irradiance scale with high accuracy in the region from 286 nm to 901 nm". Metrologia. 41(12). 401-406. 2004.

[24] Sametoglu F., "New traceability chains in the photometric and radiometric measurements at the National Metrology Institute of Turkey". Optics and Lasers in Engineering. 45(1). 36-42. 2007.

[25] Samedov F., Durak M., Bazkir O., "Filter-radiometer based realization of Candela and establishment of photometric scale at UME". Optics and Lasers in Engineering. 43(11). 1252-1256. 2005.

[26] F.Sametoglu., "Establishment of The Spectroradiometer-Based Spectral Irradiance Scale at TUBITAK UME". 13th International Conference on New Developments & Applications in Optical Radiometry (NEWRAD2017). p.155-156. 13-16 June 2017. Tokio. Japan.

[27] Sametoglu. F., Celikel. O., Witt F., "A differential spectral responsivity measurement system constructed for determining of the spectral responsivity of a single-and triple-junction photovoltaic cells". European Physical Journal of Applied Physics. 80(2). 21001. 2017.

[28] Ojanen, M, Shpak, M, Kärhä, P, Leecharoen, R and Ikonen, E 2009 Uncertainty evaluation for linking a bilateral key comparison with the corresponding CIPM key comparison Metrologia 46(5) 379-403

Appendix A

Relative Data

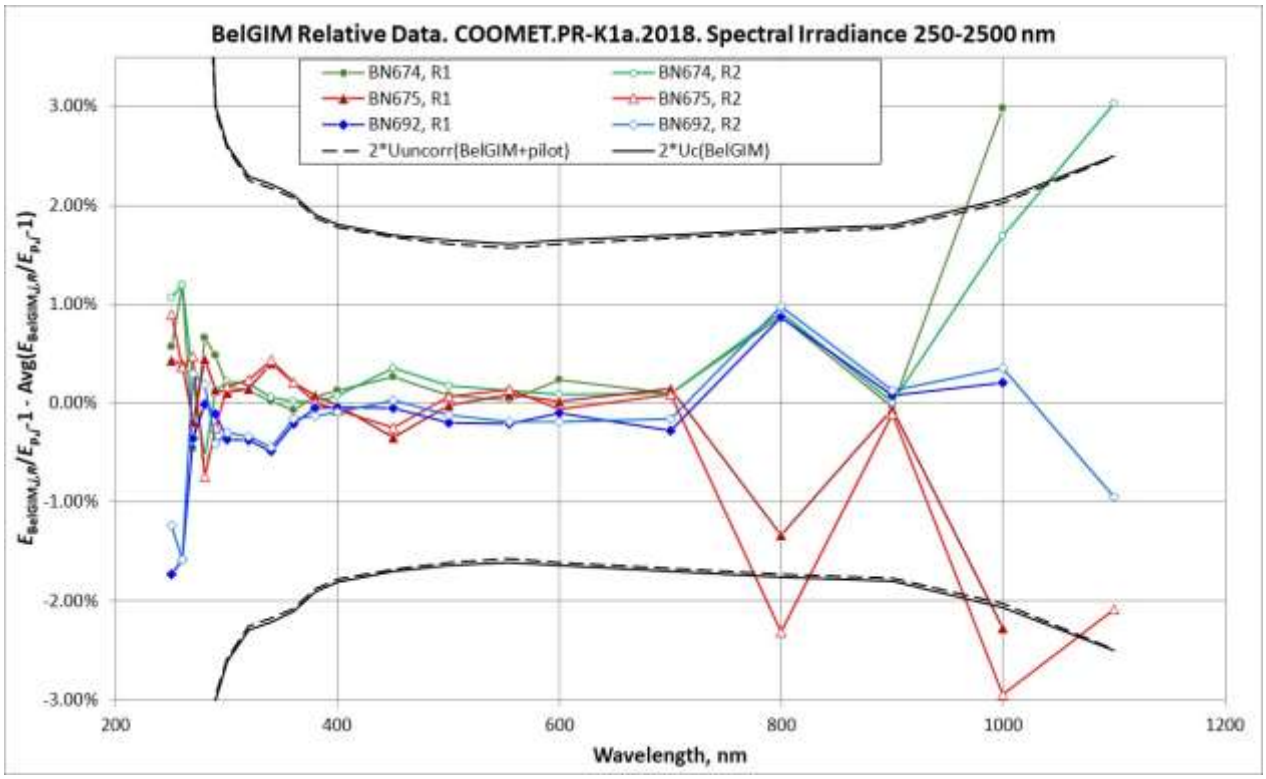

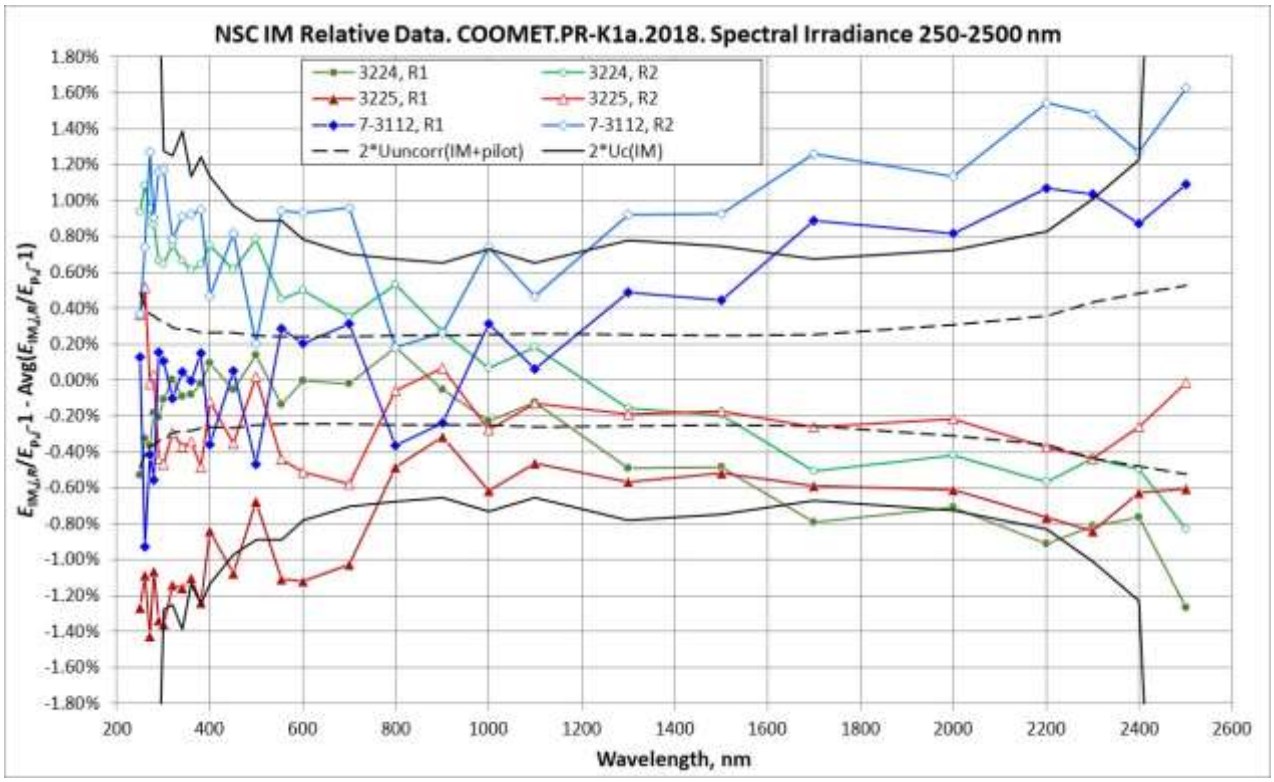

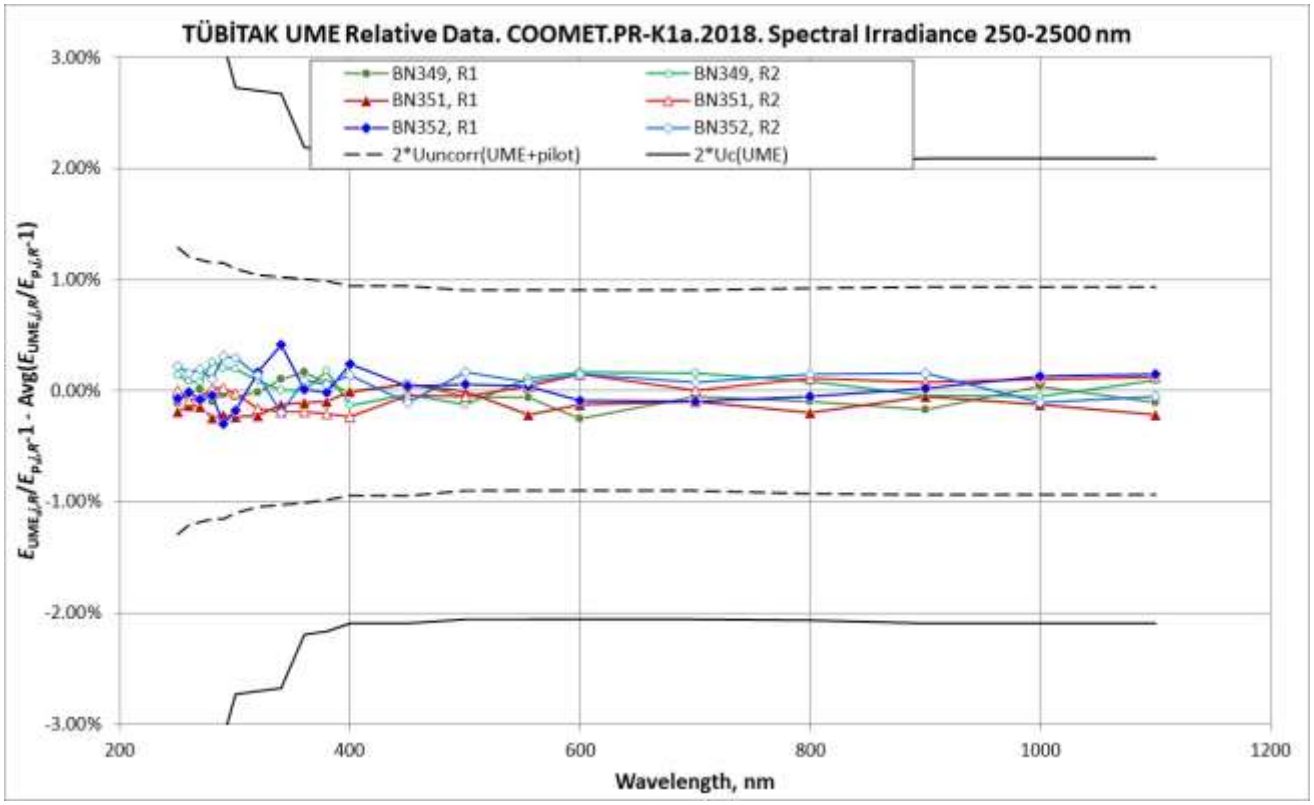
TÜBİTAK UME Relative Data. COOMET.PR-K1a.2018. Spectral Irradiance 250-2500 nm
BN349, R1
BN349, R2
BN351, R1
BN351, R2
BN352, R1
BN352, R2
2*Uuncorr(UME+pilot)
2*Uc(UME)
3.00%
2.00%
1.00%
0.00%
-1.00%
-2.00%
-3.00%
200
400
600
800
1000
1200
Wavelength, nm